QUANTIFYING MONTHLY AREAL RAINFALL UNCERTAINTY USING A DATA-BASED STOCHASTIC RAINFALL GENERATOR

Nhlakanipho Mkhize

A research report submitted to the Faculty of Engineering and the Built Environment, University of the Witwatersrand, in fulfilment of the requirements for the degree of Master of Science in Engineering

Johannesburg, 2014

DECLARATION

I declare that this research report is my own unaided work. It is being submitted to the Master of Science to the University of the Witwatersrand, Johannesburg. It has not been submitted before for any degree or examination to any other University.

_____

Signature of Applicant

Date:

ABSTRACT

This study aims to establish whether a data-based model of incorporating uncertainty in daily areal rainfall estimates can be adapted to a coarser monthly time scale and still provide reasonable uncertainty estimates for water resource modelling applications. The daily generator was formulated as a simple, efficient and robust model of stochastically generating sequences of uncertainty-impacted areal rainfall estimates from point rainfall measurements.

The data - based model is tested on 8 catchments spread across South Africa. It is found that the selected rain gauge combinations have an impact on one of the parameters of the model (the scaling factor) and the degree of bias on the standard deviation and skewness values of the generated stochastic sequences. A correlation-based rain gauge selection approach is proposed to minimise this bias.

Statistical analysis of the generated stochastic areal rainfalls shows that the data-based model provides realistic uncertainty estimates. However the actual bias on the low rainfalls (< 20^{th} percentile) is between 0.9 – 46.8%. The importance of these rainfalls in water resource modelling applications though is low.

ACKNOWLEDGEMENTS

I would like to express my sincere gratitude to Professor John Ndiritu, my supervisor, for all the assistance, patience and guidance he provided me in the preparation of this research.

Knight Piésold Consulting for providing me with the financial assistance and enabling me to fulfil my dream of writing this research report. A special thanks to Mr Edwin Lillie for all the support and encouragement.

My friends and family, who have been supportive and patient with me throughout this process, and for the All Mighty God for all the strength he gave me in this period .

To all, I am eternally grateful. I pray that this is a first step towards many more achievements.

TABLE OF CONTENTS

LIST OF FIGURES

LIST OF TABLES

LIST OF APPENDICES

APPENDIX D: Average proportion of zero rainfalls

1. INTRODUCTION

1.1 BACKGROUND

The temporal and spatial accuracy of areal rainfall is an important consideration for determining surface hydrological properties for water resource planning and management in Southern Africa, as it is the dominate source of all surface and underground waters (Ngonogondo et al, 2011). Therefore, the precise estimation of areal rainfall is an important input to human livelihoods in the region (Xu et al (2013) and Agnostopoulou et al (2003)).

Droughts for example can severely affect societies with little resilience and readiness (Nyabeze, 1999). Therefore use is made of the Standard Precipitation Index (SPI) to provide forewarning and to advice on the drought mitigation measures and decisions (Dlamini, 2013). The reduction of the number of rainfall observation stations in Southern Africa however complicates the accurate calculation of areal rainfall which informs this index.

The projection of future crop production is limited by the spatial and temporal accuracy of the climatic data used (Watson, 2013). This is an important consideration in Southern Africa, because agriculture is seen as a key development node. Watson (2013) found that crop model studies in regions where rainfall is limited are very sensitive to the rainfall data. This sensitivity has implications on food production and security as well as on the adaption options formulated. Consequently, Watson (2013) recommends that observed data should be accompanied by confidence ranges to plan for the risks associated with the inaccurate estimate of areal rainfall.

In flood prediction, a key question is how the spatial variability of rainfall impacts flow response from a catchment (Bell and Moore, 2000). This is especially important in semi - arid regions where slight changes in the magnitude of rainfall can result in dramatic changes in the runoff from a region (Fekete *et al*, 2003). Bell and Moore (2000) found that runoff sensitivity is strongest during convective rainfall events, during which, a broader range of hydrographs may result.

In water resource planning it is necessary to estimate demands and predict the effects of developments on the water balance of an area (Menne, 1961). As the Southern African region continues to develop, competition for the resource will certainly increase. However, planning relies on the availability of adequate data (Midgley, 1961). Lumsden *et al* (2009) and Warburton *et al* (2005) found that perturbations of the rainfall are amplified by the hydrological system. In South Africa for example, a 10% change in precipitation can result in a streamflow change of up to 30% and more (Warburton et al, 2005). Despite these implications, the common approach in Southern Africa is to compute a single areal rainfall and to assume that it is error free (Ndiritu, 2013a).

Areal rainfall can either be directly measured using radar or indirectly estimated using satellite images or rain gauge networks. However, due to the stochastic nature of rainfall and the limitations of the available measuring instrumentation, areal rainfall estimates are uncertain (Anagnostopoulou *et al*, 2008).

Radar coverage has increased over the last few decades and has the potential to provide rainfall measurements over large spatial areas. The radar transmits a pulse of electromagnetic energy as a beam in a direction determined by a movable antenna. The radiated wave is then partially reflected by rainfall particles and returns to the radar. Information of the rainfall can then be interpreted from the energy returned to the radar (Linsley *et al*, 1975). Radar measurements however are taken in the atmosphere and the conversion of the raw data into volumetric rainfall magnitudes is problematic due to the differences in the measured radar areal rainfall estimates based on point rainfall measurements. These differences are related to the non – uniform vertical profile of reflectivity, drifts in the radar calibration constant and biased reflectivity to rain rate relationships (McMillian *et al*., 2011).

Satellites also have an excellent spatial coverage. Satellite areal rainfall estimates require the evaluation of a rainfall coefficient on the basis of the amount and type of clouds and the probability and likely intensity of rainfall associated with each cloud (Linsley *et al*, 1975). However, because of their limited temporal resolution and the intermittency of rainfall in space, areal rainfall measurements based on satellite observations are uncertain (Steiner, 1996).

The accuracy of areal rainfall estimates based on rain gauge measurements are closely related with the density of the rain gauge network. In Southern Africa, the locations of these gauges is often associated with development centres such as mines, mission stations and railway lines which does not enable the optimal sampling of the spatial distribution of rainfall over an area (Singh and Chowdhury (1986); Mwelwa, 2005; Eagleson (1970) and Dent *et al* (1987)). The closure of many stations in the region has also affected the spatial coverage of rain gauge networks (Lynch, 2004). Errors in areal rainfall estimates based on rain gauge networks are well documented. Rainfall varies in form and scale, the measured rainfall depths are a function of the areas surrounding the measuring instrument and the measured rainfall depths themselves are subject to random and systematic errors (Dreaver and Hutchinson (1974)). Quantifying areal rainfall uncertainty in areal rainfall estimates based on point rainfall measurements is therefore an important consideration.

The quantification of areal rainfall uncertainty enables the decision maker the latitude to make an informed decision based on some form of risk analysis and enables the modeller to produce results that are comparable with those of other modellers,

encouraging a more transparent science (Kapangaziwiri (2010), Pappenberger and Beven (2006)).

There are a number of studies that focus on the uncertainty in satellite and/or radar based areal rainfall measurements. Steiner (1996) investigated the uncertainty caused by the finite sampling resolutions of satellites against ground based observations and his results indicate that the sampling uncertainty in satellite observations is constrained by the rainfall depth, sampling frequency and domain size. Vogel (2013) investigated a geostatistical method that combines radar and rain gauge data to generate the best areal rainfall estimate and to simulate ensembles of random rainfall fields that represent the inherent analysis uncertainty in Switzerland. Vogel (2013) concludes that both the accuracy and reliability of areal rainfall estimates can be improved by increasing the number of rain gauges rather than by increasing the radar information available. It is common for studies that focus on the uncertainty in satellite and radar based areal rainfall measurements to be either directly or indirectly associated with ground based observations. However, radar and satellite data are not readily available in Southern Africa and span for shorter time periods than rain gauge data sets (Ndiritu, 2013a).

Methods for quantifying areal rainfall uncertainty in point rainfall measurements can be grouped into parametric and non – parametric methods. Parametric based methods have wide applicability but require reliable quantitative information to describe the probabilistic models and should generally be used in the climatic regimes in which they were developed (UNESCO, 2005). Non – parametric (or data – based) methods are based on observed data and can be adapted to the rain gauge data available and any unique spatial rainfall features of an area, as they implicitly incorporate the patterns or characteristics of the actual recorded data (Ndiritu, 2013a). In Southern Africa however, there are very few studies that focus on non – parametric methods of quantifying uncertainty in areal rainfall estimates based on rain gauge networks.

The quantification of areal rainfall in point rainfall measurements can ensure that optimistic development proposals are kept within reasonable bounds, minimizing the potential for failure of water related projects (Menne, 1961). However, the uncertainty in areal rainfall estimates based on rain gauge networks is often not considered in water resource planning and management in Southern Africa (Ndiritu, 2013a). Non – parametric methods of quantifying uncertainty in areal rainfall are indiscriminate and have the potential to promote the incorporation of uncertainties in areal rainfall estimates based on rain gauge networks in the region. The objective of this research is therefore to demonstrate a data - based model of quantifying realistic uncertainty estimates in areal rainfall estimates based on point rainfall measurements in Southern Africa, for water resource modelling applications.

A review of methods of areal rainfall uncertainty estimation detailed in Chapter 2 revealed the approach developed recently by Ndiritu (2013a) as practical, simple and robust. The method quantifies areal rainfall uncertainty by computing the differences in areal rainfall obtained by alternate selection of rain gauges for areal rainfall determination. Ndiritu (2013a) found that the cumulative probability density (cpd) curves of these differences obtained at a lower rain gauge density could be mapped into those of a higher rain gauge density by a scaling factor. This scaling factor is used with the appropriate cumulative probability density curve to stochastically obtain perturbations on the areal rainfall. The model therefore generates an ensemble of plausible areal rainfalls that incorporate this uncertainty and is described in more details in Section 2.3. The model however had been formulated and tested using data at a daily time step while many water resources assessments in Southern Africa apply a monthly time step. Since the statistical characteristics of rainfall at the daily and the monthly time step are distinctly different, this study is aimed at assessing the applicability of the model by Ndiritu (2013a) at the monthly time step. Additionally, the model had been tested on only 2 South African catchments and this study aimed at assessing the model using more catchments spread across various rainfall zones in South Africa.

1.2 RESEARCH OBJECTIVE

To assess whether the data – based stochastic areal rainfall generator by Ndiritu (2013a) can be adapted to a monthly time step and realistically quantify areal rainfall uncertainty in monthly rainfall.

This study also aims to find out what improvements could be made to the stochastic areal rainfall generator model by Ndiritu (2013a) for application at the monthly time step.

1.3 STRUCTURE OF THE RESEARCH REPORT

Chapter 2 is the literature review. It informs about the complexity of areal rainfall estimation and then reviews models of quantifying areal rainfall uncertainty. The review then presents a detailed description of the data – based model selected for this study.

The data used to test the data – based model on a coarser monthly time interval is provided in Chapter 3. This Chapter details the quality of the data used and explains how the rain gauges in each catchment were selected. The current status of ground based rainfall measurement in South Africa is also reviewed.

The methodology adopted in this study is presented in Chapter 4. This chapter assesses the assumptions and procedures followed during the formulation of the data

– based model and evaluates whether these remain reasonable when dealing with coarser monthly rainfalls.

The statistics of the generated stochastic areal rainfalls are analysed in Chapter 5 and the results are discussed in Chapter 6. Chapter 7 reflects on the findings of the study and draws conclusions and recommendations.

2. LITERATURE REVIEW

2.1 THE ESTIMATION OF AREAL RAINFALL FROM POINT RAINFALL MEASUREMENTS

The accurate capturing of the rainfall process over a catchment using fixed point measurements is extremely complex due to the dynamics of the rainfall event and the instruments of measurement used to quantify it.

Rainfall events are classified according to the conditions that generate vertical air motion (Nandalal, 2010). For example:

- Convective rainfall results from the upward movement of air due to heating (see Figure 2.1). These events are usually in the form of light showers or thunderstorms of high intensity and short duration.

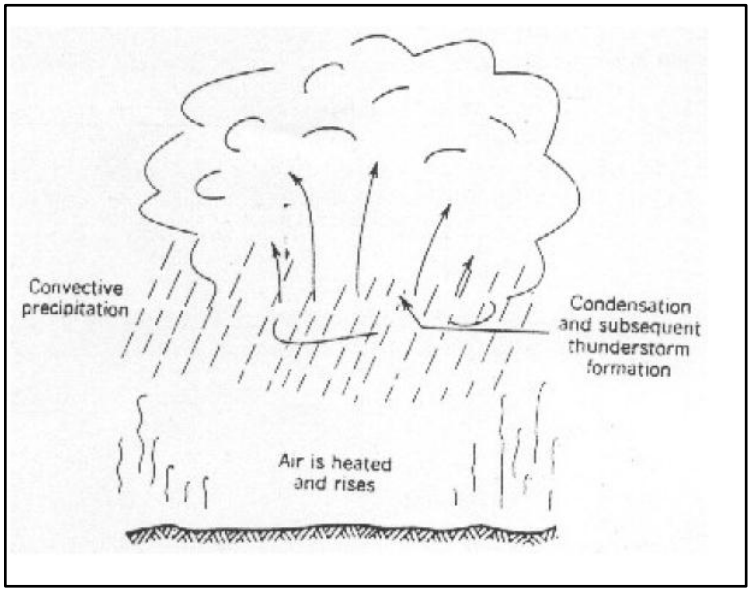

Figure 2.1: Convective Rainfall (from Nandalal, 2010)

- Orographic rainfall results from the mechanical lifting of moist horizontal air currents due to natural barriers such as mountains (see Figure 2.2). Rainfall due to this phenomenon is usually steady and continuous and occurs on the windward side of mountains.

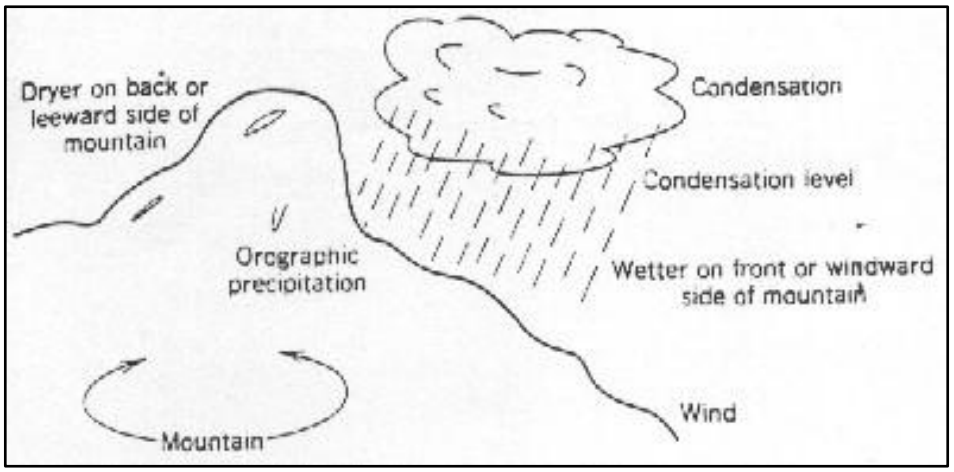

Figure 2.2: Orographic Rainfall (from Nandalal, 2010)

- Cyclonic rainfall is associated with the movement of air masses from high pressure regions to low pressure regions as a result of the unequal heating of the earth's surface (see Figure 2.3). This type of rainfall may be classified as frontal or nonfrontal.

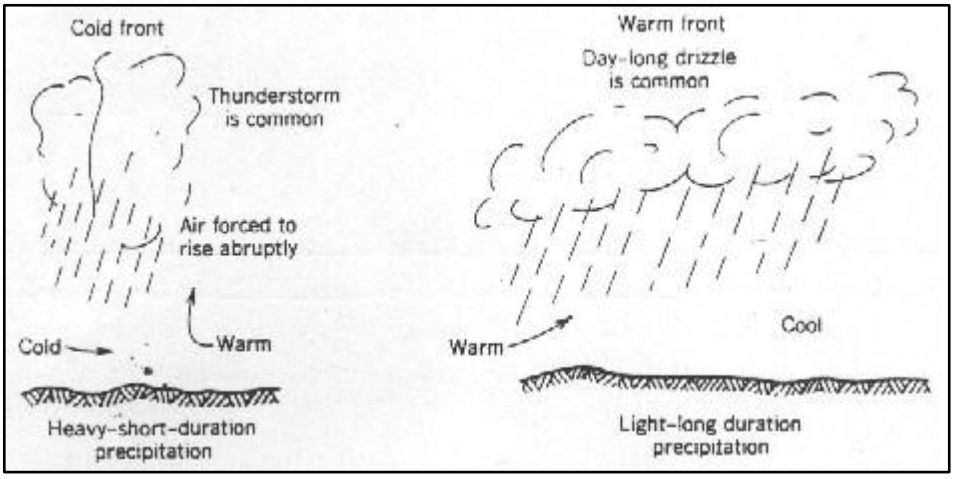

Figure 2.3: Cyclonic Rainfall (from Nandalal, 2010)

As these different rainfall events move across a fixed rain gauge network, differences in the measured rainfall depths are observed. These differences are a function of the scale of the rain event. Meteorologists classify rainfall events into three scales:

- Convective scale (or microscale) - This is the smallest scale and the range of the cellular structure can extend anywhere from one to a few kilometres. These structures generally move under the force of wind and may last up to 30 minutes. However, to the fixed observer these are often seen as bursts lasting only a few minutes.

- Mesoscale - During this event, the conditions which spawn convective cells persist more or less continuously. The droplets translate at a characteristic angle with respect to the mean wind direction. The cells of this event include thunderstorms and may extend 8 to 50 kilometres.

- Synoptic scale - These cells are associated with intense low pressure centres and may extend several hundred kilometres. These are in essence a train of mesoscale events.

In the context of rainfall measurement, the synoptic scale events can be captured most readily by ground based observation instruments, as they usually last for long periods and rainfall is produced at fixed points on the ground (Eagleson, 1970).

The measured rainfall depth during a rain event is a decreasing function of the distance from the storm centre as seen from a fixed position. Due to the random distribution of these centres over a catchment, rain gauges can measure rainfall that is sometimes near the storm centre, sometimes at the periphery of the storm and sometimes inbetween the two (Eagleson,1970). This is one of the reasons why increasing the density of rain gauges is usually associated with an increase in the estimated average areal rainfall.

2.2 DATA – BASED MODELS OF QUANTIFYING AREAL RAINFALL UNCERTAINTY

Reichle et al. (2002) used perturbations with a standard deviation of 50% of the rainfall total at each time step. However, given the importance of input data to the calibration of parameters for hydrological modelling, this approach can no longer be justified.

Ndiritu (2013b) assessed a non – parametric multiplier based method of generating stochastic daily areal rainfall from point rainfall. Ndiritu (2013b) then incorporated these uncertainties on the storage-yield reliability and found that areal rainfall uncertainty had a significant impact on the storage-yield relationship. One of the problems encountered was that the calibration process was more difficult and it was necessary to constrain the multipliers iteratively to avoid bias and to prevent the generation of unrealistically large perturbed areal rainfalls.

Ndiritu (2013a) demonstrated a simple, efficient and robust non – parametric model of stochastically generating sequences of realistic uncertainty – impacted daily areal estimates from point rainfall measurements. This data – based model by Ndiritu (2013a) fulfils two requirements that are of importance within the Southern African context. The data – based model is able to:

1. Quantify realistic uncertainties estimates in areal rainfall based on rain gauge measurements and

2. Quantify the proportion and magnitudes of rainfall events that are missed out by rain gauge networks of an inadequate density.

Ndiritu (2013a) tested the data – based model on two South African catchments and found that the model could be used as a simple and effective method of quantifying and incorporating uncertainty in areal rainfall in the region. In water resource modelling applications however, a time of one month is usually to minimise areal rainfall variations and the influence of different storm periods (Pitman (1973) and Hughes (1995)).

Research by Wagener *et al* (2007) and Hutchinson (1969) suggests that different or independent information is present at various time scales which may affect the performance of a model at a daily and a monthly time scale, particularly since monthly rainfalls are distributed normally according to the Central Limit Theorem whilst daily rainfalls are usually taken to be distributed according to the Gamma function. Alvarez and Henry (1970) through their experiments found that the density of rain gauges required to estimate monthly areal rainfall is less than that required for daily areal rainfall because the spatial variation of rainfall reduces as the averaging period increases. Jackson (1969) found that over a flat uniform terrain the integration of individual storms over a month leads to a decrease in the rainfall gradients between rainfall stations.

To promote the quantification of uncertainty in areal rainfall estimates based on point rainfall measurements in Southern Africa, a simple and practical model is required. A survey was conducted to identify other models of quantifying areal rainfall uncertainties. However, no other models were identified that respond to the issues facing the region. Therefore, the data – based model by Ndiritu (2013a) was used in this study. The data – based model by Ndiritu (2013a) is superior to the multiplier based model because it is capable of infilling missed rainfalls in catchments were the rain gauge network is inadequate and because of the problems associated with constraining the multipliers to avoid bias in the generated stochastic sequences.

The data – based model by Ndiritu (2013a) however was based on a number of assumptions found to be reasonable on a daily time scale. Consequently, due to the suggested differences in areal rainfall at different scales, the application of the data - based model by Ndiritu (2013a) at a coarser monthly time interval needs to be assessed before it can be used for water resource modelling purposes.

2.3 THE DATA – BASED STOCHASTIC AREAL RAINFALL GENERATOR

This section summarises all the literature available on the data – based stochastic areal rainfall generator model by Ndiritu (2013a). It also informs the approach adopted in this study.

2.3.1 DETERMINATION OF STOCHASTIC PERTURBED AREAL RAINFALLS

The data – based model by Ndiritu (2013a) is based on the assumption that the perturbed rainfall is the sum of the catchment average rainfall and the perturbation. The catchment average rainfall H_t is the best estimate of areal rainfall available, obtained from all the rainfall stations available.

The perturbations used in generating the stochastic rainfalls are based on the differences in areal rainfall estimates obtained from two or more rain gauge groups of lower rain gauge densities. To compute these perturbations, the available rain gauges are divided into groups of lower rain gauge densities with the aim of achieving a uniform catchment coverage. The areal rainfall estimates from these groups are represented by L^1_t and L^2_t. The computed differences (P^i_t) at period t are then given by:

$$P_t^1 = L_t^1 - L_t^2 \qquad (2.1)$$
$$P_t^2 = L_t^2 - L_t^1 \qquad (2.2)$$

The magnitudes of P_t^1 and P_t^2 are the same, however, one is positive and the other is negative. This ensures that the mean of the computed stochastic areal rainfall remains unbiased and also ensures that no negative areal rainfall estimates result once the computed differences P^i_t are added to the areal rainfall estimate H_t. Depending on the number of rain gauges available, these areal rainfall differences can be computed down to the lowest possible rain gauge density (i.e. 1 rainfall station). These differences in areal rainfall cannot be computed for a single rain gauge group (e.g. 1 group of 8 stations) and when only one rainfall station is available (e.g. 1 group of 1 station).

Intuitively, Ndiritu (2013a) expected these areal rainfall differences to reduce as the rain gauge density increases. Consequently, the differences obtained from a lower rain gauge density need to be reduced and constrained before being applied to the areal rainfall estimates obtained at a higher rain gauge density. This is achieved using an uncertainty factor *u*, which can take any value between 0 and 1. The value of the uncertainty factor *u* is quantified based on a scaling factor found to exist between cumulative probability plots of areal rainfall differences at various rain gauge densities.

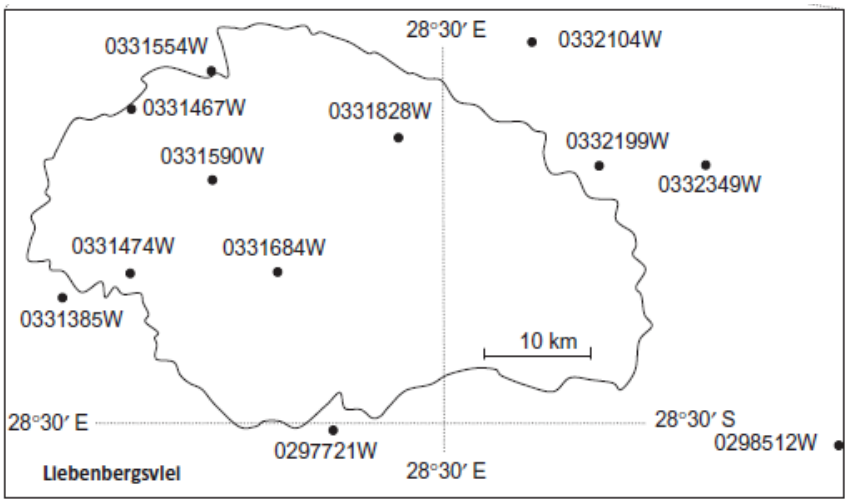

Figure 2.4: Liebenbergsvlei catchment (from Ndiritu, 2013a)

To illustrate the computation of the scaling factor, Ndiritu (2013a) selected 8 rain gauges from the 12 available on the Liebenbergsvlei catchment shown in Figure 2.4. This is because 8 rainfall stations provide 4 doubling up rain gauge densities (8, 4, 2 and 1) while 12 rain gauges only provide 3 (12, 6 and 3). The 8 stations were then divided with the aim of achieving a uniform catchment coverage into 2 groups of 4 stations (indicated by the thick black line in Figure 2.5a)); 4 groups of 2 stations (indicated by the dotted line in Figure 2.5 a)) and 8 groups of 1 station (indicated by the dashed line in Figure 2.5a)). The areal rainfall was then computed using the IDW method at these various rain gauge densities. A single sequence of P^i_t was obtained from rain gauge groups of 4 stations each; two sequences of P^i_t from rain gauge groups of 2 stations each and 4 sequences of P^i_t from rain gauge groups of 1 station each. Where there is more than one sequence of P^i_t for certain rain gauge density, Ndiritu (2013a) obtained an average and the differences were used to generate the cumulative probability plots shown in Figure 2.5a) using the Weibull plotting formula.

It was found that by scaling the cumulative plots from the various densities by a unique value, it is possible to obtain the cumulative probability plot of a different rain gauge density. This value is referred to as the *scaling factor*. Figure 2.5 (b) shows that a scaling factor of 0.57 exists between the cumulative probability plots of 4 groups of 2 stations and 2 groups of 4 stations and Figure 2.5 (c) shows that a scaling factor of 0.7 exists between the cumulative probability plots of 8 groups of 1 station and 4 groups of 2 stations. The horizontal axis indicates the proportion of perturbations less than a given perturbation within a sample of areal rainfall differences computed at various rain gauge densities.

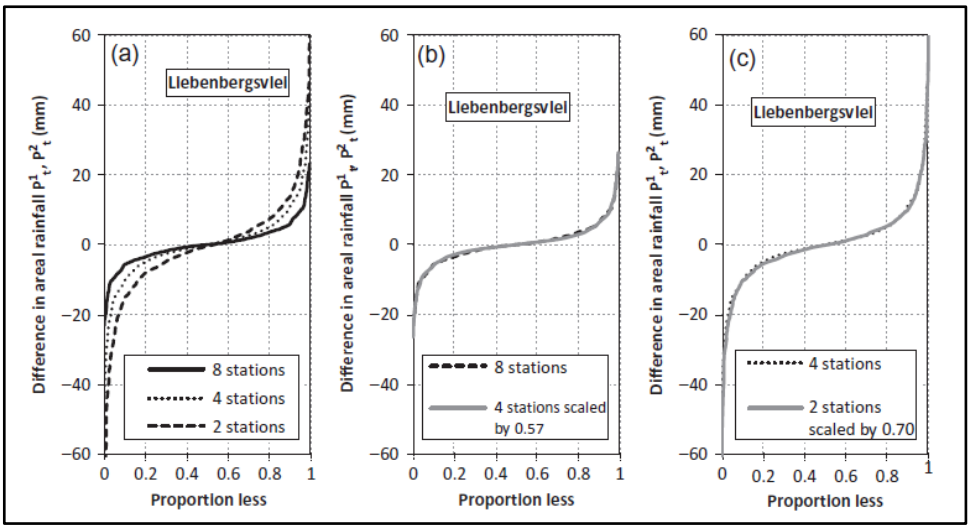

Figure 2.5: Cumulative density plots of areal rainfall differences for different rain gauge densities and the determination of scaling factors for Liebenbergsvlei (from Ndiritu, 2013a)

Intuitively Ndiritu (2013a) expected the areal rainfall differences P^i_t to increase as H_t increases. This was investigated as shown in Figure 2.6. Figure 2.6 shows that for very high rainfalls a reduction in the differences is evident. This reduction indicates that very high rainfalls cover very large catchment areas and therefore the recorded rainfall amongst the rain gauges does not vary appreciably.

The value of the computed perturbation P^i_t is therefore a function of the areal rainfall magnitude H_t, as defined by the rainfall groups (RG) 1 to 8 in Figure 2.7. These rainfall groups are selected with the aim of ensuring a reasonable sample size of perturbations within each group and based on the observed variation of the computed differences with rainfall magnitude.

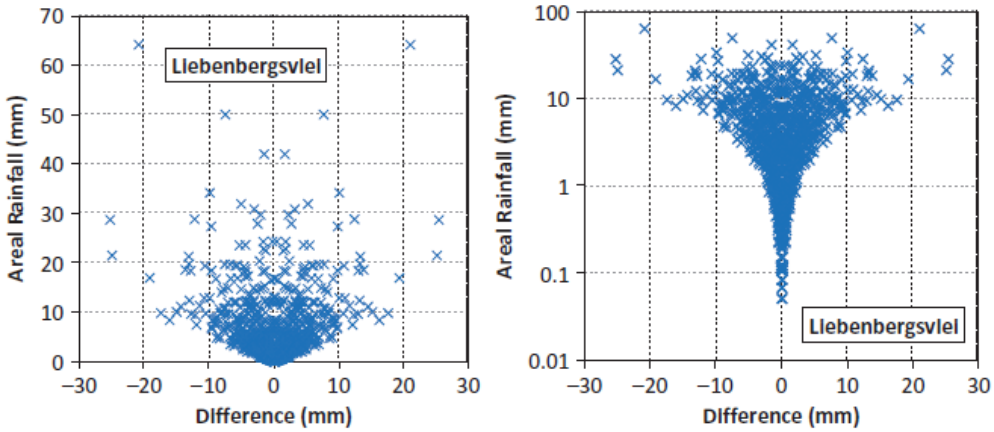

Figure 2.6: Variation of areal rainfall differences with areal rainfall depth

The final perturbed rainfall is the sum of the areal rainfall obtained from the highest available rain gauge density H_t and the scaled areal rainfall differences from the lower rain gauge density by an uncertainty factor *u*. This is illustrated in Figure 2.7. The value of the uncertainty factor *u*, is informed by the computed scaling factor. In the Liebenbergsvlei catchment for example the value of the scaling factor ranged between 0.57 and 0.72 for the considered rain gauge densities. Therefore any uncertainty factor within this range is considered to be realistic.

The perturbation of the catchment average rainfall H_t is different from the approach by Willems (2001). Willems (2001) represented the sources of rainfall input errors (point measurement errors and spatially averaged error) by stochastic terms added to a deterministic model. Willems (2001) assumed that the estimation error on the catchment average rainfall can be neglected and the quantification of the areal rainfall uncertainties of the two less dense networks was based on comparison with the densest network. However, this approach ignores the uncertainty in the catchment average rainfall.

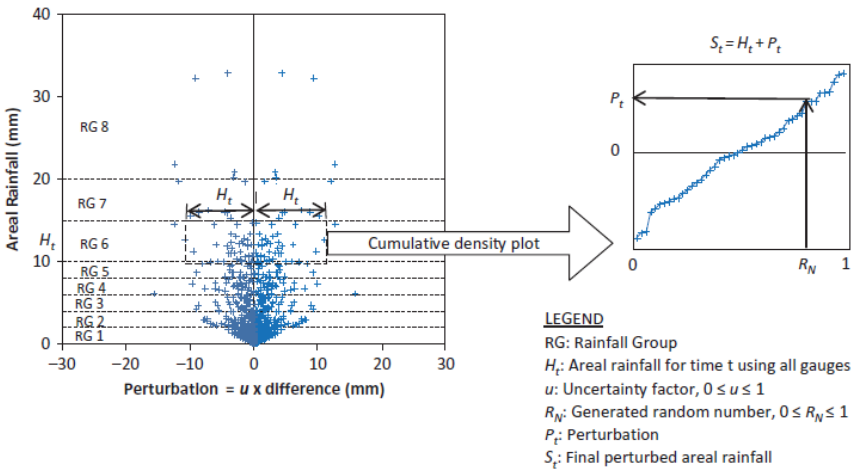

Figure 2.7: Computation of perturbations for non - zero rainfalls (from Ndiritu, 2013a)

The scaled areal rainfall differences (u x P_t^i) are then used to develop another cumulative density plot from which the applicable perturbation (P_t), which corresponds to the random number R_N, is determined (see Figure 2.4). The perturbation is then added to the catchment average rainfall H_t for that day ($H_t + P_t$) to obtain the final perturbed areal rainfall. This process can be used to generate as many sequences of perturbed areal rainfalls as required.

2.3.2 INFILLING OF MISSED OUT RAINFALLS

The proposed method for filling in missed out (or zero) rainfalls requires an expression that characterises the variation in the proportion of missed out rainfalls with rain gauge density (Ndiritu, 2013a). Ndiritu (2013a) tested and found that the relationship between the average proportion of zero rainfalls (or missed rainfalls) and an index of the rain gauge density n (where $n = log_2$(number of rain gauges) is linear. Figure 2.8 shows the average proportion of zero rainfalls obtained at various rain gauge densities for the Berg and Liebenbergsvlei catchments. Based on the linear relationship, doubling the rain gauge density reduces the number of zero rainfalls by half.

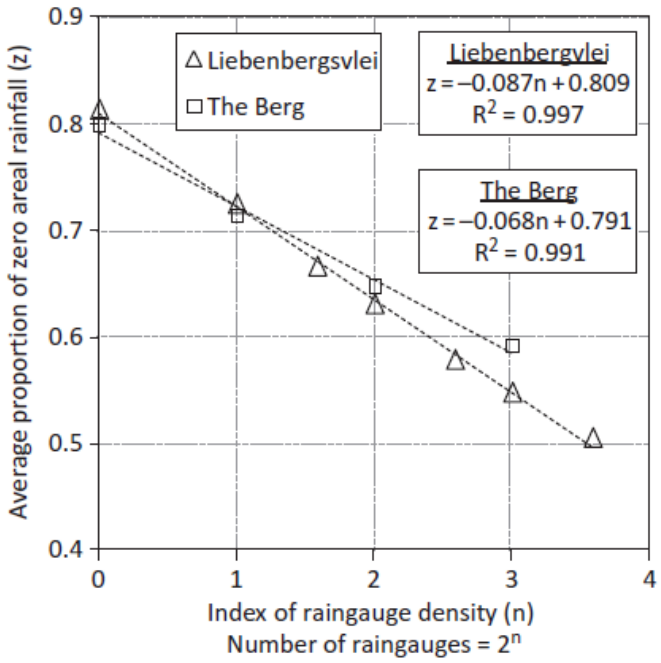

Figure 2.8: Variation in the proportion of zero rainfalls

The method also requires knowledge of the number of times the available rain gauge density needs to be doubled to obtain a rain gauge density of full capacity. Ndiritu (2013a) defined a full capacity rain gauge density as one with a sufficient number of rainfall stations to give a reliable estimate of the areal distribution of rainfall over a catchment. The method therefore can be derived as follows:

If z_i is the percentage of areal rainfall records recorded as zero at density d_i, then the proportion by which the missed out rainfalls reduce when doubling the rain gauge density can be computed as z_2/z_1, where d_2 is the existing rain gauge density and d_1 is the density at half the actual rain gauge density.

If the number of times the rain gauge density needs to be doubled to obtain a rain gauge density of full capacity is represented by n_{max}. Then, the proportion of zero rainfalls at a full capacity rain gauge density can be obtained as:

$$z_{nmax} = z_2 \left(\frac{z_2}{z_1}\right)^{nmax-2} \qquad (2.3)$$

The proportion of non – zero rainfalls that have been missed out at the existing rain gauge density (z_f) can therefore be obtained as the difference between z_2 and z_{nmax}.

$$z_f = z_2 - z_{nmax} = z_2 \left(1 - \left(\frac{z_2}{z_1}\right)^{nmax-2}\right) \qquad (2.4)$$

If the expected proportion of zero rainfalls is to be achieved, the proportion z_f of the rainfalls calculated as zero at the current rain gauge density needs to be replaced with non – zero rainfalls. The non – zero rainfalls are filled in based on a cumulative probability plot obtained from rainfalls computed as non – zero at the current density (d_2) but as zero at half the current density (d_1). The rainfall replacing the non – zero rainfall was then obtained by generating a random number from a cumulative distribution function and finding the rainfall value corresponding to this number. The rainfall value was then perturbed as before. Figure 2.9 illustrates this procedure.

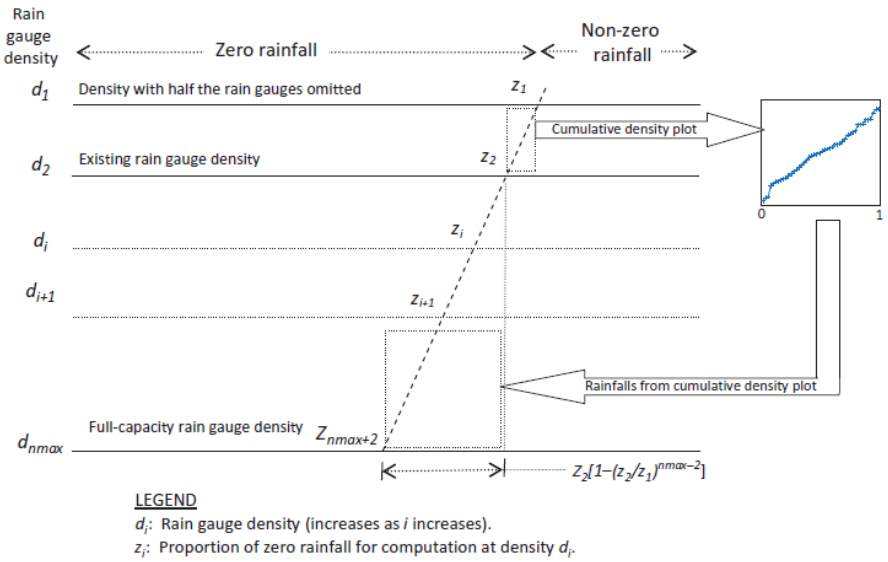

Figure 2.9: Determination of the proportion and magnitude of missed out rainfall (from Ndiritu, 2013a)

2.3.3 THE STOCHASTIC GENERATOR MODEL RESULTS

Ndiritu (2013a) tested the data – based model on two catchments: the Liebenbergsvlei and the Berg catchments. 100 sequences of daily areal rainfalls and the statistics of the generated sequences were compared against the statistics of the historical rainfall data. The uncertainty factor was set to equal the scaling factor and the limiting value of 1, to test the impact of the scaling factor on the generated stochastic sequences. The component of the generator that fills in the missed rainfalls was also activated and the parameter n_{max} (representing the doubling required for a full capacity rain gauge density) was set at 5.

Box plots of the mean, standard deviation and skewness of the generated stochastic rainfalls were unbiased when the procedure for filling in missed rainfalls was not activated. However, when the infilling component was activated, the mean rainfall increased by 5.5% and 10.3% for the Liebenbergsvlei and Berg catchments

respectively. Applying the limiting uncertainty of 1.0 was found to increase both the average value and the variability of the standard deviation and skewness value. An uncertainty factor of 1 was also significantly altered the mean rainfall of the Berg catchment.

Box plots representative of individual rainfalls revealed a large variability of generated stochastic rainfalls across the range of rainfall magnitudes, although the means remained unbiased.

3. DATA AND STUDY AREA

3.1 RAINFALL DATA USED IN THIS STUDY

The nature of this study dictates that comprehensive, good quality precipitation data be utilised. Consequently, the rainfall data for this research was sourced from the Water Resources of South Africa 2005 study, obtained from the Department of Water Affairs (DWA) Water Resources Information Management System (WRIMS) database. The two main data sources for this database is the DWA database (or HYDRSTA) and the WRC Project 1156 by Lynch (2004). The data consists of observed (unpatched) data and patched data (Sejamoholo and Lillie, 2004).

The WRC dataset was sourced from various stakeholders including the South African Weather Service (SAWS), the Agricultural Research Council (ARC), the South African Sugar Association (SASA), the Institute of Commercial Forestry Research (ICFR), municipalities, mines and other private individuals (PVT). The data was used to process the monthly and annual rainfall statistics over the Southern African region. Table 3.1 shows the number of rainfall stations used in WRC Project from the different organisations. The database consists of observed and patched daily rainfall values from 12 598 rainfall stations across South Africa collected up to November 2002, from which monthly rainfalls were generated. However, not all of these stations were operational up to November 2002.

Table 3.1: WRC Project rainfall stations

Organisation	No. of rainfall stations
SAWS	8 281
ARC	2 661
SASA	161
ICFR	445
PVT	1 050
Total	**12 598**

SAWS is the single largest dataset in the country and recent reports on the SAWS rainfall observation infrastructure suggest that the number of operational rainfall stations is approximately 1613. A breakdown of the type of rainfall stations is given in Table 3.2 and their localities are shown in Figure 3.1. Evidently, the density of the rainfall stations increases near the big cities and towns.

Table 3.2: SAWS operating rainfall observation stations

Surface Observations	No. of rainfall stations
Automatic Weather stations - unmanned	156
Automatic weather stations - manned	35
Automatic rainfall stations	165
Standard rainfall stations	1 257
Total	**1 613**

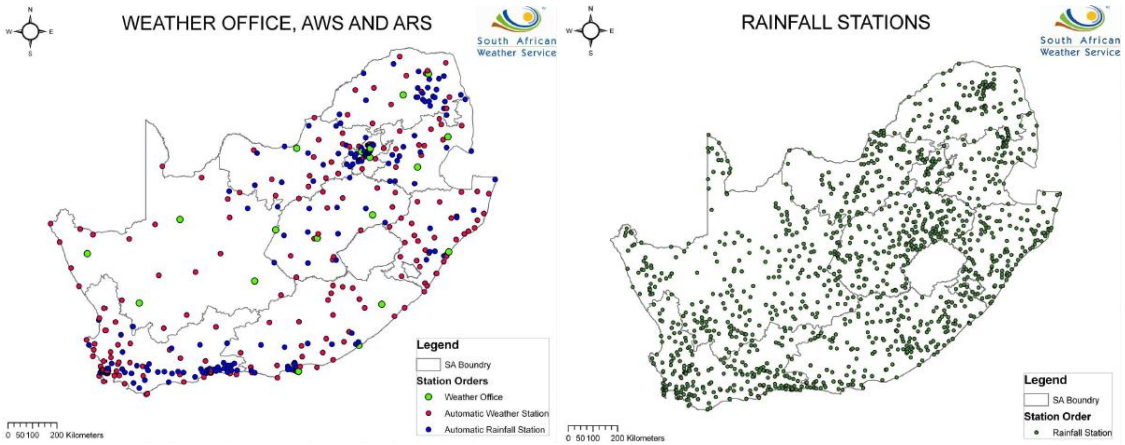

Figure 3.1: SAWS operating rainfall observation stations (from SAWS (2013))

The DWA database comprises the SAWS dataset as well as rainfall records at the DWA sites (i.e. dam sites) (Sejamoholo and Lillie, 2004). This database only contains observed data. The rainfall stations in this database can be obtained from the following website: http://www.dwaf.gov.za/hydrology/HyCatalogue.aspx. The dataset consists of 484 rainfall stations located as shown in Figure 3.2. The earliest rain gauge reading in this dataset was taken in 1904 and only 176 (36%) of these stations have data up to year 2014. The operating rainfall stations are indicated by the red dots in Figure 3.2.

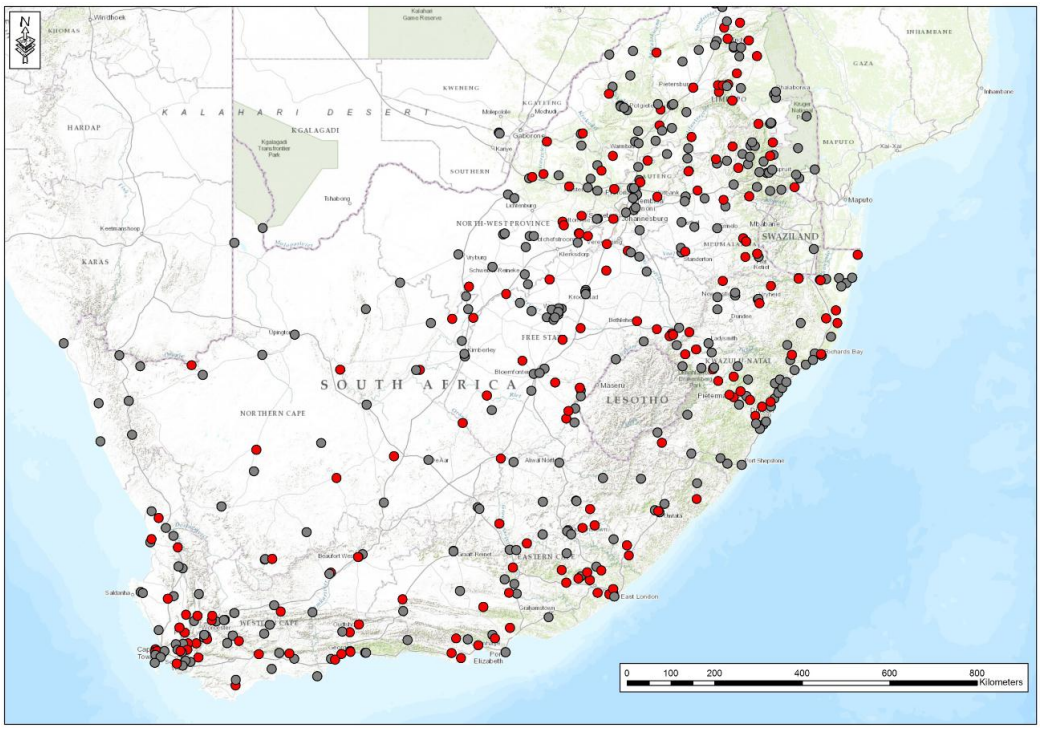

Figure :3.2 DWA observational stations

There is extensive overlap in the data available from these two sources, particularly in the data managed by SAWS. Nevertheless, the decline in the number of operational rainfall stations is evident.

The WRIMS data records are subject to some errors owing to rainfall not being measured on a particular day or gauges being dysfunctional (Sejamoholo and Lillie, 2004). Consequently, the data was provided with quality codes to give an indication of the accuracy of the recorded value. To maximise the validity of the results of this study, only accurately observed records were used. The measured rainfall depths were available in 0.1mm units.

3.2 STUDY AREA DESCRIPTION

Eight catchments were selected across South Africa as shown on Figure 3.3. The catchments consist of multiple quaternary sub - catchments formalised during the Surface Water Resources of South Africa Study 1990 by Midgley *et al* (1994). Each quaternary sub – catchment represents areas of similar runoff response (Midgley *et al*, 1994). Midgley *et al* (1994) also delineated rainfall zones to compliment the quaternary sub – catchments. These zones indicate areas of similar rainfall characteristics.

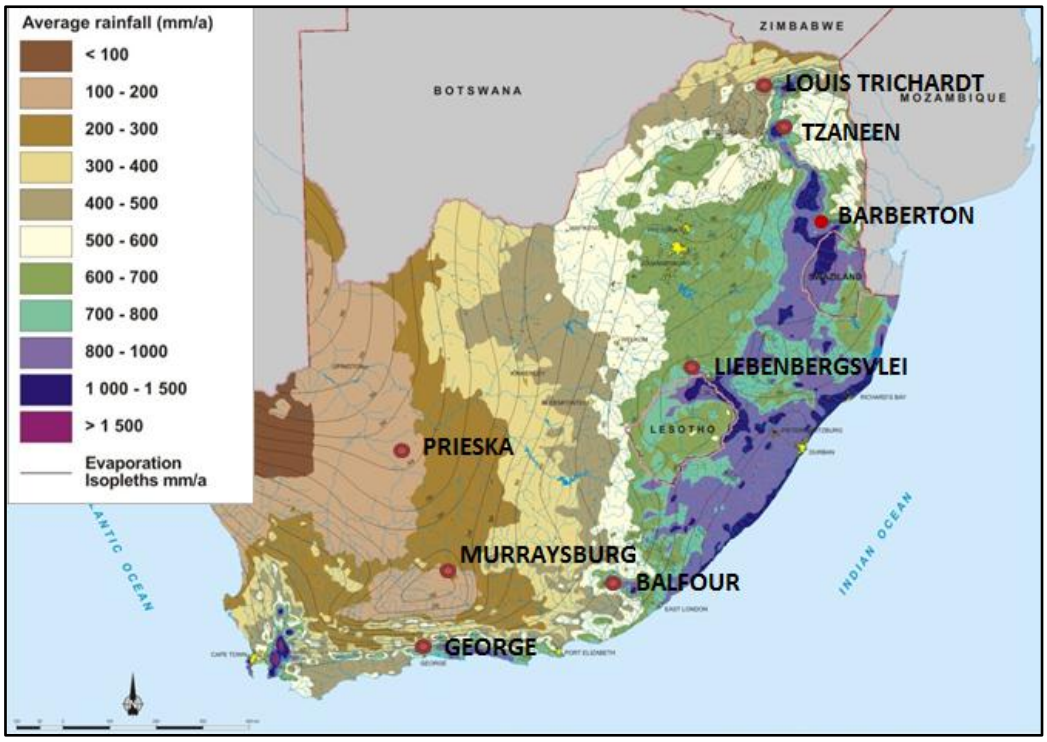

Figure 3.3: South African catchments used in this study (from DWA (2013))

Eight rainfall stations were selected in each catchment to provide 4 doubling up rain gauge densities (1, 2, 4 and 8) for the analysis. An illustration of these doubling up densities is shown on Figure 3.5 for the Balfour catchment. These stations were selected with the aim of obtaining reliably long overlapping record of observed data and spread across the catchment to provide a uniform catchment coverage. In some cases, this resulted in the selection of rainfall stations located beyond the catchment boundary. This however was not a concern as the rainfall stations in each catchment are within the same rainfall zone and the IDW method accounts for them. A description of the catchments now follows.

BALFOUR

Balfour is located within the Nkonkobe Local Municipality in the Eastern Cape of South Africa. The area is located within the Fish to Tsitsikamma Water Management Area (WMA) and has a catchment area of approximately 981km^2. The climate varies from arid and semi – arid moderate midlands to arid and semi – arid cold high lying land. The northern mountain ranges record the highest rainfall and the southern areas record the least. Figure 3.4 shows the location of the selected rain gauges across the catchment.

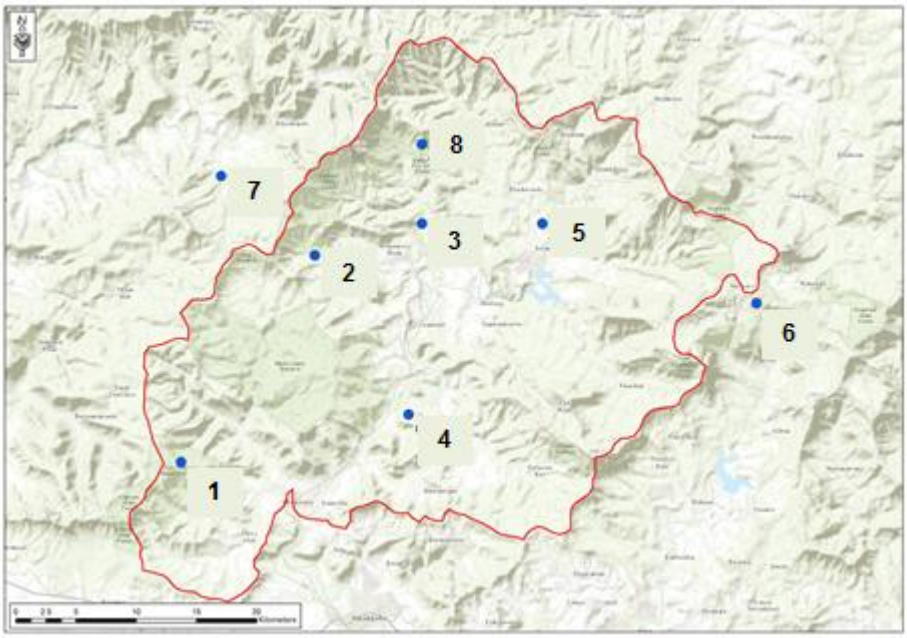

Figure 3.4: Location of rain gauges in the Balfour Catchment

The topography of the northern region is characterised by the mountain range of the Winterberg and flattens out towards the south. Large parts of the area are rural and people either have no access to water or have to walk very long distances to access it.

Table 3.3 shows the rainfall characteristics of the area, the statistics of the rain gauge data is given in Appendix A. The largest proportion of rain falls between August and May while the lowest rainfall period is between June and July. March receives the highest rainfall. The largest elevation difference across the catchment is approximately 697m.

Table 3.3: Balfour rainfall data

Map ID number	Gauge Number	Location	MAP (mm)	Period (years)	Approximate Elevation (mamsl)
1	077 881	32 41S 26 30E	982	1920 - 1950	1101
2	078 153	32 33S 26 36E	846	1920 - 1950	873
3	078 272	32 32S 26 40E	564	1920 - 1950	699
4	078 279	32 39S 26 40E	507	1920 - 1950	690
5	078 453	32 33S 26 46E	547	1920 - 1950	788
6	078 755	32 35S 26 56E	1208	1920 - 1950	1387
7	100 060	32 30S 26 32E	553	1920 - 1950	1099
8	100 329	32 29S 26 41E	995	1920 - 1950	1026

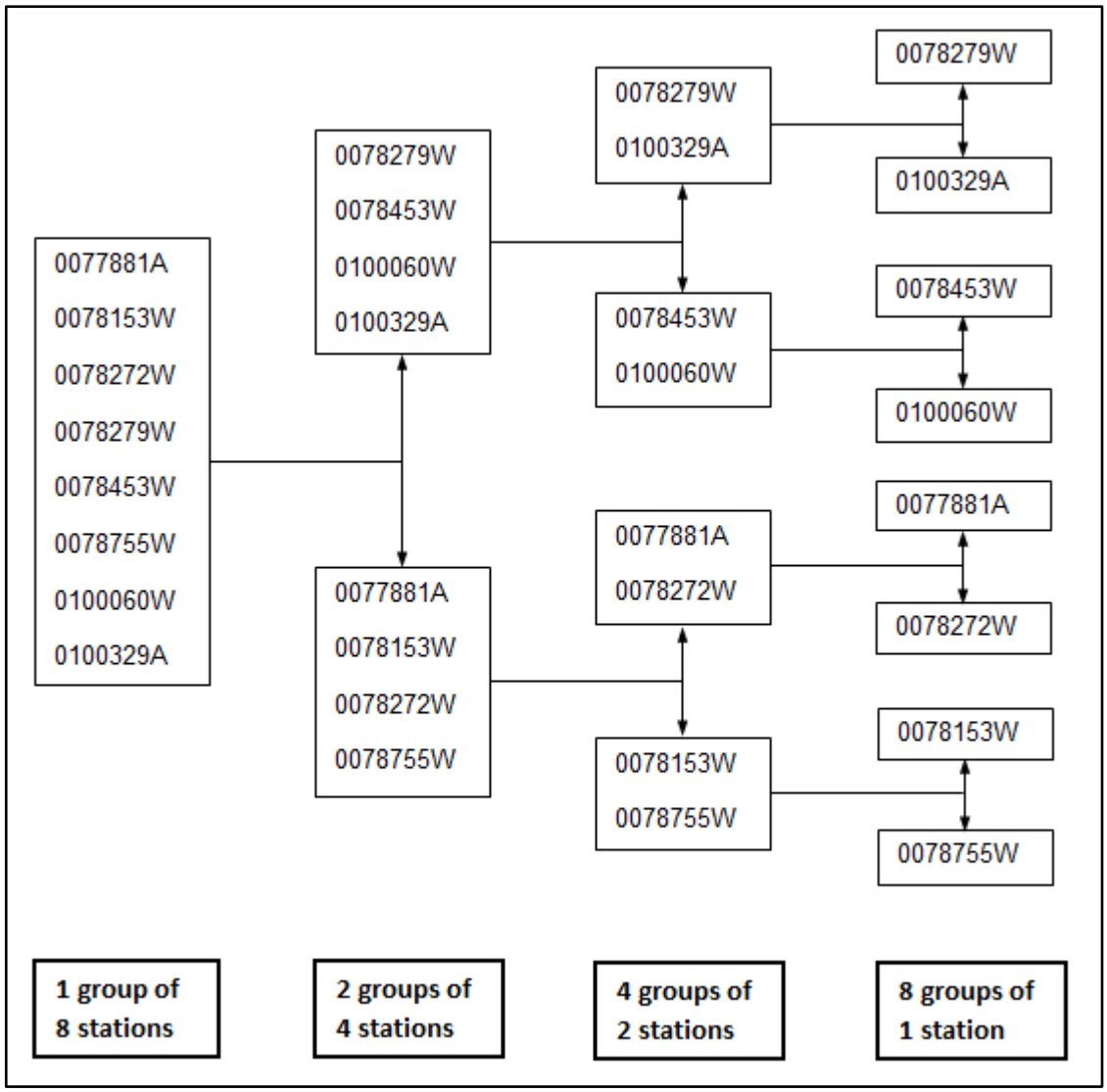

Figure 3.5: Balfour rain gauge station groups

BARBERTON

Barberton forms part of the Umjindi Local Municipality in the Mpumalanga Province of South Africa. The area is located within the Inkomati WMA and has a catchment area of approximately 490km^2. Figure 3.6 shows the location of the selected rain gauges across the catchment.

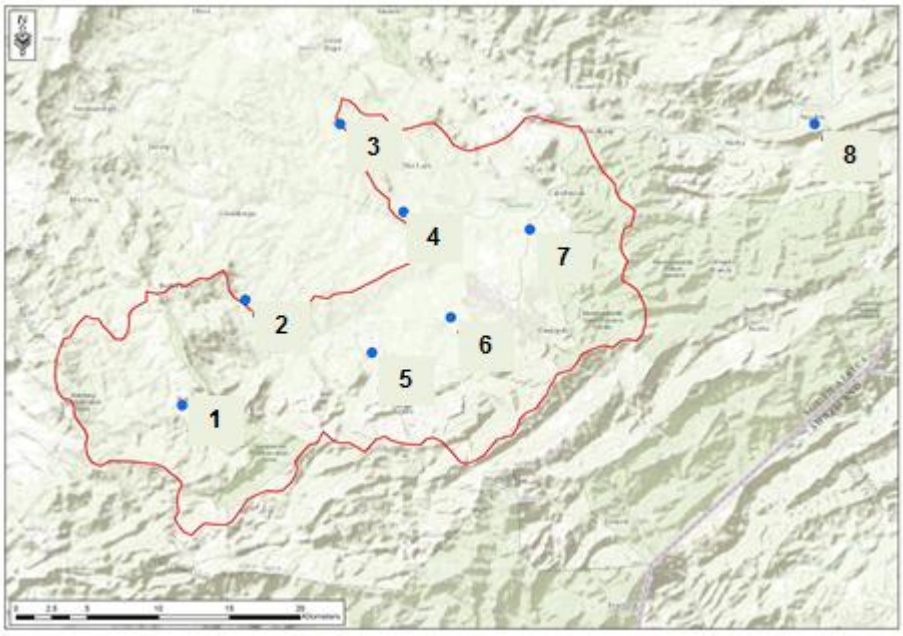

Figure 3.6: Location of rain gauges in the Barberton Catchment

Warm summers and moderate winters characterise the climate in this region. The area is mainly covered by the Lowveld Sour Bushveld and the North – Eastern Mountain sour veld. The area is predominantly semi-rural and water provision remains a priority and a constraint to development.

Table 3.4 provides details of the rainfall stations in the catchment. The detailed rain gauge statistics are available in Appendix A. The maximum elevation difference across the catchment is approximately 757m and the rainfall in the region is highly variable from month to month.

Table 3.4: Barberton Rainfall Data

Map ID number	Gauge Number	Location	MAP (mm)	Period (years)	Approximate Elevation (mamsl)
1	518 589	25 49S 30 50E	1118	1950 - 1971	1442
2	518 676	25 46S 30 53E	1074	1950 - 1971	913
3	518 759	25 39S 30 56E	850	1950 - 1971	902
4	518 822	25 42S 30 58E	819	1950 - 1971	722
5	518 859	25 59S 30 59E	804	1950 - 1971	1024
6	518 886	25 46S 30 60E	764	1950 - 1971	685
7	519 134	25 44S 31 05E	691	1950 - 1971	745
8	519 310	23 38S 31 10E	742	1950 - 1971	836

GEORGE

George is located within the winter rainfall region of South Africa, almost halfway between Cape Town and Port Elizabeth. The town generally experiences an oceanic climate. The catchment is located within the Gouritz WMA and is approximately

813km^2. Figure 3.7 shows the location of the selected rain gauges across the catchment.

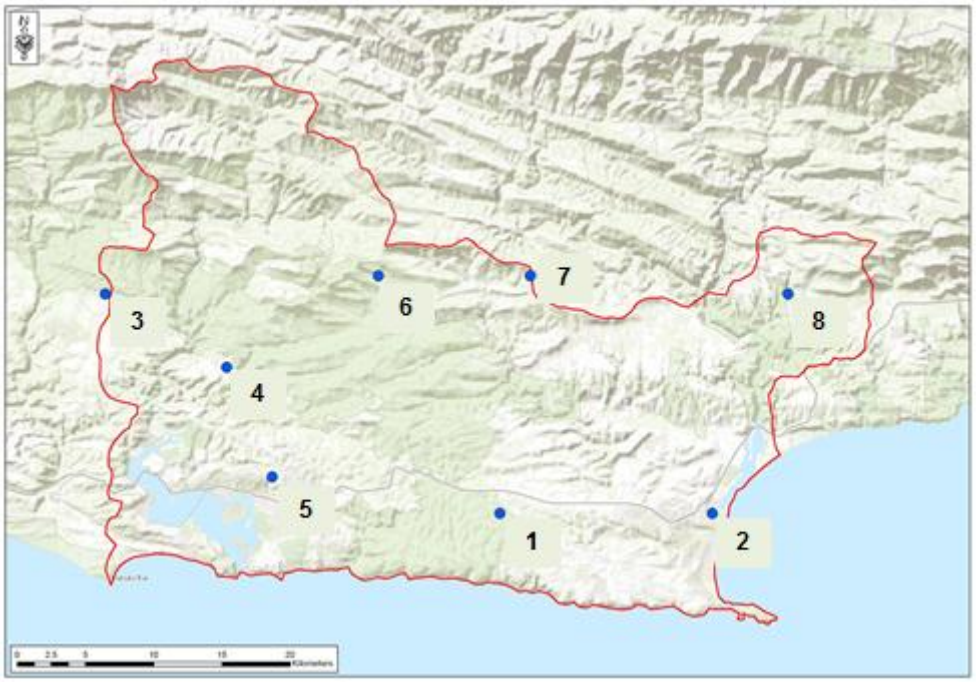

Figure 3.7: Location of rain gauges in the George Catchment

Rainfall in George is generally consistent and has a low variance from month to month. The highest rainfall volume is measured in August and the largest elevation difference across the catchment is approximately 479m. Table 3.5 gives details of the rainfall stations in this catchment. Detailed statistics of the rain gauges are given in Appendix A.

Table 3.5: George Rainfall Data

Map ID number	Gauge Number	Location	MAP (mm)	Period (years)	Approximate Elevation (mamsl)
1	014 393	34 02S 23 13E	986	1948 - 1983	254
2	014 633	34 03E 23 22S	693	1948 - 1983	60
3	029 805	33 55E 23 58S	861	1948 - 1983	239
4	030 088	33 58E 23 03S	948	1948 - 1983	381
5	030 090	34 01E 23 04S	865	1948 - 1983	191
6	030 265	33 55E 23 09S	1130	1948 - 1983	539
7	030 446	33 55E 23 15S	874	1948 - 1983	385
8	030 775	33 55E 23 25S	863	1948 - 1983	245

LIEBENBERGSVLEI

Liebenbergsvlei is located within the Dihlabeng Local Municipality, in the southern eastern part of the Free State Province, South Africa. Large parts of the area have slopes exceeding 7%. This aspect affects solar heating, air temperature and moisture

over the region. Rainfall is strongly seasonal and mostly occurs in the form of thunderstorms during the summer period. The area forms part of the Upper Vaal river catchment where water is mainly used for irrigation and rural purposes. Figure 3.8 shows the location of the selected rain gauges across the catchment. The catchment area is approximately 997km^2.

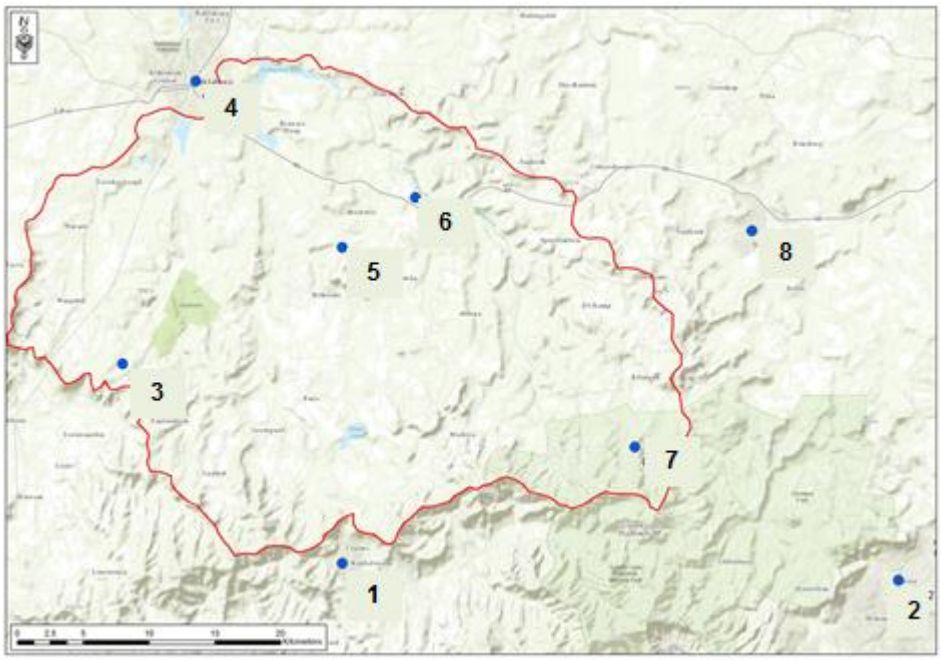

Figure 3.8: Location of rain gauges in the Liebenbergsvlei Catchment

Rainfall in the region mainly occurs between August and May. The highest rainfall is usually measured in January and the largest elevation difference across the catchment is approximately 753m. Table 3.6 gives details of the rainfall stations selected in this catchment. Detailed statistics of the gauges are provided in Appendix A.

Table 3.6: Liebenbergsvlei rainfall

Map ID number	Gauge Number	Location	MAP (mm)	Period (years)	Approximate Elevation (mamsl)
1	297 721	28 31S 28 25E	725	1940 - 1965	1126
2	298 512	28 31S 28 48E	790	1940 - 1965	1677
3	331 474	28 24S 28 16E	687	1940 - 1965	1879
4	331 554	28 14S 28 19E	667	1940 - 1965	1635
5	331 740	28 20S 28 25E	726	1940 - 1965	1725
6	331 828	28 18S 28 28E	700	1940 - 1965	1675
7	332 206	28 26S 28 37E	770	1940 - 1965	1850
8	332 349	28 19S 28 42E	706	1940 - 1965	1128

LOUIS TRICHARDT

The Louis Trichardt catchment is located at the foot of the Soutpansberg mountain range in the Limpopo Province, South Africa. The catchment is approximately 507km^2 and is located within the Luvuvhu and Letaba WMA, and drains towards the Luvuvhu River. Figure 3.9 shows the location of the selected rain gauges across the catchment. As can be seen, a number of the gauges lie outside of the catchment boundary, which according to the IDW method reduces the influence of these gauges in the calculation of the average catchment rainfall. The earliest rain gauge reading was recorded in 1915.

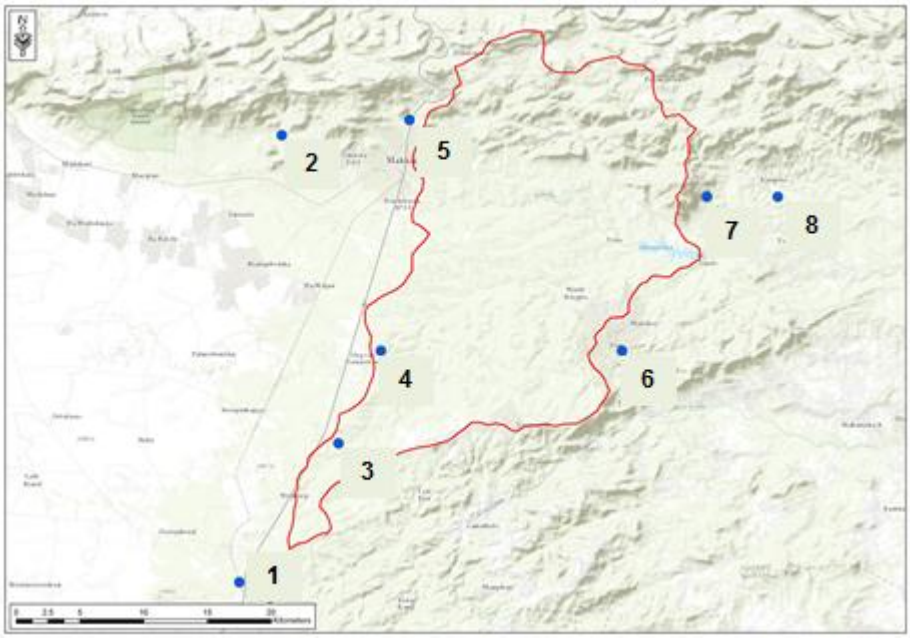

Figure 3.9: Location of rain gauges in the Louis Trichardt Catchment

Louis Trichardt is located in the lowveld of Limpopo and is characterised by a sub humid climate. The winters are usually dry and frost free and 90% of the rainfall falls within the summer months between October and March. Evaporation remains higher than rainfall, affecting surface runoff and the volume of storage dams.

The annual precipitation varies from 400mm at its most eastern point to 1000mm at its most western point. Table 3.7 gives details of the rain gauges used in this catchment. Detailed statistics of the gauges are available in Appendix A. The maximum elevation difference across the catchment is approximately 347m.

Table 3.7: Louis Trichardt rainfall data

Map ID number	Gauge Number	Location	MAP (mm)	Period (years)	Approximate Elevation (mamsl)
1	722 529	29 49E 23 19S	441	1962 - 1982	1099
2	722 571	29 50E 23 01S	650	1962 - 1982	1101
3	722 614	29 51E 23 14S	495	1962 - 1982	1038
4	722 700	29 54E 23 10S	476	1962 - 1982	963
5	722 721	29 55E 23 01S	690	1962 - 1982	1069
6	723 070	30 03E 23 01S	710	1962 - 1982	877
7	723 155	30 06E 23 05S	713	1962 - 1982	820
8	723 334	30 12E 23 04S	957	1962 - 1982	754

MURRAYSBURG

The Murraysburg catchment is located within the Central Karoo District of the Western Cape, South Africa. The Karoo is categorized as a semi – arid region with significantly low rainfall patterns on a limited number of rainy days, high temperatures and significantly high evaporation rates. This region is regarded as having a very fragile ecosystem, which needs to be managed if economic growth and development is to occur (Central Karoo IDP, 2010). Figure 3.10 shows the location of the rain gauges across the catchment used for the analysis. The southern side of the catchment has a flat topography and is divided by a 450m high escarpment running in a northerly direction.

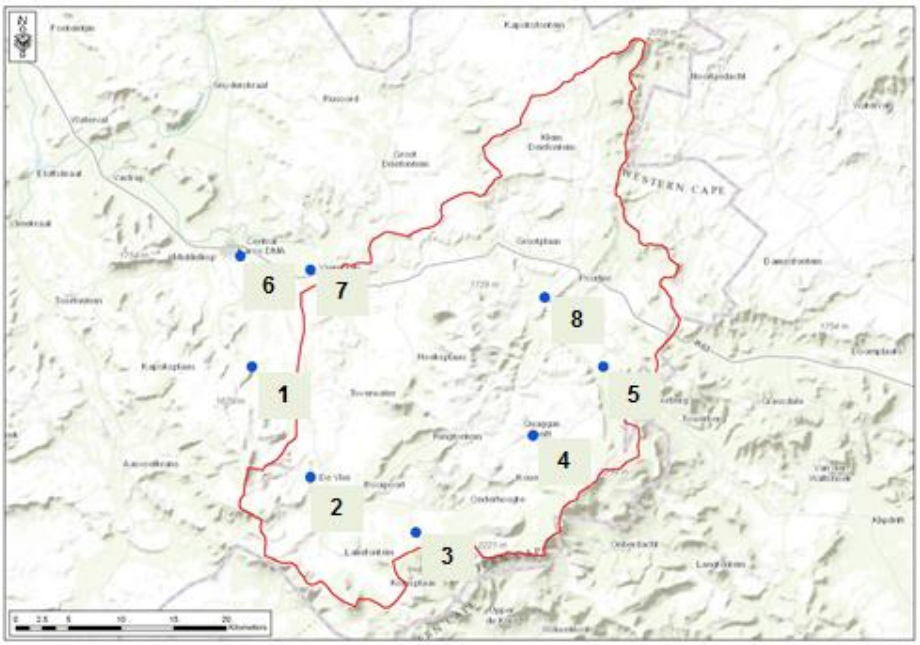

Figure 3.10: Location of rain gauges in the Murraysburg Catchment

Murraysburg is located within the Fish to Tsitsikamama WMA. The catchment area is approximately 865km^2 and drains in a west – easterly direction towards the Buffels

River. The earliest gauge reading was recorded in 1878. Murraysburg receives most of its rain between October and May. The highest rainfall is typically measured in March and the maximum elevation difference is approximately 401m. Table 3.8 gives details of the rainfall stations in this catchment. Detailed statistics of the stations are provided in Appendix A.

Table 3.8: Murraysburg Rainfall Data

Map ID number	Gauge Number	Location	MAP (mm)	Period (years)	Approximate Elevation (mamsl)
1	094 513A	32 03S 23 48E	318	1952 - 1975	1317
2	094 578	32 08S 23 50E	342	1952 - 1975	1418
3	094 730	32 10S 23 55E	422	1952 - 1975	1481
4	095 006	32 06S 24 01E	405	1952 - 1975	1588
5	095 123	32 03S 24 05E	440	1952 - 1975	1527
6	117 447	31 57S 23 45E	284	1952 - 1975	1187
7	117 749	31 59S 24 01E	293	1952 - 1975	1278
8	118 029	31 59S 24 01E	380	1952 - 1975	1405

PRIESKA

Prieska forms part of the Siyathema Local Muncipality in the Northern Cape Province, South Africa. It is located on the southern bank of the Orange (or Gariep) River, South Africa's largest river. The catchment is approximately 2200km^2 and is located within the Lower Orange WMA. Figure 3.11 shows the location of the selected rain gauges across the catchment.

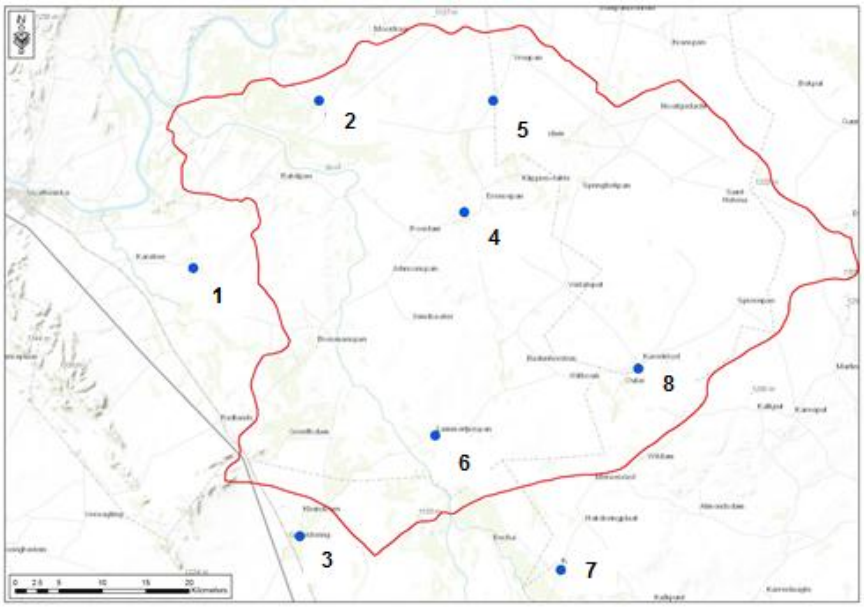

Figure 3.11: Location of rain gauges in the Prieska Catchment

Prieska has a flat terrain and is located in the arid, sparsely populated Karoo region of South Africa. The region receives very little rainfall particularly between May and

August. The highest rainfall month is usually March and the maximum elevation difference across the catchment is approximately 86m. Table 3.9 gives details of the rainfall stations in this catchment. The statistics of these stations are given in Appendix A.

Table 3.9: Prieska Rainfall Data

Map ID number	Gauge Number	Location	MAP (mm)	Period (years)	Approximate Elevation (mamsl)
1	224 734	29 44S 22 55E	215	1936 - 1969	996
2	225 065	29 34S 23 03E	224	1936 - 1969	997
3	225 118	29 58S 23 01E	212	1936 - 1969	999
4	225 311	29 40S 23 12E	215	1936 - 1969	1023
5	225 395	29 34S 23 13E	247	1936 - 1969	1060
6	225 413	29 52S 23 13E	199	1936 - 1969	1003
7	225 540	28 00S 23 18E	210	1936 - 1969	1032
8	225 679	29 49S 23 22E	238	1936 - 1969	1082

TZANEEN

Tzaneen is situated in the eastern quadrant of the Limpopo Province, South Africa, within the Mopani District Municipality. The area is approximately 650km^2 and is located within the Luvhuvhu Letaba WMA where water provision is one of the most pressing needs. Figure 3.12 shows the location of the selected rain gauges across the catchment (Mopani IDP, 2011). The catchment area is approximately 650km^2 and is characterised by uneven topography.

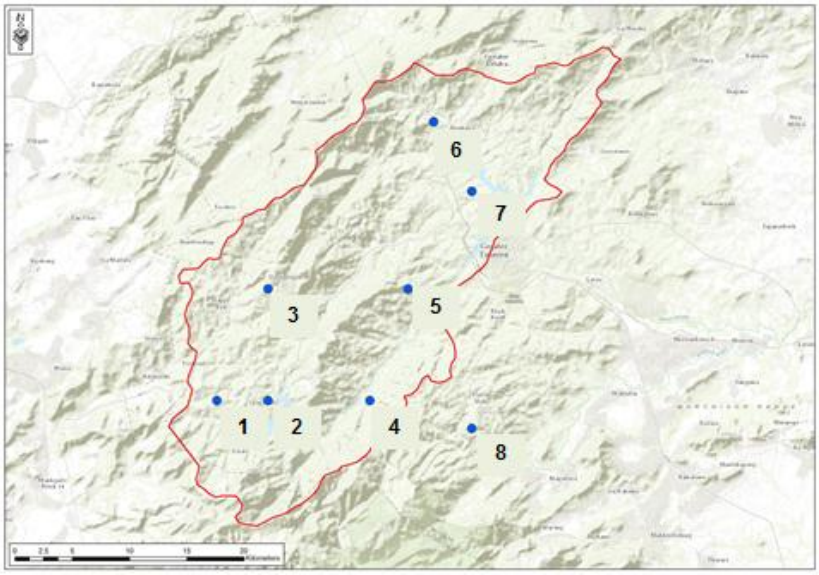

Figure 3.12: Locations of rain gauges in the Tzaneen Catchment

Tzaneen has the highest monthly rainfall variability and the largest elevation difference (802m) out of the catchments considered in this study. The lowest rainfall is measured

between May and August whilst the wettest month is usually measured in January. Table 3.10 gives details of the rain gauges used in this catchment. The statistics of the rain gauges are available in Appendix A.

Table 3.10: Tzaneen rainfall data

Map ID number	Gauge Number	Location	MAP (mm)	Period (years)	Approximate Elevation (mamsl)
1	678 776	23 56S 29 56E	840	1958 - 2002	1455
2	678 836	23 56S 29 58E	1074	1958 - 2002	1420
3	678 858	23 48S 29 59E	2051	1958 - 2002	1602
4	679 086	23 56S 30 03E	1074	1958 - 2002	897
5	679 141	23 51S 30 05E	1430	1958 - 2002	1031
6	679 164	23 44S 30 06E	1196	1958 - 2002	920
7	679 197	23 47S 30 07E	1123	1958 - 2002	800
8	679 267	23 57S 30 09E	1441	1958 - 2002	998

4. METHODOLOGY

To fulfil the objectives set out in Chapter 2, the original model code of the data – based stochastic generator was adapted to a monthly time step by Ndiritu (2013a). The adapted model code requires the rainfall data and the positions of the stations across the catchments to compute the areal rainfall using the IDW method, the rain gauge groups to calculate the perturbations at various rain gauge densities and an estimate of the uncertainty factor to constrain the computed perturbations. It then outputs the following files for the selected rain gauge groups in a textfile format:

- The historical (or observed) perturbations;
- The historical areal rainfalls;
- Data for the cumulative probability plot;
- The stochastic perturbations for the stated number of sequences and
- The stochastic areal rainfalls for the corresponding number of sequences.

The rain gauge groups were therefore selected to initiate the study. These groups were selected with the aim of achieving a uniform catchment coverage, as was done by Ndiritu (2013a). However, after a number of iterations, it became evident that this framework for selecting the rain gauges in each rain gauge group, leads to multiple reasonable rain gauge combinations.

A study by Morrisey *et al* (1995) demonstrates that the error in the estimation of areal rainfall is fundamentally based on the rain gauge sampling scheme used for the computation of the catchment average rainfall. Morrisey *et al* (1995) results show that the rain gauge sampling (or grouping) scheme must consider the existing network geometry and the relationship of the rain gauge group and the averaging area. Consequently, methods for guiding the optimal selection of rainfall stations for areal rainfall estimation were investigated.

The best estimate of areal rainfall was considered to be an important consideration during the grouping of the rainfall stations. Therefore, the problem consists of determining which rainfall stations are the best estimators of areal rainfall over a catchment (or the key stations) and developing a means of grouping these stations in a manner that maintains the best areal rainfall estimate for each rain gauge group and ensures that a uniform catchment wide coverage is maintained (Cheng *et al*, 2012). Studies by Hutchinson (1969) suggest that the correlation between two gauges (or between a single gauge and a number of gauges) is dependent on the areas surrounding the gauges and is an important consideration when estimating the catchment rainfall. Consequently, a correlation-based method of selecting the rain gauges was also assessed and compared against the prescribed method of selecting the stations by Ndiritu (2013a). This would also be used to examine whether the

grouping of rainfall stations impacts affects the generated stochastic areal rainfall sequences.

4.1 A CORRELATION BASED METHOD OF SELECTING THE RAINFALL STATIONS IN EACH RAIN GAUGE GROUP

It was assumed that the 'key stations' can be determined by computing the correlation coefficient between the station and the catchment average rainfall (obtained using all 8 stations). Consequently, the station having the highest correlation with the catchment average rainfall is regarded as the key station. The next key station is the station with the next highest correlation and so on. This process was used to determine four key stations for each catchment, to ensure that there is at least one key station in each rain gauge group with more than one station.

The key stations were then paired with the non – key stations to give an equally satisfactory estimate of areal rainfall. To achieve this, the areal rainfall was computed from the station pairs using the IDW method, and the correlation coefficient was computed between the estimated areal rainfall obtained from the station pairs and the catchment average rainfall. The correlation between the areal rainfall from the station pairs and the average catchment rainfall was then compared, and the key and non - key station combinations with the highest correlations were grouped. If it was found that more than one key station correlates best with the same non – key station, the key station with the highest correlation with the remaining ungrouped non – key station was grouped first.

Once all rainfall stations had been paired, the 4 station pairs were then grouped with other station pairs with the aim of achieving a uniform catchment coverage. In the event that there are 4 or less rain gauges available on a catchment, the rain gauge catchment coverage would have to be considered during the pairing of the stations. An example of this process is demonstrated below for the Balfour catchment:

Step 1: Using the IDW method, determine the catchment average rainfall using all the stations. This is considered the best areal rainfall estimate available. (see results in Appendix C)

Step 2: Determine the correlation coefficient between the estimated catchment average rainfall and the measured rainfall volumes at each rainfall station using Equation 4.1:

$$c = \frac{\sum(x-\bar{x})(y-\bar{y})}{\sqrt{\sum(x-\bar{x})^2(y-\bar{y})^2}} \qquad (4.1)$$

Where $\bar{x}$ and $\bar{y}$ are the sample mean averages of the catchment average rainfall and the measured point rainfall respectively. x and y are the magnitudes of the catchment average rainfall and the measured point rainfall for each month.

The correlation coefficients are based on differences between the estimated catchment average rainfall and the measured rainfall volumes at each rainfall station for each corresponding month. The correlation coefficients between the measured point rainfall and the estimated catchment rainfall are given in Table 4.1.

Table 4.1: Rain Gauge Correlations for Balfour

Map ID number	Gauge Number	Correlation with catchment areal rainfall
1	077 881	0.950
2	078 153	0.970
3	078 272	0.861
4	078 279	0.916
5	078 453	0.905
6	078 755	0.915
7	100 060	0.836
8	100 329	0.949

Step 3: Identify the rainfall stations with the highest correlation coefficients as the key stations. The number of key stations identified should be sufficient to ensure that there is at least one key station in each in each rain gauge group with more than one rainfall station.

Table 4.2: Identification of Key Stations

Map ID number	Gauge Number	Correlation with catchment areal rainfall	Identification
1	077 881	0.950	Key station
2	078 153	0.970	Key station
3	078 272	0.861	Non – key station
4	078 279	0.916	Key station
5	078 453	0.905	Non – key station
6	078 755	0.915	Non – key station
7	100 060	0.836	Non – key station
8	100 329	0.949	Key station

Step 4: Compute the catchment average rainfall using each of the key stations in combination with each of the non – key stations.

Step 5: Compute the correlation coefficient *c* between the paired stations (key and non- key station from step 4) and the estimated catchment average rainfall estimate obtained from using all the rainfall stations.

Table 4.3 shows that the correlation between any pair of these stations (1 key station and 1 non key station) and the catchment average rainfall is high (> 90%). This is an expected result.

Table 4.3: Key Station Pairing

Key station	Non Key station	c	Non Key station	c	Non Key station	c	Non Key station	c
1	3	0.977	5	0.980	6	0.975	7	0.963
2	3	0.969	5	0.973	6	0.975	7	0.975
4	3	0.943	5	0.939	6	0.961	7	0.923.
8	3	0.934	5	0.972	6	0.949	7	0.961

Step 6: Compare the computed correlation coefficient between the paired stations and the estimated catchment average rainfall. Table 4.3 shows that station 1 has the highest correlation when paired with station 5; station 2 has the highest correlation when paired with station 6 or 7; station 4 has the highest correlation when paired with station 6 and station 8 has the highest correlation when paired with station 5.

Station 3 remains unpaired. Therefore, one of the key stations between station 1 and 8 must be paired with station 3, to ensure that the key stations are evenly distributed between the groups. The station with the highest correlation with 3 between the two stations (1 and 8) is station 1.

Therefore the final grouping is station 1 and 3; station 2 and 7; station 4 and 6 and station 8 and 5.

Some of the pairings, such as 2 and 7 and 8 and 5 (see Table 4.2 and Figure 4.1), obtained from this correlation analysis are considered unrealistic on the basis of reasonable areal coverage. The clustering of stations is undesirable because it may lead to biased output results in favour of the rainfall characteristics of part of the catchment (Midgley *et al*, 1994). A more sensible rain gauge pairing would be 4 and 8 and 5 and 7 which correspond to combination 1 used for this catchment (see Appendix B).

Step 7: Combine the station pairs into groups of 4 (or any other higher densities) with the aim of ensuring uniform catchment coverage. These groups need to be checked for catchment coverage graphically on the catchment map.

For example, if the stations are grouped into the following two groups: 1;3;2;7 (Group 1) and 4;6;5;8 (Group 2) (ensuring that each pair is within the same group), graphically the groups can be represented as shown in Figure 4.1. The dotted polygons are drawn using the rain gauges as the vertices and show the spatial coverage of each rain gauge group.

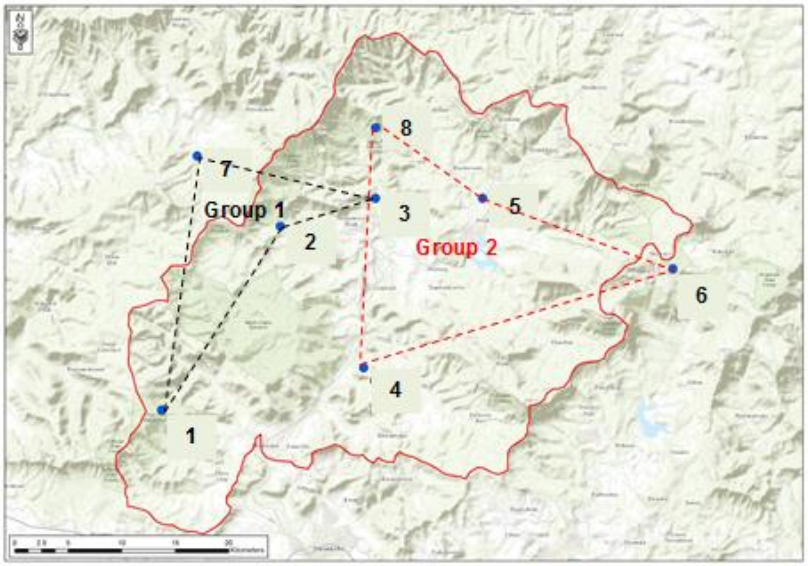

Figure 4.1: Nonuniform catchment coverage

According to Figure 4.1, this rain gauge grouping is undesirable because the two groups do not exhibit a uniform catchment coverage but are representative of different parts of the catchment. To prevent this happening, it was assumed that the area of the polygons (delineated by the lines connecting the pair of stations) must at least overlap to be considered as being representative of the catchment rainfall, for rain gauge groups with 3 or more stations. The larger the area at which the two rain gauge groups overlap, the more representative of the entire catchment rainfall they are. On this basis, groups 2;4;6;7 (Group 1) and 1;5;3;8 (Group 2) were selected. Figure 4.2 shows these two groups graphically.

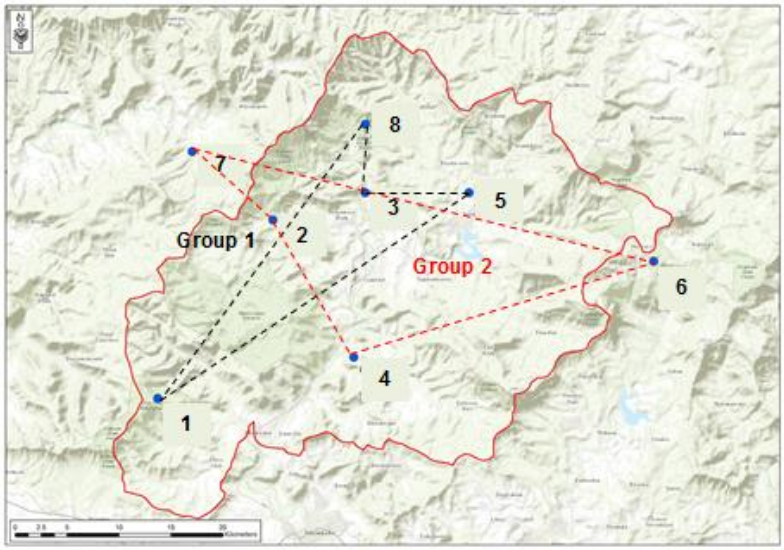

Figure 4.2: Rain gauge grouping for combination 4 (Balfour)

To evaluate the influence that the selection of the rain gauge groups has on the outputs of the adapted data – based stochastic rainfall generator, four possible rain

gauge combinations were selected for each catchment. The first three combinations (combinations 1; 2 and 3) were selected with the aim of achieving a uniform catchment coverage as prescribed by Ndiritu (2013a) and a fourth combination (combination 4) was selected using the correlation based method (described in steps 1 to 7 above).

4.2 AVERAGINCUMULATIVE DENSITY FUNCTIONS OBTAINED FROM MULTIPLE RAIN GAUGE GROUPS OF THE SAME DENSITY

The development of the cumulative density plots is discussed in Section 2.2.1. Data for two cumulative probability plots were obtained from the 4 groups of 2 stations each and data for four cumulative probability plots were obtained from the 8 groups of 1 station each. To compute the scaling factors between the two sets of rain gauge groups, the average cumulative probability plot had to be obtained.

Ndiritu (2013a) averaged the cumulative probability plots by simply computing the average perturbation at specified percentiles, for the rain gauge groups with a common rain gauge density. This is referred to as averaging without considering time alignment (Not TA). However, the averaging of cumulative density functions can also be done through time aligned averaging (TA). With TA, the average perturbations are obtained from the same month before ranking them to create the cumulative probability plot and then the averages are ranked for all time periods to obtain the cumulative probability plot. Time aligned averaging is the more realistic method of averaging as it ensures that the rainfalls occurring within each month are compared. Consequently, the cumulative probability plots from the two averaging methods were compared to investigate whether there is any benefit to be gained by using time aligned averaging.

The results indicate that the cumulative probability plots obtained from the two averaging techniques are similar, and the differences between them decrease as the rain gauge density increases. The shape of the cumulative probability plot in the TA case is associated to the rainfall characteristics of the catchment and the number of zero or very small measured rainfall volumes.

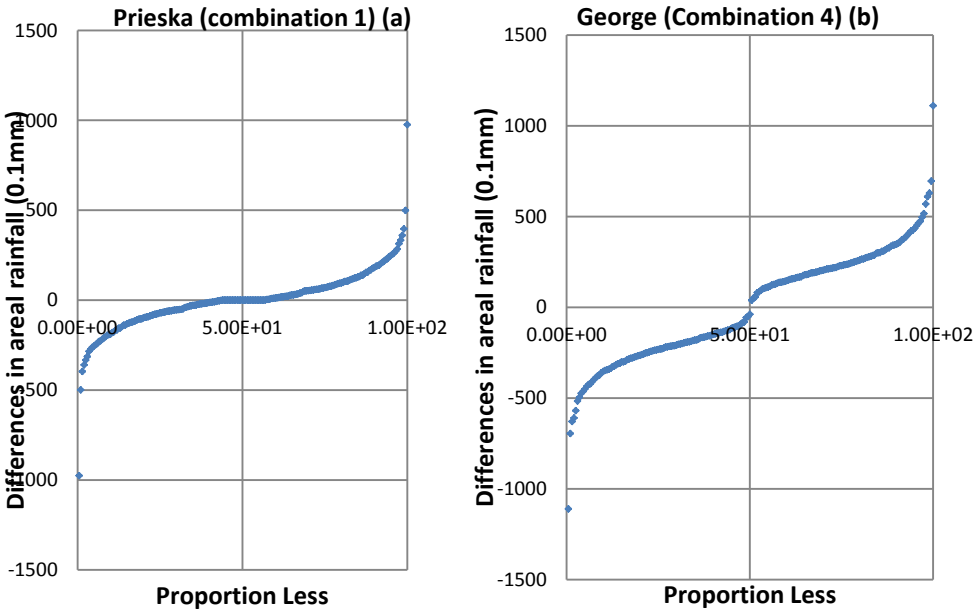

Figure 4.3: Time aligned average cumulative probability plots for Prieska and George

Figure 4.3 shows the cumulative probability plots of the eight groups of one station each for the Prieska and George catchments. The graphs show that the number of zero or very small rainfalls has an impact on the slope of the cumulative probability plot at the 50th percentile. A flat slope (such as in Figure 4.3a) indicates that a considerable number of zero or very small rainfall volumes were measured at the catchment while a very steep slope (or translation) at the 50th percentile (such as in Figure 4.3b) indicates that there were none or very few measured zero rainfalls at the catchment.

Figure 4.4 shows the cumulative probability plots for the same rain gauge combinations considered in Figure 4.3, without considering time alignment (Not TA). The graphs show that the attributes found to exist at the 50th percentile during time aligned averaging are lost when averaging without considering time alignment. The computed scaling factors based on the TA case and the Not TA case are however similar.

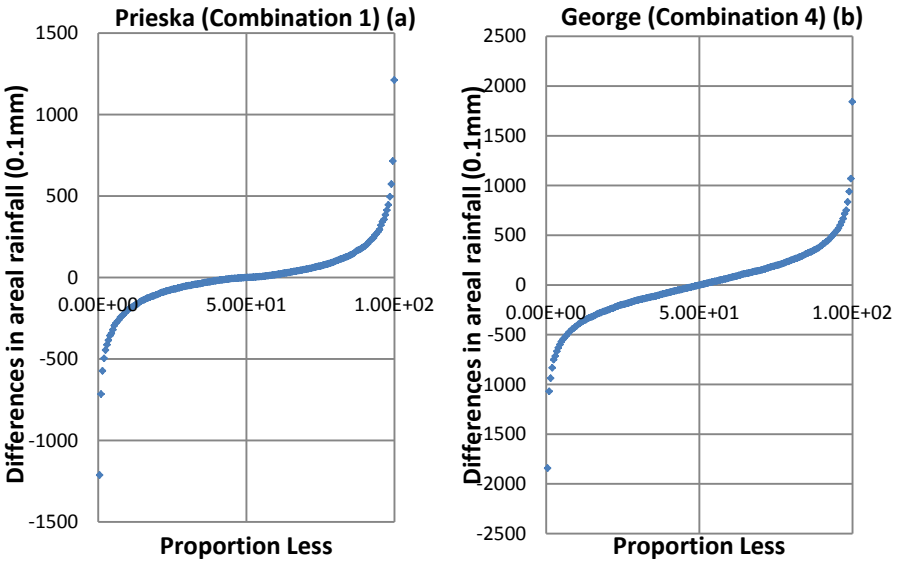

Figure 4.4: Not time aligned cumulative probability plots for Prieska and George

The computation of the scaling factors is explained in Section 2.3 and is illustrated by an example using the George catchment. Figure 4.5 shows the average cumulative density plots obtained from the TA case and the Not TA case for the George catchment. Scaling factors of 0.75 and 0.50 were found to exist between the average cumulative density plots obtained from 8 groups of 1 station and 4 groups of 2 stations as well as 4 groups of 2 stations and 2 groups of 4 stations respectively, for both averaging approaches. Therefore, averaging without considering time alignment was used in this study.

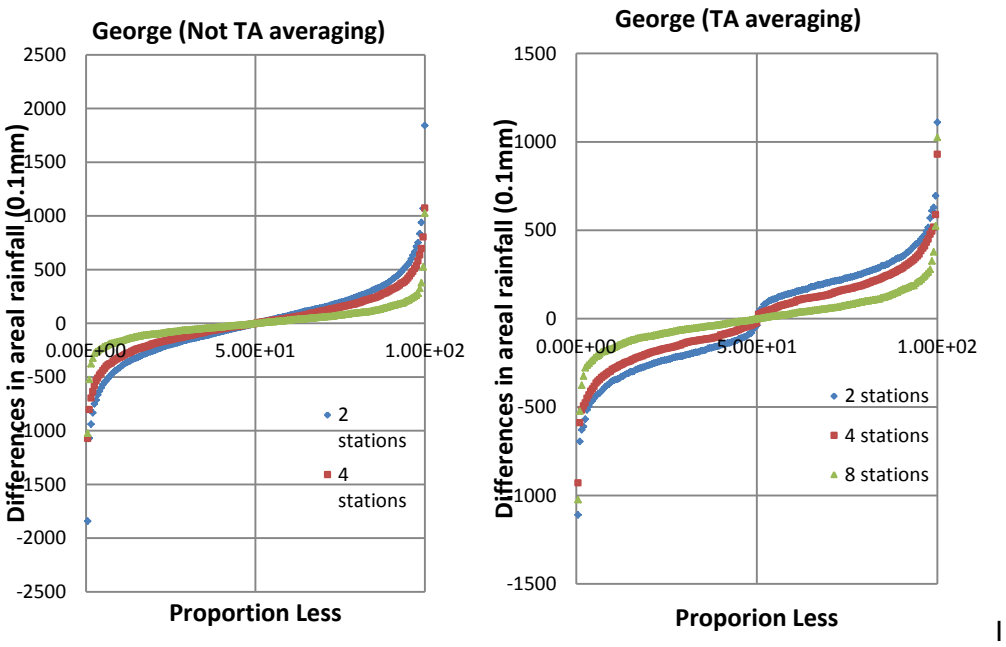

Figure 4.5: Different averaging techniques for the George catchment

4.3 THE ESTIMATION OF SCALING FACTORS AT VARIOUS RAIN GUAGE DENSITIES

Scaling factors were computed for the various rain gauge combinations as shown in Table 4.4. The rain gauges selected in each rain gauge combination are given for each catchment in Appendix B.

For the basis of comparison, it was assumed that a difference in scaling factor >10% is considerable, Table 4.4 shows that scaling factors computed for the Prieska and Barberton catchments were affected least by the rain gauge grouping process. However, the scaling factors obtained from the Balfour, Liebenbergsvlei and Tzaneen catchments were considerably affected by the selected rain gauge groups. The scaling factors obtained between 2 to 4 stations for the George, Louis Trichardt and Murraysburg catchments were also not considerably affected by the rain gauge groups, however, the influence of these rain gauge groups becomes more pronounced in the scaling factors computed between 4 and 8 rainfall stations.

Table 4.4: Computed scaling factors from the various rain gauge combinations

Balfour		
Combination	**2 to 4 stations**	**4 to 8 stations**
1	0.52	{1.25; 1.50}
2	0.35	0.82
3	0.90	0.60
4	{0.30,0.40}	0.65
Barberton		
Combination	**2 to 4 stations**	**4 to 8 stations**
1	{0.50, 0.90}	0.50
2	0.70	0.47
3	0.70	0.52
4	0.70	0.47
George		
Combination	**2 to 4 stations**	**4 to 8 stations**
1	0.70	1.00
2	0.80	0.70
3	0.72	0.70
4	0.75	0.50
Liebenbergsvlei		
Combination	**2 to 4 stations**	**4 to 8 stations**
1	0.72	0.75
2	0.70	0.75
3	0.60	0.80
4	0.60	0.90
Louis Trichardt		
Combination	**2 to 4 stations**	**4 to 8 stations**
1	0.55	0.60
2	0.48	1.00
3	0.45	1.00
4	0.50	0.65
Murraysburg		
Combination	**2 to 4 stations**	**4 to 8 stations**
1	0.60	0.60
2	0.57	0.60
3	0.55	0.80
4	0.65	0.80
Prieska		
Combination	**2 to 4 stations**	**4 to 8 stations**
1	0.68	0.65
2	0.70	0.65
3	0.65	0.65
4	0.70	0.60
Tzaneen		
Combination	**2 to 4 stations**	**4 to 8 stations**
1	0.70	0.60
2	0.92	{1.00,1.15}
3	0.95	0.50
4	0.85	0.35

Some of the computed cumulative probability plots had unique features. Figure 4.6a shows an example of a case where a single scaling factor between the differences

obtained from 2 groups of 4 stations and 4 groups of 2 stations could not be found. Figure 4.6b shows a case where the scaling factor between the differences obtained from 4 groups of 2 stations and 2 groups of 4 stations was found to be greater than 1. A scaling factor that is greater than 1 is not realistic as it implies that the variability of the rainfall at a higher gauge density exceeds that at a lower gauge density.

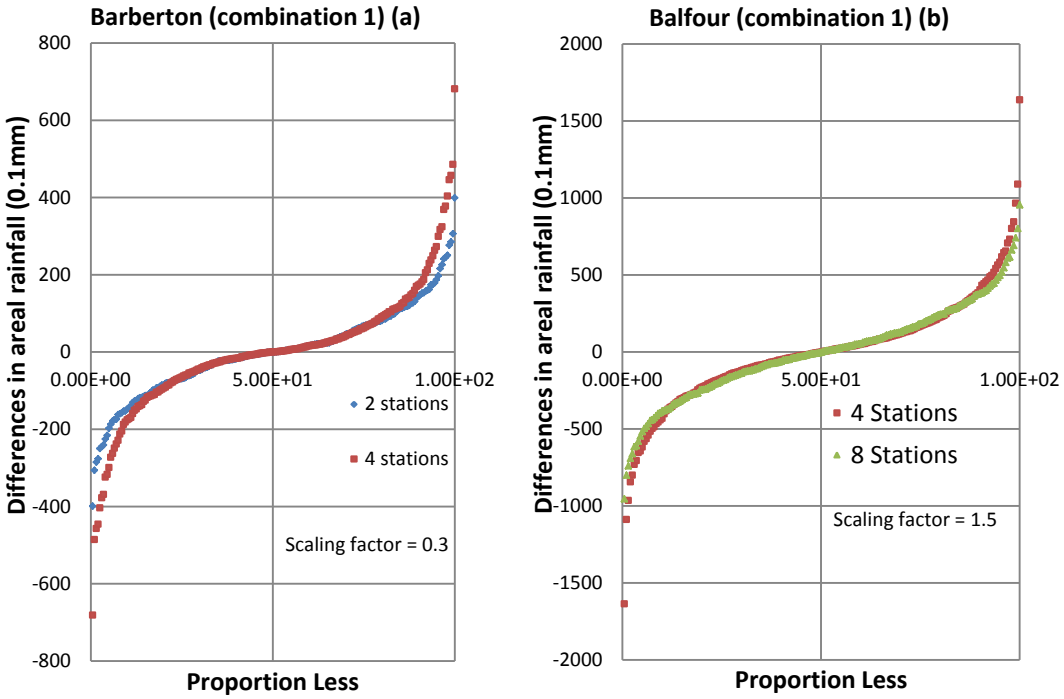

Figure 4.6: Scaled Cumulative Probability Plots with unique features

These results show that the selection of the rainfall stations within each rain gauge group is not a trivial exercise. The selection of stations in each rain gauge group may lead to considerably different scaling factors and in some cases scaling factors with unrealistic values (i.e scaling factor > 1). Scaling factors with unrealistic values may be an indication of an unsuitable combination of rainfall stations. The impact of these computed scaling factors on the generated stochastic areal rainfalls are evaluated in Chapter 5.

4.4 DEALING WITH MISSED MONTHLY RAINFALLS

To assess whether a linear relationship exists between the average proportion of zero rainfalls and the index of rain gauge density ($\log_2$(number of rain gauges)) for longer averaging periods, graphs showing the average proportion of zero rainfalls against rain gauge density were plotted for all the combinations mentioned in Section 4.1.

The relationship between the average proportion of zero rainfalls and the rain gauge density was best approximated by the power function in the form:

$$y = ax^{-b} \qquad (4.1)$$

Where *y* represents the average proportion of zero rainfalls, x is the number of rain gauges and *a* and *b* are constants dependent on the rain gauges selected in each group. Therefore, each catchment could have a number of values for a and *b*.

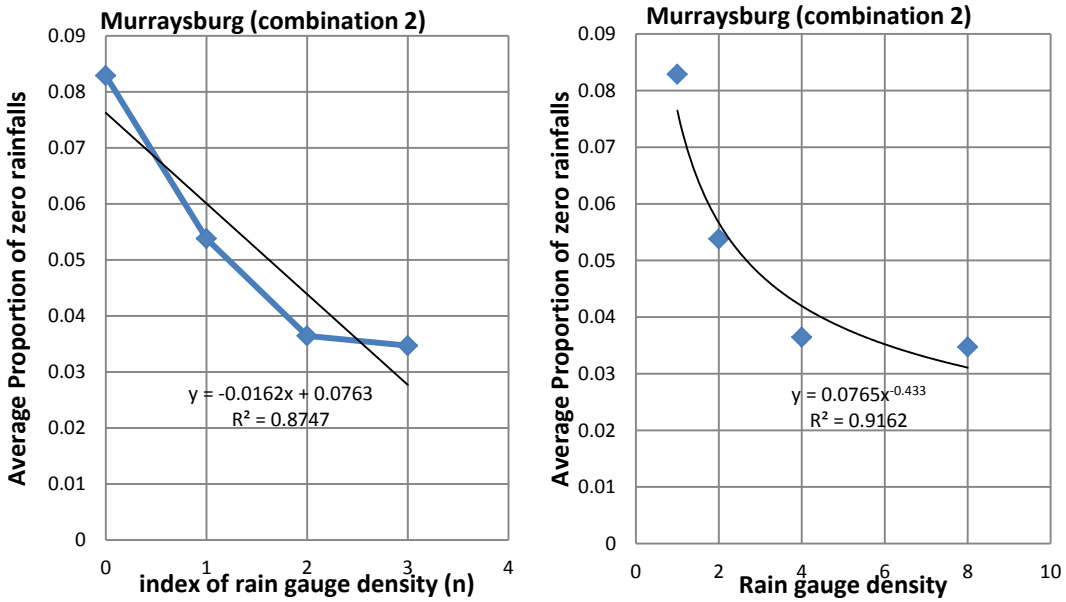

Figure 4.7: Proportion of average zeros for Murraysburg.

Figure 4.7 shows that the rate at which the average proportion of zero rainfalls decreases with rain gauge density tends towards zero, which is not adequately accounted for by the logarithmic function proposed by Ndiritu (2013a). This was also evident for the Murraysburg, Tzaneen, Louis Trichardt and Barberton catchments (see Appendix D). The power function could not however be used to approximate the average proportion of zero rainfall against rain gauge density for the Balfour and George catchments. As the average proportion of zero rainfalls reduces to 0 at rain gauge density of 4 stations for all combinations in Balfour and no zero rainfalls were observed in George.

Table 4.5 gives a list of the various combinations that yielded the highest R^2 values for each catchment where a relationship between the average proportion of zero rainfalls and the rain gauge density could be established. The constants *a* and *b* are also included for comparison.

Table 4.5: Power function constant values for each catchment for the relationship between proportion of zero rainfalls and rain gauge density

Catchment	Combination	a	b	R^2
Tzaneen	4	0.002	-1.816	0.99
Louis Trichardt	2	0.096	-0.603	0.99
Murraysburg	1	0.077	-0.403	0.95
Prieska	1	0.235	-0.263	0.97
Barberton	2	0.092	-0.918	0.93
Liebenbergsvlei	4	0.091	-0.572	0.97

The computed scaling factors from the rain gauge combinations yielding the highest R^2 values listed in Table 4.5 were evaluated, to establish whether these can be used to inform the selection of the most ideal rain gauge combination. The results however showed that the combination yielding the highest R^2 value in Louis Trichardt is not spatially representative. The areal rainfalls from which the perturbations are derived are computed from different parts of the catchment and therefore are not representative of the whole catchment. In other rain gauge combinations the proportion of zero rainfalls increased with the rain gauge density (see Figure 4.8), although the magnitude of the increases (7% for Murraysburg and 12.5% for Louis Trichardt) were not considered significant enough to warrant concern given the magnitude of the proportion of zero rainfalls being considered. Therefore, using the R^2 value to inform the most ideal rain gauge combination was not considered.

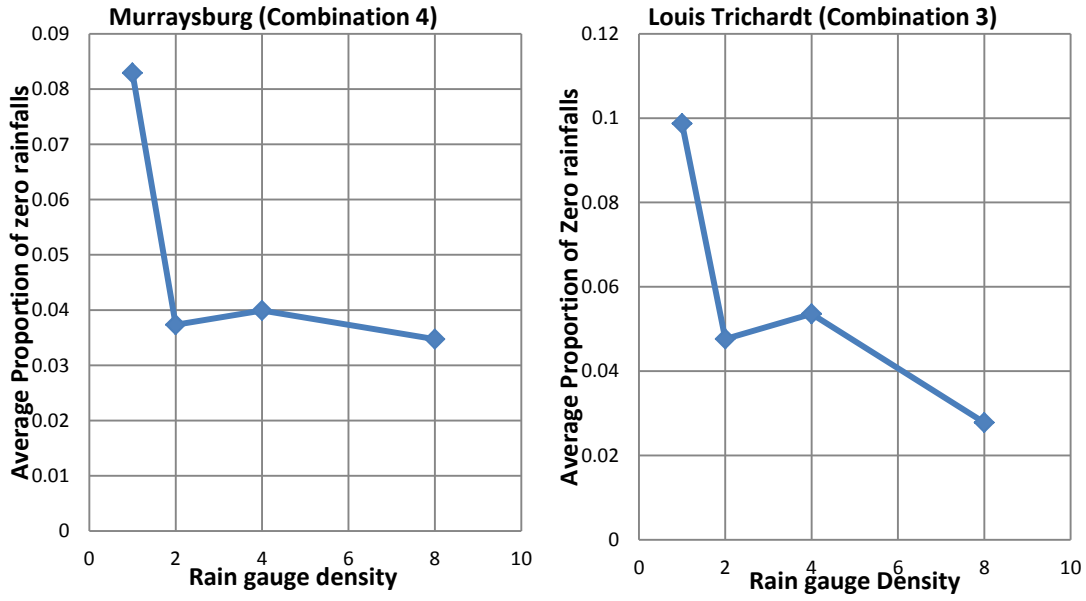

Figure 4.8: Proportion of average zeros for Murraysburg and Louis Trichardt

Depending on the output of monthly hydrological model, the magnitude of missed rainfalls may be important. However, in this study the catchments considered have a low average proportion of zero rainfalls (<10%) and not much benefit can be obtained from activating the infilling of missed rainfalls component of the data – based model.

Therefore, this component was not activated. The results however provide some insight in to how the infilling of missed rainfalls should be dealt with in cases where the proportions of missed monthly rainfalls are found to be significant.

5. STOCHASTIC AREAL RAINFALL GENERATION RESULTS

Before applying the areal rainfall differences to the catchment average rainfall computed using all eight (or available) stations, they have to be scaled down using an uncertainty factor *u*, quantified based on the scaling factor as explained in Section 2.2.1 and Figure 2.4. All the scaling factors in Table 4.4 are considered to be realistic estimates of the uncertainty factor *u*. Therefore, *u* was set to equal the scaling factor obtained between the average cumulative probability plots between the 4 groups of 2 rainfall stations each and the 2 groups of 4 rainfall stations each listed in Table 4.4. The data – based model was then used to generate 100 stochastic areal rainfall sequences.

To assess the credibility of the adapted data – based model for monthly applications and the impact of the various rain gauge combinations on the generated stochastic areal rainfalls, bias in the generated sequences was evaluated. Bias can be visualised as the deviation of the box plot mean obtained from the generated stochastic rainfalls, from the associated historical rainfall statistic. In this study the mean, standard deviation and skewness values are considered, due to the importance of these statistics in water resource modelling applications.

Ideally, the degree of bias in the generated stochastic sequences must be negligible for the adapted data – based model to be considered a realistic uncertainty estimator. The results of the simulation are summarised in Section 5.1 below.

5.1 STATISTICAL ANALYSIS OF THE GENERATED STOCHASTIC AREAL RAINFALLS

BALFOUR

Mean

Figure 5.1a and Table 5.1 show that the stochastic mean rainfalls are unbiased and at least 50% of the data across all combinations overlap. The interquartile range from each combination varies. Combination 4 yields data with the lowest variability and combination 1 yields data with the highest variability.

Standard Deviation

Figure 5.1b and Table 5.1 show that the stochastic mean values of combination 2, 3 and 4 are very similar and close to the historic mean. It is expected that the historical standard deviation would at least plot within the range of sequences generated. However, the entire range of data resulting from combination 1 is well above the historical. In this combination noticeably, a scaling factor of 1.5 was used.

Combination 4 yields data with the least bias and with an interquartile range much shorter than those obtained from the other rain gauge combinations.

Skewness

According Figure 51c, the probability distributions of the data resulting from combinations 1and 3 are shifted significantly. The mean of combination 4 is closest to the historical skewness value, and plots within the interquartile range of the box plot. Combination 4 has the least bias on the probability distribution of the historical data.

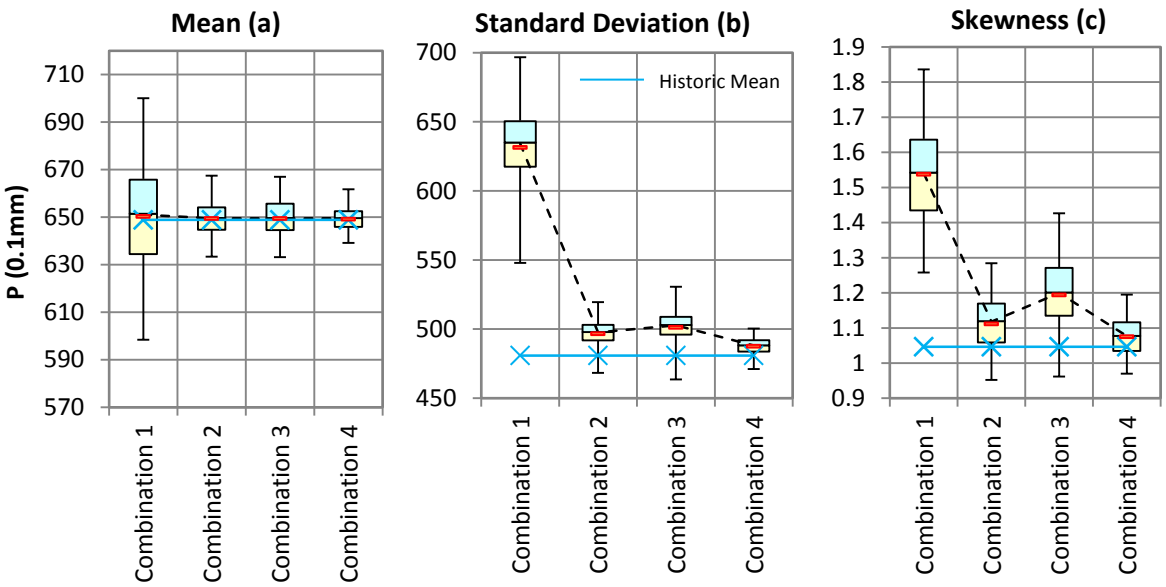

Figure 5.1: Comparison of the rainfall statistics for the Balfour catchment

BARBERTON

Mean

Figure 5.2a and Table 5.1 show that the mean rainfall value remains unbiased for all combinations and at least 50% of the interquartile range overlaps. Combination 3 yields the largest distribution of results while combination 4 has the shortest.

Standard Deviation

Figure 5.2b and Table 5.1 show that the stochastic means are also very similar while the interquartile ranges differ, the historical deviation plots on the 25th percentile for all combinations, however, the degree of bias remains less than 1%. The computed scaling factors for this catchment were also very similar. Combinations 2 and 4 yield data with the shortest interquartile range.

Skewness

Figure 5.2c and Table 5.1 show that the stochastic means of all combinations are close to the historical skewness value and data – based model has very little impact on the historical probability distributions. The box plots of combination 1 and 3 are shifted such that the historical skewness value corresponds approximately to the 25th percentile. However, the percentage bias is negligible (see Table 5.2).

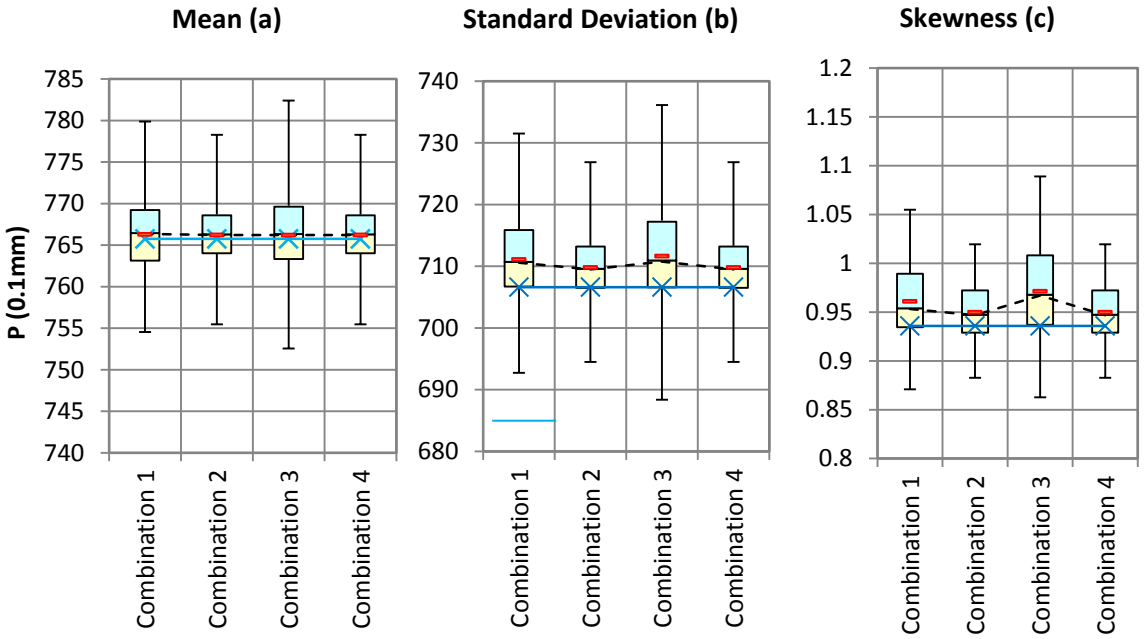

Figure 5.2: Comparison of the rainfall statistics for the Barberton catchment

GEORGE

Mean

Figure 5.3a and Table 5.1 show that the means are unbiased and the interquartile range from all the considered combinations varies and overlaps for the majority of the generated data. Combination 4 has the smallest interquartile range and combination 1 has the largest. Data from Combination 1 also has the highest variability. The box plot of combination 4 is positively skewed suggesting that the upper portion has a larger variability.

Standard Deviation

In Figure 5.3b, the box plots for combinations 1, 2 and 3 are above the historical, which is not realistic as it is expected that the historical standard deviation would at least plot within the box plot range. However, the percentage bias of the results from combination 2 and 3 are not considerable (< 10%). In combination 4, the historical plots between the 0th and 25th percentile. Noticeably, a scaling factor of 1.0 was used for combination 1.

Skewness

Figure 5.3c shows that only the stochastic mean of the skewness box plot from combination 4 equals the historical skewness. The means from the other combinations all plot below the historical skewness value, although the magnitude of the bias is negligible.

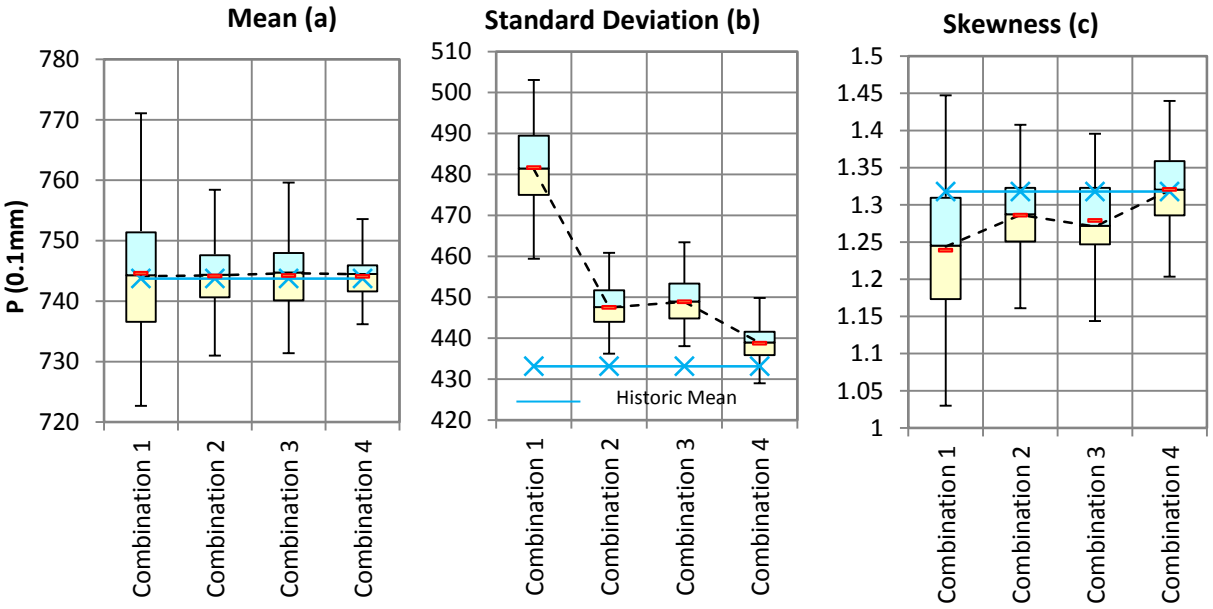

Figure 5.3: Comparison of the rainfall statistics for the George catchment

LIEBENBERGSVLEI

Mean

Figure 5.4a and Table 5.1 show that the stochastic means of the box plots are unbiased and the interquartile ranges overlap. Combination 3 yields the shortest interquartile range while combination 4 has the largest. Combination 4 also has a large range of results.

Standard Deviation

Figure 54b and Table 5.1 show that the stochastic generator has negligible bias on the dispersion of the results, ranging between 1.7 and 3.8%. The historical standard deviation plots between the 0^{th} and 25^{th} percentile for all combinations and the mean standard deviation of combination 3 is the closest to the historical value. The upper proportion of the box plots from combinations 1, 2 and 4 are less variable than the lower proportion.

Skewness

Figure 5.4c and Table 5.1 show that the probability distributions of all combinations experience a degree of bias with combination 4 experiencing the most. Combination 4 also yields the largest range of results whilst combination 3 yields the shortest.

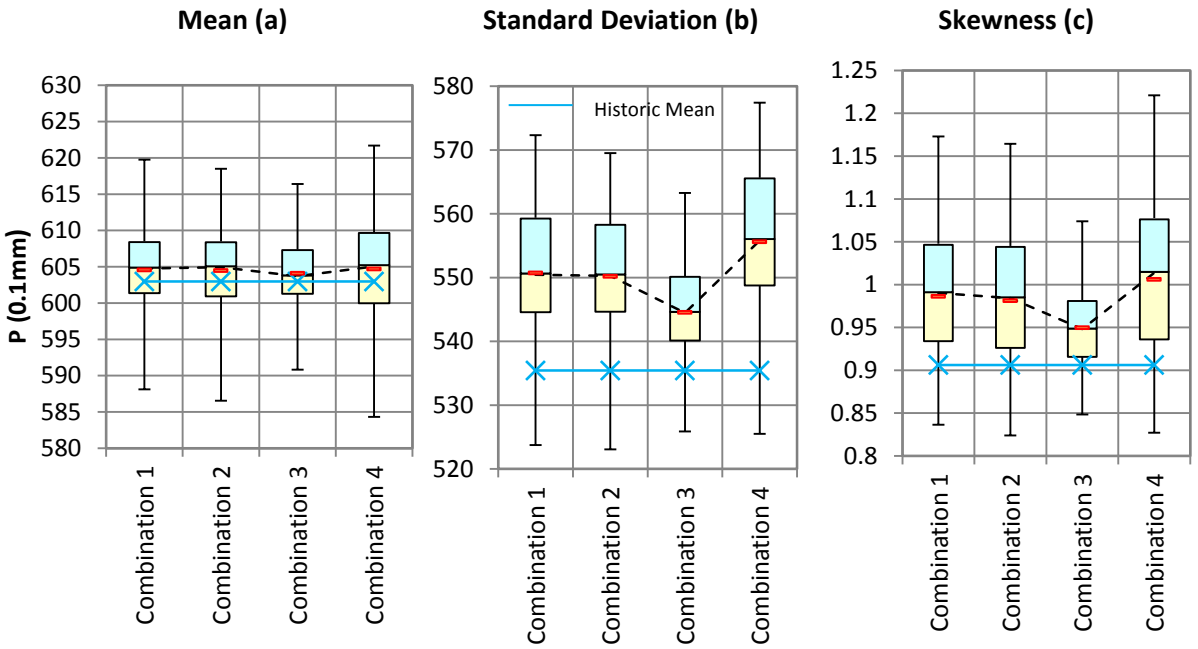

Figure 5.4: Comparison of the rainfall statistics for the Liebenbergsvlei catchment

LOUIS TRICHARDT

Mean

Figure 5.5a and Table 5.1 shows that the stochastic mean values are unbiased. Combinations 1 and 4 yield results with the shortest interquartile range while combination 2 has the largest range of results. Combination 3 yields data with the highest variability.

Standard Deviation

Figure 5.5c and Table 5.1 show that combination 2 and 3 yield results with a small degree of bias. The historical standard deviation plots within the interquartile range for combinations 1 and 4. All the box plots are positively skewed.

Skewness

Figure 5.5c and Table 5.1 show that the stochastic mean skewness values from combinations 1 and 4 equals the historical value. The box plots of these combinations also have the shortest interquartile range and distribution of results. Combinations 2 and 3 yield results with the most biased data and have the largest range of results.

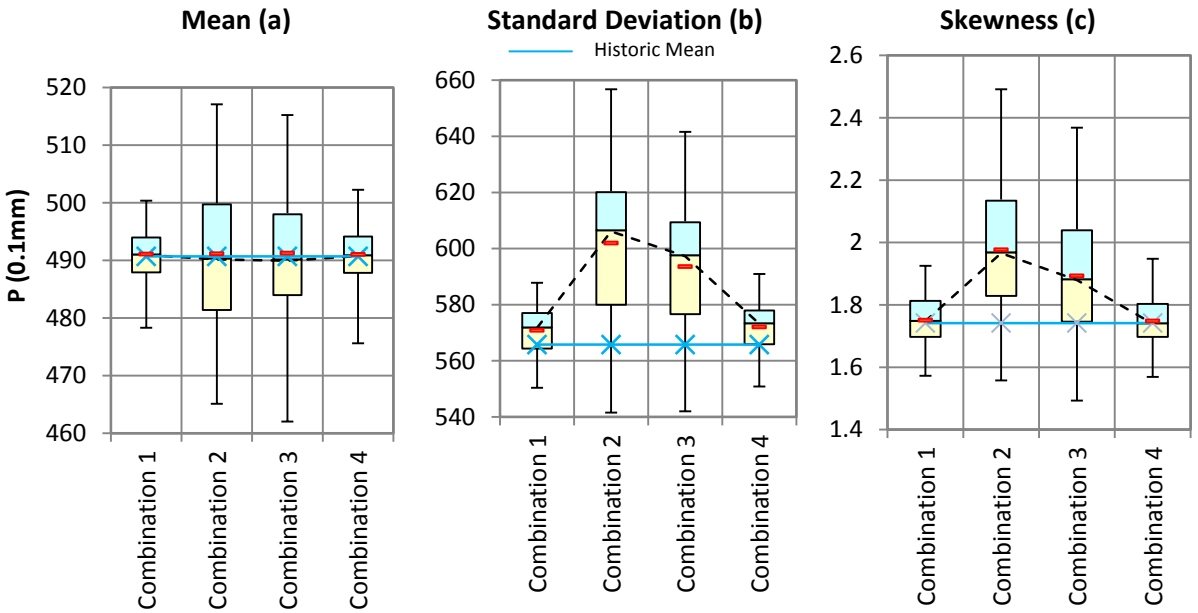

Figure 5.5: Comparison of the rainfall statistics for the Louis Trichardt catchment

MURRAYSBURG

Mean

Figure 5.6a and Table 5.1 show that the stochastic means remain unbiased and the box plots are all negatively skewed. Combinations 1 and 2 yield the shortest interquartile range and combinations 3 and 4 have the largest. Combinations 2 and 4 also have the shortest and largest distribution of data respectively.

Standard Deviation

Figure 5.6b and Table 5.1 show that all the combinations experience negligible bias. The historical standard deviation plots within the interquartile range of the data from combination 1. For all other combinations, the historical value plots between the 0^{th} and 25^{th} percentiles.

Skewness

Figure 5.6c and Table 5.1 show that the stochastic mean skewness from combinations 1, 2 and 4 are all very similar and equal to the historical skewness value. All combinations yield results with negligible bias.

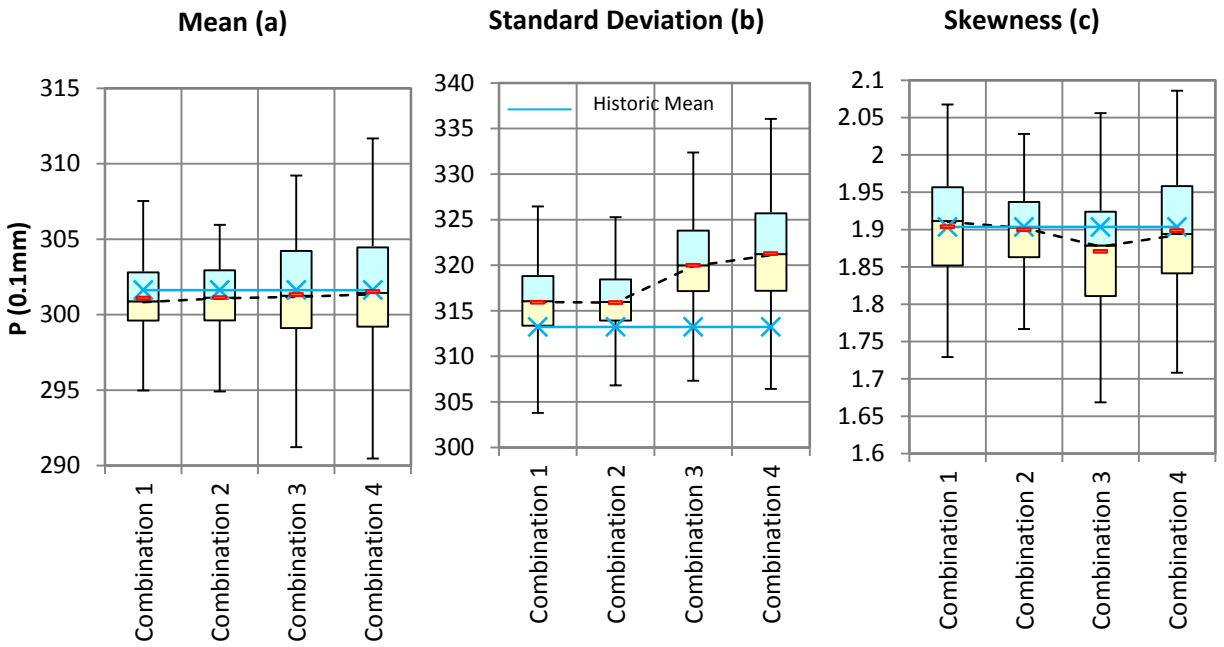

Figure 5.6: Comparison of the rainfall statistics for the Murraysburg catchment

PRIESKA

Mean

Figure 4.7a and Table 5.1 show that the stochastic means are unbiased and the interquartile range of the box plots overlap. Combinations 3 and 4 yield the largest and shortest interquartile range respectively. The box plots from combinations 1, 2 and 4 are all positively skewed. Combination 3 yields the data with the highest variability.

Standard Deviation

Figure 5.7b and Table 5.1 show that the dispersion of the monthly rainfalls is increased by all combinations as the historical standard deviation value plots between the 0^{th} and 25^{th} percentile. However the magnitude of the bias is insignificant. The means of the box plots from combinations 2 and 4 are closest to the historical value. The interquartile range of the data from combinations 2 and 4 are also shorter than that from combinations 1 and 3.

Skewness

Figure 5.7c and Table 5.1 show that the mean of the skewness box plot of combination 4 is equal to the historical skewness value. The historical skewness value plots between the lower interquartile range of combinations 1, 2 and 3. The box plots are all positively skewed. The variability of the lower percentiles is also larger than that of the upper percentiles. The increase in the dispersion of the results is negligible for all combinations, least of all the results from combination 4.

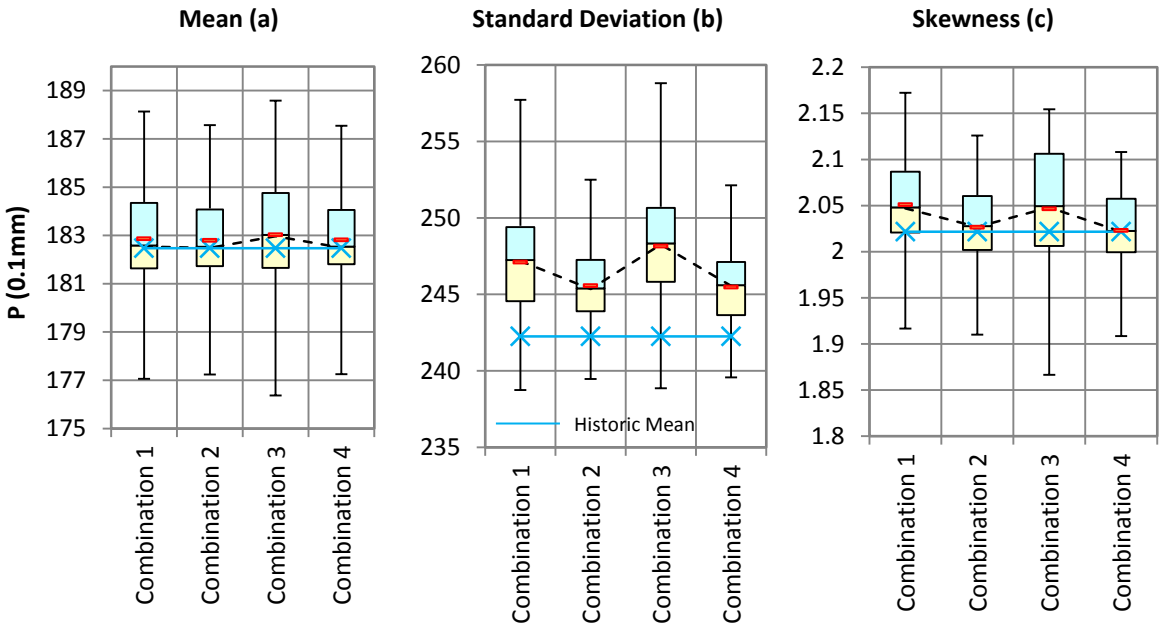

Figure 5.7: Comparison of the rainfall statistics for the Prieska catchment

TZANEEN

Only three rain gauge combinations were considered as a unique scaling factor could not be obtained for rain gauge combination 2.

Mean

Figure 5.8a and Table 5.1 show that the stochastic means of all box plots are unbiased and the interquartile ranges overlap. Combinations 1and 4 yield the shortest and largest interquartile range respectively. The variability of the lower portion of results from combination 3 and 4 is less than the upper portion.

Standard Deviation

In Figure 5.8b, the historical standard deviation plots within the lower interquartile of the box plots from combinations 3 and 4. Bias across all combinations is negligible. Combination 4 yields data with the shortest interquartile range and combination 1 yields data with the largest interquartile range.

Skewness

Figure 5.8c and Table 5.1 show that the stochastic generator introduces negligible bias for all combinations. The historical skewness value plots within the upper interquartile range for all the combinations. Combinations 4 and 1 yield the shortest and largest interquartile range respectively.

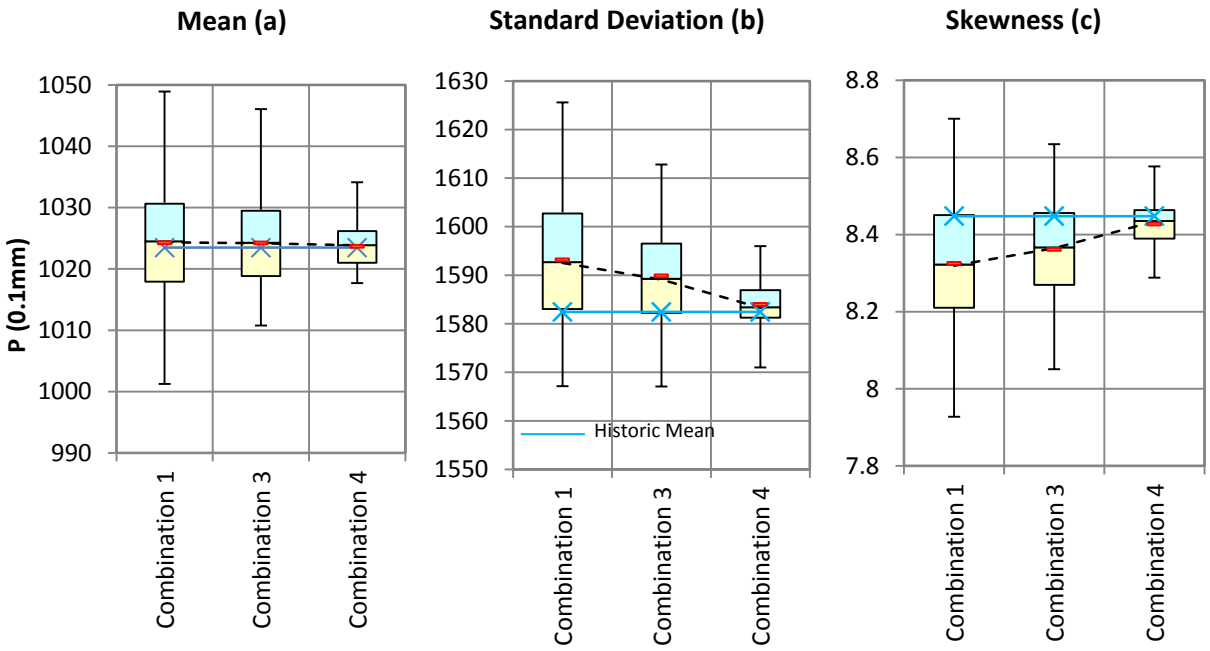

Figure 5.8: Comparison of the rainfall statistics for the Tzaneen catchment

Table 5.1: Actual bias associated with the generated areal rainfall stochastic sequences

Catchment	Statistic	Actual bias scaled to the historic value ((Box plot mean – Hist) /Hist) (%)			
		Combination 1	Combination 2	Combination 3	Combination 4
Balfour	Mean	0.22	0.09	0.09	0.05
	Standard Deviation	31.31	3.29	4.24	1.39
	Skewness	46.92	6.22	14.11	2.76
Barberton	Mean	0.07	0.06	0.06	0.06
	Standard Deviation	0.63	0.45	0.72	0.45
	Skewness	2.68	1.50	3.80	1.50
George	Mean	0.12	0.06	0.07	0.05
	Standard Deviation	11.20	3.32	3.64	1.30
	Skewness	-5.99	-2.40	-2.94	0.21
Liebenbergsvlei	Mean	0.27	0.25	0.19	0.29
	Standard Deviation	2.86	2.76	1.71	3.77
	Skewness	8.85	8.29	4.81	11.04
Louis Trichardt	Mean	0.08	0.09	0.12	0.07
	Standard Deviation	0.90	6.39	4.92	1.11
	Skewness	0.53	13.51	8.70	0.39
Murraysburg	Mean	-0.18	-0.16	-0.10	-0.03
	Standard Deviation	0.86	0.86	2.16	2.57
	Skewness	0.02	-0.20	-1.71	-0.26
Prieska	Mean	0.22	0.18	0.31	0.19
	Standard Deviation	2.01	1.37	2.44	1.33
	Skewness	1.45	0.25	1.23	0.07
Tzaneen	Mean	0.08	-	0.08	0.02
	Standard Deviation	0.68	-	0.47	0.10
	Skewness	-1.45	-	-1.02	-0.24

5.2 THE REPLICATION OF HISTORICAL RAINFALL STATISTICS BY THE DATA – BASED MODEL

The results indicate that the mean of the generated stochastic results across all combinations is unbiased. However, the degree of bias on the standard deviation and skewness values varies considerably for the different rain gauge combinations in the George, Liebenbergsvlei, Louis Trichardt and Balfour catchments. In the Barberton, Murraysburg, Prieska and Tzaneen catchments though, the rain gauge combinations

have a negligible effect on the degree of bias of the standard deviation and skewness values of the generated stochastic sequences. The rain gauge combinations also have an impact on the variability of the generated sequences.

The combinations yielding results with the least bias over all three statistics (mean, standard deviation and the skewness) for each catchment are given in Table 5.2.

Table 5.2: Combinations yielding the least biased results

Catchment	Combination
Balfour	4
Barberton	4
George	4
Liebenbergsvlei	3
Louis Trichardt	4
Murraysburg	1
Prieska	4
Tzaneen	4

According to Table 5.2, combination 4 yields results with the least bias for 6 out of the 8 catchments considered. This indicates that the correlation - based approach of selecting the rainfall stations in each rain gauge group is a good way of initiating the grouping of the rainfall stations, but does not guarantee that the most ideal solution is obtained.

Combination 3 yields results with the least bias for the Liebenbergsvlei catchment. However, bias on the skewness value is still considerable and may be associated with a variety of reasons. It may also be possible that another rain gauge combination exists that may give results with even less bias.

In Section 4.4 it is found that combination 4 in the Murraysburg catchment, yielded unrealistic results (the proportion of zero rainfalls increased with the rain gauge density, although the magnitude of the increase was considered negligible). Combination 1 yields the least biased results and the highest R^2 value for the power function approximating the relationship between the average proportions of zero rainfalls and the rain gauge density.

These results indicate the need for the selection of multiple rain gauge combinations to increase confidence in the generated stochastic sequences.

The degree of bias in the generated stochastic results where a scaling factor of 1 or greater was obtained varies for each catchment. This is indicated by the results of combination 1 in the George and Balfour catchments. Unlike the results obtained by Ndiritu (2013a), the results in this study indicate that a scaling factor of 1.0 (or greater) has a significant impact on the standard deviation of the generated stochastic results and that the range of the generated stochastic sequences, unexpectedly, does not

include the historical standard deviation value. The generated stochastic sequences are therefore considered to be unrealistic.

5.3 STATITICAL ANALYSIS OF THE INDIVIDUAL RAINFALLS GENERATED BY THE DATA – BASED MODEL

The percentile box plots of the rain gauge combinations yielding the least biased results from each catchment (shown in Table 5.3) were used to assess the impact of the adapted data – based stochastic areal rainfall generator on individual monthly rainfalls.

The 5 – 95 percentiles from each of the 100 generated stochastic sequences were first computed and then the corresponding percentiles from all the sequences were represented graphically using box plots.

BALFOUR

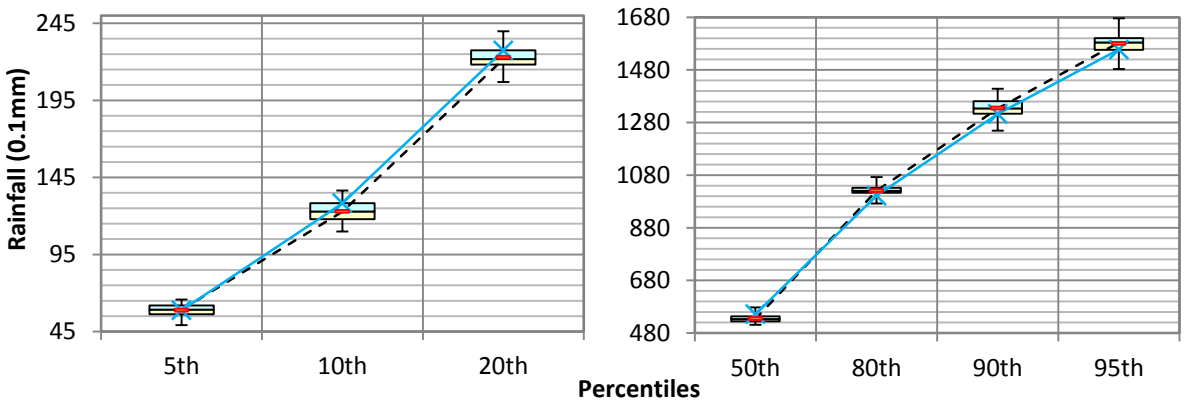

Figure 5.9: Comparison of the bias on various percentiles for the Balfour catchment

Figure 5.9 and Table 5.3 show that all the volumes above the 5th percentile experience a small degree of bias. The historical rainfalls lie just outside of the interquartile range for the areal rainfalls above the 5th percentile. All the volumes are negatively skewed except for the higher rainfall volumes (80th - 95th percentile). The small rainfall volumes (5th - 20th percentile) have the highest variability.

BARBERTON

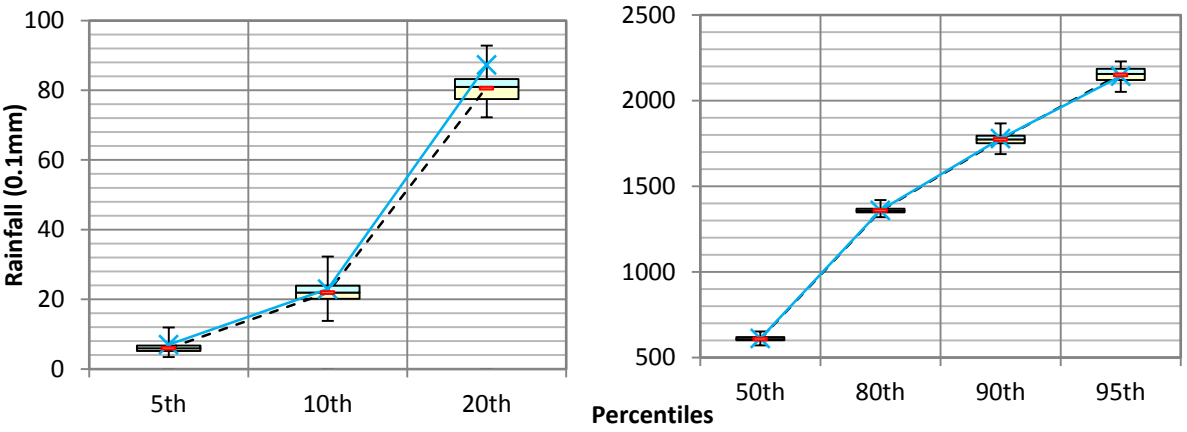

Figure 5.10: Comparison of the bias on various percentiles for the Barberton catchment

Figure 5.10 and Table 5.3 show that the smallest rainfall volumes (5th - 20th percentile) experience the most bias, however not significant to warrant concern. All volumes are negatively biased. The coefficient of variation shows that the highest variability is experienced by the smallest and the largest rainfall volumes.

GEORGE

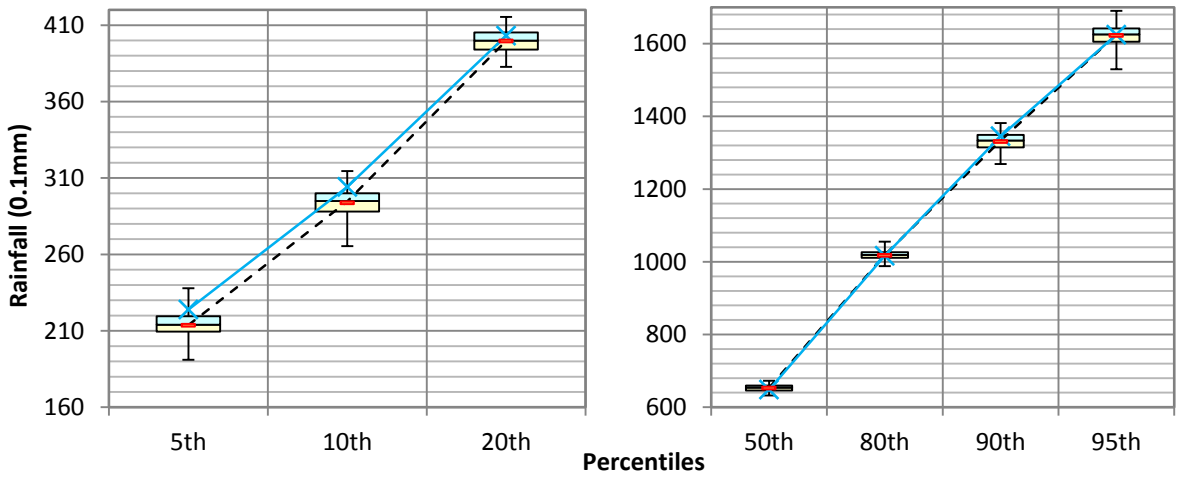

Figure 5.11: Comparison of the bias on the various percentiles for the George catchment

Figure 5.11 and Table 5.3 show that the smallest rainfalls (5th - 10th percentile) experience the most bias, however, the magnitude of the bias is not significant to warrant concern. All the small rainfall volumes (5th – 20th percentile) and the very high rainfall volumes (90 – 95th percentile) are negatively skewed. The smallest rainfalls have the highest variability.

LIEBENBERGSVLEI

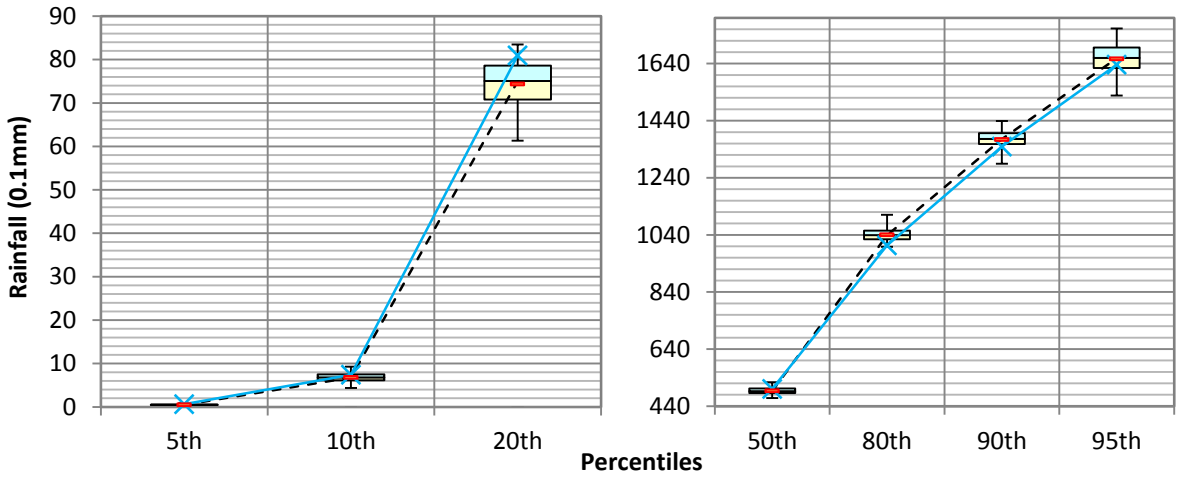

Figure 5.12: Comparison of the bias on the various percentiles for the Liebenbergsvlei catchment

Figure 5.12 and Table 5.3 show that the smallest rainfalls (5^{th} – 20^{th} percentile) experience the most bias. All the lower stochastic means (5^{th} – 50^{th} percentile) are negatively skewed. The smallest rainfalls have the highest variability.

LOUIS TRICHARDT

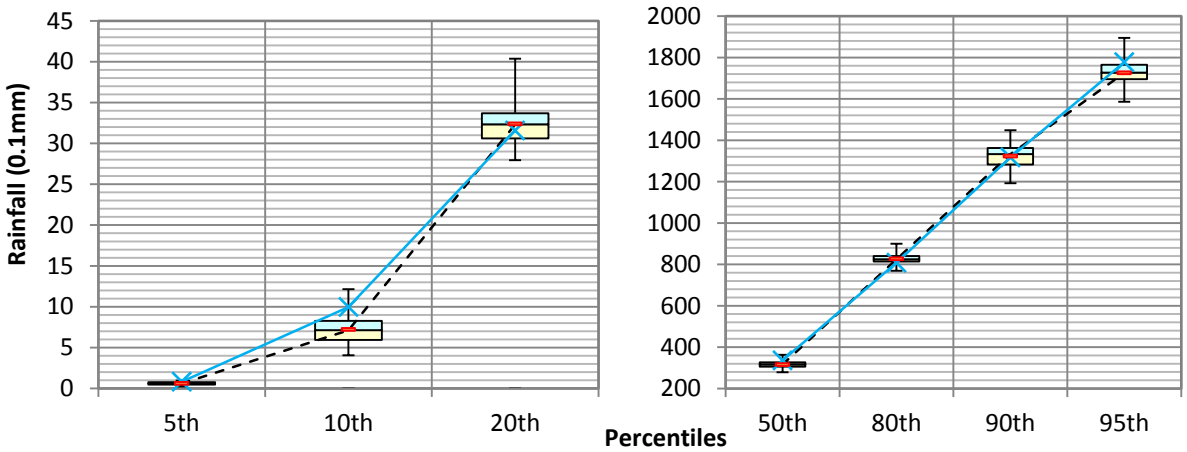

Figure 5.13: Comparison of the bias on the various percentiles for the Louis Trichardt catchment

Figure 5.13 and Table 5.3 show that the smallest rainfall volumes experience the most bias (5^{th} – 10^{th} percentile). The stochastic means of these rainfall volumes are also negatively skewed. The coefficient of variation shows that the smallest rainfalls have the highest variability.

MURRAYSBURG

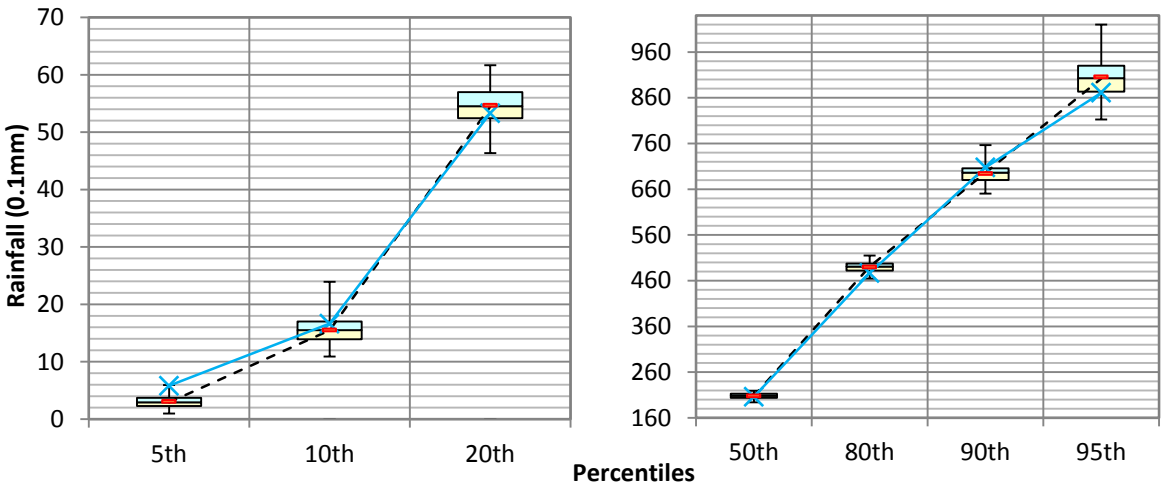

Figure 5.14: Comparison of bias on various percentiles for the Murraysburg catchment

Figure 5.14 and Table 5.3 show that the smallest rainfalls (5th – 10th percentile) experience the most significant bias and their stochastic means are negatively skewed. The coefficient of variation values show that these rainfall volumes also have the highest variability.

PRIESKA

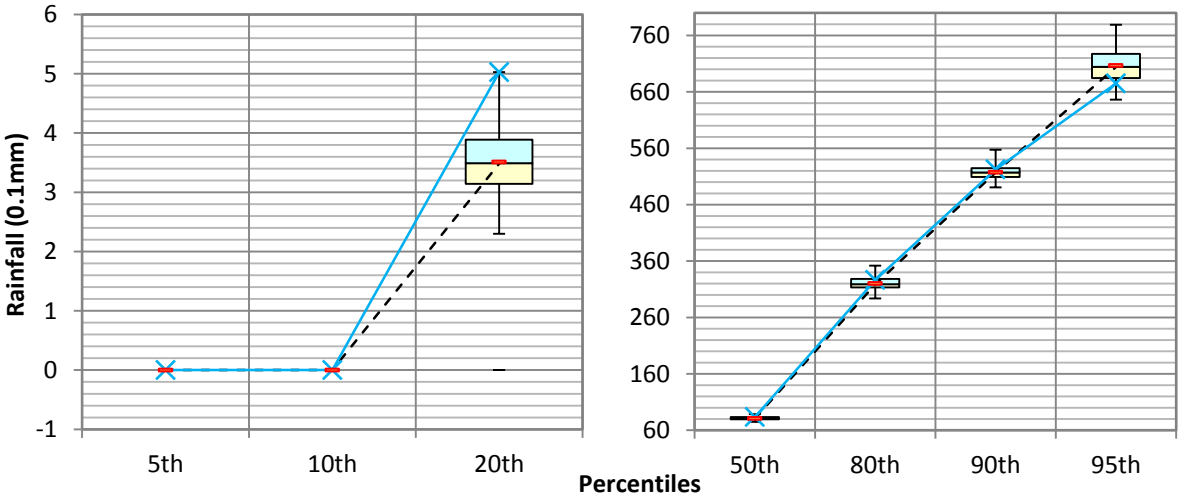

Figure 5.15: Comparison of bias on various percentiles for the Prieska catchment

Figure 5.15 and Table 5.3 show that no uncertainty is associated with the 5th and 10th percentile areal rainfall volumes. This is likely associated with the significant proportion of zero rainfalls measured at this catchment. The 20th percentile rainfall volume experiences the most significant bias and has the highest variability. All the stochastic rainfall means are negatively skewed.

TZANEEN

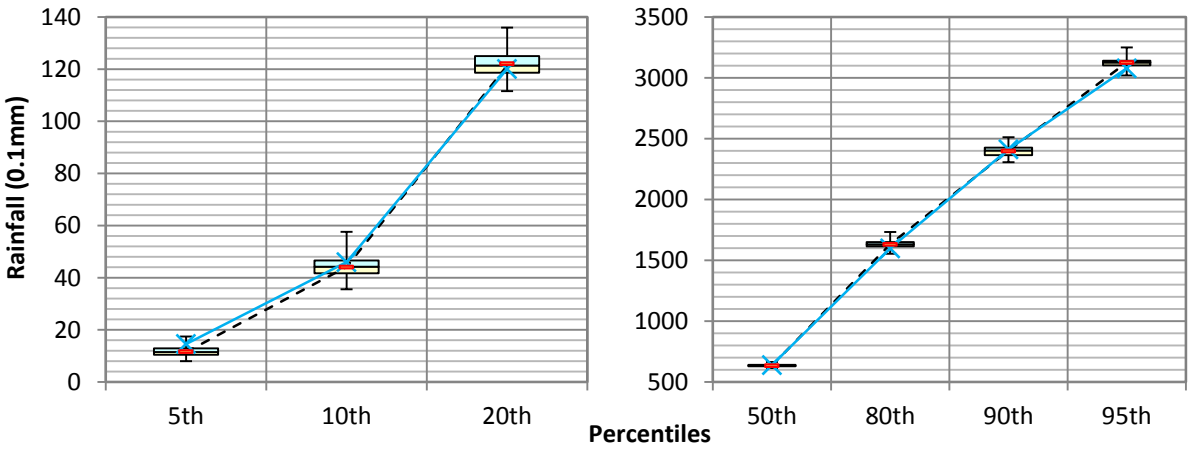

Figure 5.16: Comparison of the bias on the various percentiles for the Tzaneen catchment

Figure 5.16 and Table 5.3 show that the smallest rainfalls (5^{th} – 10^{th} percentile) experience the most significant bias. These rainfalls also have the highest variability. The stochastic means of most rainfalls are negatively skewed and the historical rainfalls lie within the interquartile range for all percentiles.

Table 5.3: Actual bias on individual monthly rainfalls for Tzaneen

Catchment	Statistic	Actual bias to the historic value (%)						
		5^{th}	10^{th}	20^{th}	50^{th}	80^{th}	90^{th}	95^{th}
Balfour	Mean	-0.86	-9.82	-6.51	-3.75	4.49	1.97	1.78
	Co. of variation	8.43	6.68	4.62	2.47	2.09	2.38	3.22
Barberton	Mean	-14.14	-4.77	-8.29	-1.31	-0.97	-1.20	-0.58
	Co. of variation	14.30	5.48	2.42	1.47	2.00	1.95	14.30
George	Mean	-4.62	-3.40	-0.86	0.69	0.13	-1.07	-0.11
	Co. of variation	3.66	3.34	1.90	1.47	1.19	1.74	1.74
Liebenbergsvlei	Mean	-31.03	-10.93	-17.81	-2.59	5.53	3.28	0.09
	Co. of variation	20.67	16.66	11.66	3.54	2.52	3.16	2.54
Louis Trichardt	Mean	-24.52	-27.51	2.59	-5.84	2.41	0.58	-2.88
	Co. of variation	27.25	21.24	7.57	4.95	2.87	3.93	3.22
Murraysburg	Mean	-46.82	-6.63	2.62	0.89	2.73	-1.85	3.97
	Co. of variation	37.99	14.18	6.32	2.85	2.27	2.83	5.00
Prieska	Mean	-	-	-30.11	-3.06	-1.92	-0.99	4.70
	Co. of variation	-	-	16.04	3.90	3.63	2.54	4.20

Tzaneen	Mean	-19.78	-4.06	1.72	-0.57	2.14	-0.54	1.56
	Co. of variation	15.66	8.52	4.26	1.58	1.72	1.70	1.22

5.4 THE REPLICATION OF INDIVIDUAL RAINFALLS BY THE DATA – BASED MODEL

The results indicate that bias is between 0.9 – 46.1% for the lowest monthly rainfall volumes (<20th percentile). The importance of these very small rainfalls must be assessed relative to their use. In rainfall - runoff modelling for example, very small monthly rainfalls are not important as these result in very little or no runoff at all. The larger rainfall volumes however experience negligible bias.

The variability of the generated stochastic sequences is different for all percentiles.

6. DISCUSSION

The results show that the generated stochastic sequences from the adapted data – based model exhibit negligible bias on crucial rainfall statistics and therefore provide realistic uncertainty estimates. This is in line with the findings by Ndiritu (2013a) based daily rainfalls. Box plots of the generated stochastic sequences of the individual rainfalls indicate that the lowest rainfalls (< 20^{th} percentile) have the highest variability and experience the most significant bias.

This study further investigates the impact of the selection of rain gauge groups on the generated stochastic sequences. It is found that the rain gauge groups selected have an impact on the value of the scaling factor obtained, the variability of the generated sequences as well as degree of bias on the standard deviation and skewness values. The value of the scaling factor in some instances may be non-unique and in other cases even greater than 1. Scaling factors that are greater than 1 are considered to be unrealistic and are an indication of inappropriate rain gauge combinations.

A correlation-based method of initiating the rain gauge grouping is evaluated and is found to yield results with generally the least bias and variability. The correlation between any pair of stations considered in this study was generally high, and is perhaps a consequence of all the stations being within the same rainfall zones. The importance of this approach therefore needs to be assessed in catchments where there the rain gauges have poorer correlations. It is important to note however that a low correlation between the estimated catchment average rainfall and point rainfall does not mean the point rainfall is less representative considering the complex dynamics of the rainfall process. It could be that the rainfall station is in an area predominantly receiving rainfall of a different type from the other stations but could still be contributing to the overall catchment rainfall substantially.

A scaling factor was found to exist between the average cumulative probability plots computed from various rain gauge densities. The generated sequences in this study are based on averaging without considering time alignment (see Section 4.2). The importance of time aligned averaging in this study may have been minimised due to the rainfall stations lying within the same rainfall zone. The impact of time aligned averaging and averaging without considering time alignment needs to be investigated further, particularly for catchments where the correlation between the rain gauges is low and also when dealing with daily rainfalls. Table 5.3 shows that the lowest rainfalls generally exhibit the highest variability. Time aligned averaging may potentially reduce the degree of bias in these rainfalls in the event that these rainfalls are of vital importance. For instance in semi – arid regions, where a small change in precipitation may result in a significant change in streamflow.

Willems (2001) assumed that the estimation error in areal rainfall based on the densest rainfall network can be neglected. Unlike Willems (2001) the model by (Ndiritu, 2013a) assumes that the areal rainfall estimation is error free only when the catchment rain guage density represents a full rain guage density i.e. a rain guage density that is able to accurately capture the temporal, spatial and magnitudinal characteristics of rainfall. Consequently, unless this condition is fulfilled, the catchment average rainfall obtained using all rainfall stations also needs to be perturbed.

During the demonstration, it was assumed that the scaling factor required to reduce the variability of areal rainfall estimate from 8 to 16 rainfall stations equates the scaling factor required to reduce the variability of 4 stations to 8 stations. An alternative would be to assume that the uncertainty factor is equivalent to the largest scaling factor obtained between the various rain gauge densities (i.e. 8, 4, 2 and 1), as this is likely to yield results with the largest perturbations. Only once some information is available regarding a full capacity rain gauge can the magnitude of the scaling factor be more precisely determined.

Montanari (2007) stated that a suitable method of uncertainty quantification must be able to take into account any type of useful information. In areal rainfall estimation the most valuable information is the measured rainfall depths themselves. These rainfall depths give unique information related to the exposure, elevation, orientation, landslope and orography of the area surrounding each rainfall station and the measured differences can be associated with the dynamics of the rain events. However, the accuracy of the information provided by each station reduces as the distance between the stations increases. Unless the rain gauge network is able to fully capture the spatial variability of rainfall over a catchment, reasonable assumptions have to be made to aid the estimation of areal rainfall uncertainty. On this basis, the adapted data – based stochastic areal rainfall generator provides reasonable uncertainty estimates in monthly areal rainfall based on point rainfall measurements.

7. CONCLUSIONS AND RECOMMENDATIONS

The objective of this research was to determine demonstrate a data – based model of quantifying realistic uncertainty estimates in areal rainfall estimates based on point rainfall measurements in Southern Africa, for water resource modelling applications.

The data – based model by Ndiritu (2013a) was identified as a simple, effective, non – parametric method of incorporating uncertainty in monthly areal rainfall estimations. This model by Ndiritu (2013a) was formulated for daily rainfalls and due to the influence of storm periods on areal rainfall characteristics, the assumptions made during the formulation of the model needed to be evaluated.

The influence of the coarser monthly time scale on the following key elements of the model was therefore investigated:

1. The scaling factor (see Section 2.1) between cumulative probability plots of the differences in monthly areal rainfall at various rain gauge densities and
2. The relationship between the average proportion of missed monthly rainfalls and rain gauge density.

The adapted data – based model was tested on 8 catchments across South Africa that varied in terms of topography and climatic conditions.

A scaling factor was found to exist between cumulative probability plots at various rain gauge densities. However, the value of the scaling factor is affected by the selected rain gauge combinations. Ndiritu (2013a) selected the rain gauges in each group with the aim of achieving a uniform catchment coverage. This objective though can lead to a number of rain gauge combinations. A correlation-based method of selecting the rain gauges is therefore proposed. The method is based on the determination of the rain gauges with most representative catchment average rainfall obtained using all available rainfall stations, identified as the key stations. These stations are obtained by computing the correlation between the rain gauge and the catchment average rainfall. The key stations are paired with the remaining stations with the aim of ensuring the best estimate of areal rainfall and then grouped with other station pairs with the aim of ensuring a uniform catchment coverage. This rain gauge selection method generally provided the most reasonable uncertainty estimates although this was not always the case.

The influence of the longer averaging period on the relationship between the average proportion of zero rainfalls and the rain gauge density is also evaluated. The relationship is found to be nonlinear and best approximated by the power function. The constants of the function are dependent on the rain gauges selected in each group. The proportion of zero monthly rainfalls is generally low and minimal benefit can be gained by activating the rainfall infilling component of the model.

Box plots of the generated stochastic areal rainfall sequences were developed and it is found that the mean monthly rainfalls remain unbiased. However the selected rain gauge combinations affect the variability of the generated stochastic sequences and the degree of bias on the standard deviation and skewness; although the degree of bias in most instances was negligible. Consequently, the adapted data – based model by Ndiritu (2013a) provides realistic uncertainty estimates. The correlation based method of rain gauge grouping yielded the least biased results for 6 out of the 8 catchments considered. This showed that the selection of rain gauge groups using the correlation based method is a more suitable method of selecting the rain gauges in each group although does not always provide the most ideal results. Replications of individual monthly rainfalls showed that the lowest monthly storm volumes (< 20^{th} percentile) experienced the most significant bias and variability. The importance of these rainfalls must be assessed relative to their use as they are likely to lead to biased model results. It is hypothesized that time aligned averaging may reduce the degree of bias of these rainfalls.

The following work is recommended on the stochastic areal rainfall generator in future studies:

1. Determining how the rainfall infilling component of the model can be adapted to infill monthly rainfalls especially in the regions that experience low rainfall with high variability.
2. The data - based model does not take into consideration measurement errors in the point rainfall measurement and it is recommended that investigations be undertaken towards extending the model to incorporate uncertainties due to measurement errors. This includes errors associated with wind, rainfall splashing, clogging of orifices and funnels and others.
3. Test the applicability of the model on catchments with rain gauges that exhibit more variable rainfall characteristics than those applied in this analysis.
4. Investigate the influence of other methods (other than the inverse distance weighting methods used in this study) of determining the catchment average rainfall using the correlation-based method of selecting rain gauges within each group.
5. Investigate the impact of incorporating monthly areal rainfall uncertainties using the data - based stochastic areal rainfall generator on water resource modelling applications.
6. Test the data – based model using catchments with very high rain gauge density.
7. Aggregate the daily stochastic rainfalls generated using the daily model by Ndiritu (2013a) and compare these with the results obtained from the monthly model.
8. Investigate the influence of time – aligned averaging particularly at shorter time scales (weeks or days). The variation of the rainfall at these time scales may be

significant and may have a greater influence on the value of the computed scaling factor and the degree of bias in the small rainfall volumes.

8. REFERENCES

Ajami, N.K., Duan, Q., Sorooshian, S., (2007) **An integrated hydrologic Bayesian multi – model combination framework: Confronting input, parameter and model structural uncertainty in hydrological prediction**. Water Resources Research. 43. DOI: 10.1029/2005WR004745.

Alvarez, F. and Henry, W.K. (1970) **Rainguge spacing and reported rainfall**. International Association of Scientific Hydrology Bulletin. 15 (1), p97 – 107.

Anagnostopoulou, C., Tolika, K., Maheras, P., Reiser, H. and Kutiel, H. (2008) **Quantifying uncertainties in precipitation: a case study from Greece**. Advances in Geosiences. 16, p19 – 26. http://www.adv-geosci.net/16/19/2008.

Bell, V.A. and Moore, R.J.(2000) **The sensitivity of catchment runoff models to rainfall data at different spatial scale,** Hydrol. And Earth Sciences. 4 (4) p653 – 667.

Chen, F.W. and Liu, C.W. (2012) **Estimation of the spatial rainfall distribution using inverse distance weighting in the middle of Taiwan**. Paddy Water Environment. 10 (3), p 209 – 222.

Cheng, C., Cheng, S., Wen, J. and Lee, J. (2012) **Effects of Rain gauge distribution on Estimation Accuracy of Areal Rainfall**. Water Resources Management. 26, p1 – 20. DOI: 10.1007/S11269 – 011 – 9898 – 7.

Dent, M.C., Lynch, S.D., Schulze, R.E. (1987) **Mapping the Mean Annual and other Rainfall Statistics over Southern Africa**. Pretoria, South Africa. Water Research Commission, WRC Report No. 27.

Department of Water Affairs (2012) **Proposed National Water Resource Strategy 2: Managing water for an equitable and sustainable future**. Pretoria, South Africa. Department of Water Affairs.

Department of Water Affairs (2013) **National Water Resource Strategy.** South Africa's water situation and strategies to balance supply and demand of the Usutu to Mhlatuze Water Management Area. Pretoria.

Dihlabeng (2010). **Integrated Development Plan**. Dihlabeng Local Municipality.

Dreaver, K.R. and Hutchinson, P. (1974) **Random and systematic errors in precipitation at an exposed site**. Journal of Hydrology. 13 (1), p54 - 63.

Dlamini, L. (2013) **Modelling standardized precipitation index using remote sensing for improved drought monitoring**. Unpublished M.Sc thesis. University of the Witwatersrand. Johannesburg, South Africa.

Eagleson., P.S. (1970) **Dynamic Hydrology: The Stochastic Nature of point precipitation**. Massachusetts Institute of Technology. McGraw Hill Book Company.

Central Karoo District Municipality (2010) **Integrated Development Plan**. Central Karoo District Municipality.

Fekete, B.M., Vorosmarty C.J., Roads O.J. and Willmott C.J. (2003) **Uncertainties in precipitation and their impacts on runoff estimates.** Journal of Climate. 17(1), p274 - 304.

George Municipality (2013) **Spatial Development Framework**. George Municipality Planning Department.

Hughes, D.A. (1995) **Monthly rainfall – runoff models applied to arid and semiarid catchments for water resource estimation purposes**. Hydrological Sciences Journal. 40 (6), p751 – 769.

Hughes, D.A (2004) **Three decades of hydrological modeling research in South Africa**. South African Journal of Science. 100 (1), p638 – 642.

Hughes, D.A., Kapangaziwiri, E. and Sawunyama T. (2010) **Hydrological model uncertainty assessment in southern Africa.** Journal of Hydrology. 387(1). p221 – 232. DOI: 10.1016/j.jhydrol.2010.04.010.

Hughes, D.A., Kapangaziwiri, E., Mallory, S.J.L., Wagener, T. and Smithers, J.C. (2011) **Incorporating uncertainty in water resources simulation and Assessment tools in South Africa.** Pretoria, South Africa. Water Research Commission, WRC Report No. 1838/1/11.

Hutchinson, P. (1969). **Estimation of rainfall in sparsely gauged areas**. Bulletin of the International Association of Scientific Hydrology. 14 (1), p101 – 119.

Jackson, I. (1969) **The persistence of rainfall gradients over small areas of uniform relief**. E. Afr. Geogr. Rev. 7 (1), p37 – 43.

Jones, S. B. (1983) **The estimation of catchment average point rainfalls**. Institute of Hydrology. Report No. 87.

Kapangaziwiri, E. and Hughes, D.A. (2008) **Towards a revised physically based parameter estimation methods for the Pitman monthly rainfall – runoff model**. Pretoria, South Africa. Water Research Commssion. Water SA, 34 (2), p183 – 192.

Klemes, V. (2002) **Common sense and other hersies chapter 2.3: Stochastic Models of Rainfall Runoff relationship**. Canadian Water Resources Association.

Klemes, V. (2002) **Common sense and other hersies chapter 4.2: Hydrological Uncertainty in Water Management Context**. Canadian Water Resources Association.

Lanza, L.G., Ramirez, J.A. and Todini, E. (2001) **Stochastic rainfall interpolation and downscaling**. Hydrology and Earth Systems. 5 (2), p139 – 143.

Layberry, R., Williams, C.J.R. and Kniveton, D.R. (2007) **Climatic and Oceanic associations with daily rainfall extremes over southern Africa**. International Journal of Climatology. 27 (1), p93 - 108

Linsley, R.K, Jr., Kohler, M.A. and Paulhus, J.L.H. (1975) **Hydrology for Engineers Second Edition**. McGraw Hill Series in water resources and environmental engineering. Tokyo, Japan.

Lumsden, T.G., Schulze, R.E. and Hewitson, B.C. (2009) **Evaluation of potential changes in hydrologically relevant statistics of rainfall in southern Africa under conditions of climate change.** Pretoria, South Africa. Water Research Commission, Water SA, 35 (5), p649 – 656.

Lynch, S.D (2004) **Development of a Raster Database of Annual, Monthly and daily rainfall for Southern Africa. Water Research Commission**. Pretoria, South Africa. Water Research Commission, WRC Report No 1156/1/04.

Malzbender, P. and Earle, A. (2006) **Water Resources of the SADC: Demands, Dependencies and Governance Responses**. Cape Town, South Africa African Centre for Water Research.
http://www.acwr.co.za/pdf_files/IGD_Water%20Resources.pdf

Menne, T.C. (1961) **The Role of Hydrology in planning the development of a country**. Inter African Conference on hydrology. Publication 66, p27 – 35.

Midgley, D.C. (1961) **Use of precipitation data by the civil engineer**. Inter African Conference on hydrology. Publication 66, p87 – 93.

M'Marete, C.K. (2003) **Climate and Water Resources of Limpopo Province**. Agriculture as a cornerstone of the economy in the Limpopo province: A study commissioned by the economic cluster of the Limpopo province government under the leadership of the department of agriculture. p1 – 49.

McMillan, H., Jackson, B., Clark, M., Kavetski, D. and Woods, R. (2011) **Rainfall uncertainty in hydrological modeling: an evaluation of multiplicative use error models**. Journal of Hydrology. 400, p83 – 94. DOI: 10.1016/j.jhydrol.2011.01.026.

Middleton, B.J. and Bailey, A.K. (2005) **Water Resources of South Africa, 2005 Study (WR 2005)**. Pretoria, South Africa. Water Research Commission, WRC Report Number TT 381/08.

Mopani District Municipality (2011) **Integrated Development Plan**. Mopani District Municipality.

Montanari, A. (2007) **What do we mean by 'uncertainty'? The need for a consistent wording about uncertainty assessment in hydrology.** Hydrological Processes. 21, p841 – 845. DOI: 10.1002/hyp.6623.

Morrissey, M.L., Maliekal, J.A., Greene, J.S. and Wang, J. (1995) **The uncertainty of simple spatial averages using rain gauge networks**. Water Resources Research. 31 (8), p2011 – 2017.

Mwelwa, E.M. (2004) **The Application of the Monthly time step Pitman Rainfall – Runoff Model to the Kafue River Basin of Zambia**. Unpublished M.Sc thesis. Rhodes University.Grahamstown. South Africa.

Nandalal, K.D.W. (2010) **Engineering hydrology lecture notes**. Department of Civil Engineering, University of Paradeniya. Paradeniya.

Ndiritu, J. (2013a) **Using data – derived perturbations to incorporate uncertainty in generating stochastic areal rainfall from point rainfalls**. Hydrological Sciences Journal. 58 (8), p1704-1717.

Ndiritu, J. (2013b) **A multiplier based method of generating stochastic areal rainfall from point rainfalls. http://dx.doi.org/10.1016/j.pce.2013.09.010**

Ngongondo, C., Xu, C., Gottshalk, B.A. and Alemaw, B. (2011) **Evaluation of spatial and temporal characteristics of rainfall in Malawi**. Theory Appl Climatol. 106, p79 – 93. doi 10.1007/s00704 – 011 – 0413 – 0.

Nkonkobe Municipality (2010) **Spatial Development Framework**. Nkonkobe Municipality.

Nyabeze, W.R.R (1999) **Development of a methodology for drought frequency analysis using sub – catchments in Zimbabwe**. Unpublished M.Sc thesis. University of the Witwatersrand. Johannesburg, South Africa.

Pappenberger, F. and Beven, K.J. (2006) **Ignorance is bliss: Or seven reasons not to use uncertainty analysis.** Water Resources Research. 42 (W05302), p1 – 8.

Pitman, W.V. (1973) **A Mathematical Model for Generating Monthly River Flows from Meteorological Data in southern Africa**. University of the Witwatersrand, HRU, Report 2/73.

Refsgaard, J.C. And Henriksen, H. J. (2004) **Modelling guidelines - terminology and guiding principles**. Advances in Water Resources. 27 (1), p71– 82. DOI: 10.1016/j.adwatres.2003.08.006.

Renard, B., Kavetski, D. Kuczera, G. Thyer, M., Franks, S.W.(2010) **Understanding predictive uncertainty in hydrologic modelling: The challenge of identifying input and structural errors**. Water Resources Research. 46 (W05521), p1 – 22.

Riechle, R.H., Walker, J.P., Koster., R.D., Houser., P.R. (2002) **Extended versus ensemble Kalman filtering for land data assimilation**. Journal of Hydrometerology. 3 (6), p728 – 740.

Sejamoholo, B. and Lillie, E. (2004) **Business support for the inclusion of rainfall records into the rain ims**. Pretoria, South Africa. Department of Water Affairs internal report.

Singh, P.V. and Chowhury, P.K. (1986) **Comparing some methods of estimating mean areal rainfall**. Water Resources Bulletin: American Water Resources Association. 22 (2), p275 – 282.

Sivapalan, M, Tekeuchi, K., Franks, S.W., Karambiri, H., Lakshmi, V., Liang, X., Oki, T., Pomeroy, J.W., Schertzer,D., Uhlenbrook, S. and Zehe, E. (2003) **IAHS Decade on Predictions in Ungauged Basins (PUB), 2003 – 2012: Shaping an exicting future for Hydrological Sciences.** Hydrological Sciences Journal. 48 (6), p857 – 880.

South African Weather Service. (2013) **Climate Services and SAWS**. Presentation by Mahlobo, D., Kruger., A., Funde, S. and Phakula, S. Document Reference: CLS – CI – 001 – 2012 – 04 – 11.

Srikanthan, R. and McMahon, T.A. (2001) **Stochastic generation of annual, monthly and daily climate data: A review**. Hydrology and Earth Sciences. 5(4), p653 – 670.

Silberstein, R.P. (2006) **Hydrological models are so good, do we still need data?** Environmental modelling and Software. 21(1), p1340 – 1352.

Steiner, M (1996) **Uncertainty of estimates of monthly areal rainfall for temporally sparse remote observations**. Water Resources Research. 32 (2), p373 – 388.

Sutcliff, J.V. (1966) **The assessment of random errors in areal rainfall estimation**. International Association of Scientific Hydrology Bulletin. 11 (3), p35 – 42.

Turton, A (undated) **The State of Water Resources in Southern Africa: What the Beverage Industry needs to know**. Pretoria, South Africa. Council of Science and Industrial Research (CSIR).
http://www.anthonyturton.com/admin/my_documents/my_files/8F6_The_State_of_Water_Resources_in_Southern_Africa1.pdf

United Nations Educational, Scientific and Cultural Organization (2002) **Water Resource Systems Planning and Management: An Introduction to Methods, Models and Applications**. UNESCO publishing. The Netherlands.

United Nations Educational, Scientific and Cultural Organization (2005) **FRIEND – a global perspective 1998 - 2002**. Centre for Ecology and Hydrology. UNESCO Publishing. Wallingford, UK.

Valimba, P. (2004) **Rainfall variability in southern Africa, its influences on streamflow variations and its relationships with climatic variations.** Unpublished Ph.D thesis. Rhodes University. Grahamstown, South Africa.

Vogel, R. (2013) **Quantifying the uncertainty of spatial precipitation analyses with radar – gauge observation ensembles**. Zurich, Switzerland. Federal Office of Meterorology and Climatology, Scientific Report MeteoSwiss No. 95.

Vrugt, J.A., Braak, C.J.F, Hyman, J.M. And Robinson, B.A. (2008) **Treatment of input uncertainty in hydrologic modeling: Doing Hydrology backward with Markov chain Monte Carlo simulation** Water Resources Research. 44 (W00B09), p1 – 15.

Wagner, T., Sivaplan, M., Troch, P., and Woods, R. (2007) **Catchment classification and Hydrologic Similarity**. Geography Compass. 1(4), p 901 – 931.

Warburton, M. and Schulze, R. (2005) **Historical precipitation trends over Southern Africa: A Hydrology Perspective**. Water Research Commision. WRC Report 1430/1/05, Chpt 19, p325 – 338.

Willems, P. (2001) **Stochastic description of the rainfall input errors in lumped hydrological models**. Stochastic Environmental Research and Risk Assessment. 15 (2), p132 – 152.

Winter, C.L. (2004) **Stochastic Hydrology: practical alternatives exist.** Stochastic Environmental Research and Risk assessment. 18, p282 - 284. DOI: 10.1007/s00477 – 004 – 0198 – 0.

Xu, H., Xu, C., Chen, H., Zhang, Z., and Li, L. (2013) **Assessing the influence of rain gauge density and distribution on hydrological model performance in a humid region of China**. Journal of Hydrology. 505, p1 – 12. http://dx.doi.org/10.1016/j.jhydrol.2013.09.004

APPENDIX A

BALFOUR

0077881A												
	Jan	Feb	Mar	Apr	May	Jun	Jul	Aug	Sep	Oct	Nov	Dec
Mean (10mm)	1057.8	1197	1424.6	668.8	504	299.2	344	301.1	703.4	935	1236	1149
Standard Deviation (10mm)	451.08	576	585.48	670.4	528	243	349	243.6	497.5	511	849	531
Minimum (10mm)	223	522	452	0	74	0	15	0	144	115	307	435
Maximum (10mm)	1995	2985	2560	3067	2460	888	1654	800	1974	2484	3766	2772
Skewness	0.3283	1.62	0.0579	1.982	2.64	0.957	2.4	0.428	1.157	1.13	1.56	1.2
Coefficient of Variation	0.4264	0.48	0.411	1.002	1.05	0.812	1.02	0.809	0.707	0.55	0.69	0.46

0078153W												
	Jan	Feb	Mar	Apr	May	Jun	Jul	Aug	Sep	Oct	Nov	Dec
Mean (10mm)	949.5	1001	1197	574	423	244	282	264	614.32	787	1044	1082.7
Standard Deviation (10mm)	365.1	465.7	576.5	418	414	195	263	198	427.58	385.4	611.5	503.9
Minimum (10mm)	249	461	500	18	48	0	28	6	61	242	239	366
Maximum (10mm)	2126	2245	2765	1708	1813	860	1411	858	1609	1737	2657	2351
Skewness	0.977	1.189	0.752	1.36	2.27	1.25	2.81	1.02	0.8555	0.768	1.052	0.7375
Coefficient of Variation	0.384	0.465	0.482	0.73	0.98	0.8	0.93	0.75	0.696	0.49	0.586	0.4654

0078272W												
	Jan	Feb	Mar	Apr	May	Jun	Jul	Aug	Sep	Oct	Nov	Dec
Mean (10mm)	652.61	654.4	880.7	455.9	241	166.58	210	202	397.2	478.45	665	635.94
Standard Deviation (10mm)	323.54	376.2	528	366.1	202	132.84	228	190	314.4	302.81	545	428.87
Minimum (10mm)	0	0	0	36	0	0	0	0	0	0	0	0
Maximum (10mm)	1285	1582	2204	1444	938	427	1173	916	1156	1245	2367	1604
Skewness	0.358	0.635	0.522	1.173	1.66	0.6059	2.8	1.92	0.967	0.4566	1.37	0.4296
Coefficient of Variation	0.4958	0.575	0.6	0.803	0.84	0.7974	1.08	0.94	0.792	0.6329	0.82	0.6744

0078279W												
	Jan	Feb	Mar	Apr	May	Jun	Jul	Aug	Sep	Oct	Nov	Dec
Mean (10mm)	454.29	541	768.77	376	319	177.65	197	183	365.4	441.6	643	601.13
Standard Deviation (10mm)	262.92	369	431.29	360	375	170.64	218	188	296.6	272	495	376.44
Minimum (10mm)	99	94	66	0	0	0	0	0	0	0	0	25
Maximum (10mm)	1067	1666	1692	1550	1458	581	1163	723	1161	954	2286	1472
Skewness	0.586	1.3	0.3804	1.67	2.16	0.9803	3.06	1.21	0.899	0.333	1.48	0.6091
Coefficient of Variation	0.5787	0.68	0.561	0.96	1.17	0.9605	1.11	1.03	0.812	0.616	0.77	0.6262

0078453W												
	Jan	Feb	Mar	Apr	May	Jun	Jul	Aug	Sep	Oct	Nov	Dec
Mean (10mm)	535.7	583.6	873.87	418.13	342	194	233	168	366	437.9	666	650.161
Standard Deviation (10mm)	351.2	368.1	498.53	369.89	313	194	263	178	317	264.4	461	447.549
Minimum (10mm)	101	0	46	13	0	0	0	0	0	0	28	15
Maximum (10mm)	1278	1422	2006	1304	1517	802	1197	770	1386	1065	2045	1846
Skewness	0.849	0.815	0.3833	0.9992	2.1	1.43	2.09	1.35	1.57	0.604	1.06	0.72093
Coefficient of Variation	0.656	0.631	0.5705	0.8846	0.91	1	1.13	1.06	0.87	0.604	0.69	0.68837

0078755W												
	Jan	Feb	Mar	Apr	May	Jun	Jul	Aug	Sep	Oct	Nov	Dec
Mean (10mm)	1487	1363	1473.9	802.52	586	392.6	432	410	905.8	1186	1501	1534.4
Standard Deviation (10mm)	553.1	515.4	695.44	630.61	441	273.3	391	395	565.3	497.8	766	690.16
Minimum (10mm)	533	477	390	0	0	0	25	46	23	261	236	320
Maximum (10mm)	3026	2719	2929	2194	2131	1028	1884	1838	2483	2536	4232	2845
Skewness	0.687	0.888	0.628	0.9871	1.69	0.426	1.86	1.94	0.853	0.483	1.38	0.4252
Coefficient of Variation	0.372	0.378	0.4718	0.7858	0.75	0.696	0.9	0.96	0.624	0.42	0.51	0.4498

0100060W												
	Jan	Feb	Mar	Apr	May	Jun	Jul	Aug	Sep	Oct	Nov	Dec
Mean (10mm)	467.94	642.81	738.94	433	407	194	270	209	391.4	453.4	715.3	606
Standard Deviation (10mm)	284.84	404.07	367.31	416	435	223	272	213	293.8	308.8	602.3	445.2
Minimum (10mm)	41	0	0	0	0	0	0	0	0	0	0	0
Maximum (10mm)	1150	1521	1480	1811	1901	838	1212	909	1160	1292	2338	1783
Skewness	0.565	0.6381	0.0953	1.42	2.13	1.38	1.64	1.21	0.923	0.609	1.074	0.763
Coefficient of Variation	0.6087	0.6286	0.4971	0.96	1.07	1.15	1.01	1.02	0.751	0.681	0.842	0.735

0100329A												
	Jan	Feb	Mar	Apr	May	Jun	Jul	Aug	Sep	Oct	Nov	Dec
Mean (10mm)	1246	1206	1423.8	643	437	241	284	297	715.52	878.6	1242	1331.4
Standard Deviation (10mm)	539	541	569.55	478	375	184.2	256	230	457.29	410.2	721	608.28
Minimum (10mm)	291	633	523	61	68	5	33	0	44	241	297	370
Maximum (10mm)	3209	2806	2950	2119	1630	784	1293	1016	1775	1822	3454	2775
Skewness	1.51	1.54	0.429	1.41	2.05	0.965	2.17	1.13	0.7995	0.7	1.31	0.4543
Coefficient of Variation	0.43	0.45	0.4	0.74	0.86	0.764	0.9	0.77	0.6391	0.467	0.58	0.4569

BARBERTON

0518589W												
	Jan	Feb	Mar	Apr	May	Jun	Jul	Aug	Sep	Oct	Nov	Dec
Mean (10mm)	1734	1389.7	1083.5	735.82	283	109	127	206	456	1151.4	1846	2064.2
Standard Deviation (10mm)	862.2	945.16	585.7	415.5	222.7	173	179	259	363	524.06	542.37	893.51
Minimum (10mm)	558	376	170	119	0	0	0	0	57	388	478	736
Maximum (10mm)	3893	3437	2400	1535	789	773	703	1169	1645	2238	3007	4329
Skewness	0.777	1.0443	0.5162	0.2129	0.981	2.88	1.97	2.6	1.68	0.634	-0.2596	0.6661
Coefficient of Variation	0.497	0.6801	0.5405	0.5647	0.787	1.59	1.41	1.26	0.8	0.4552	0.2938	0.4329

0518676W												
	Jan	Feb	Mar	Apr	May	Jun	Jul	Aug	Sep	Oct	Nov	Dec
Mean (10mm)	1686.5	1435	1294.5	742.4	268	94	109.3	162	390	1062.77	1752	1742.5
Standard Deviation (10mm)	764.514	747.4	825.11	460.2	253	133	146	302	371	469.476	658.2	819.26
Minimum (10mm)	615	495	150	27	0	0	0	0	0	335	595	570
Maximum (10mm)	3390	3102	3055	2040	1070	510	507	1338	1458	2188	3390	3565
Skewness	0.81975	0.85	0.667	0.763	1.73	2.04	1.352	2.97	1.13	0.61931	0.405	0.5918
Coefficient of Variation	0.45331	0.521	0.6374	0.62	0.95	1.41	1.335	1.86	0.95	0.44175	0.376	0.4702

0518759W												
	Jan	Feb	Mar	Apr	May	Jun	Jul	Aug	Sep	Oct	Nov	Dec
Mean (10mm)	1342	1044	954.05	597.3	255.95	65.9	79.6	159	264.32	846.14	1320.1	1567.2
Standard Deviation (10mm)	785.7	537	493.05	462.1	232.63	126	121	256	260.91	387.67	534.71	754.71
Minimum (10mm)	300	455	160	0	0	0	0	0	0	205	297	442
Maximum (10mm)	3330	2365	2123	1460	750	530	415	958	895	1737	2403	2913
Skewness	1.177	1.009	0.5584	0.249	0.8521	2.61	1.61	1.98	0.6629	0.3232	0.0299	0.3424
Coefficient of Variation	0.585	0.514	0.5168	0.774	0.9089	1.92	1.52	1.61	0.9871	0.4582	0.4051	0.4816

0518822W												
	Jan	Feb	Mar	Apr	May	Jun	Jul	Aug	Sep	Oct	Nov	Dec
Mean (10mm)	1224	1067	899.2	558.45	246.227	91.7	60.1	157	270	771.64	1274.7	1567
Standard Deviation (10mm)	654.5	615.3	557.5	403.52	225.179	161	97.4	295	299	393.08	463.33	741
Minimum (10mm)	360	210	80	12	0	0	0	0	0	145	201	377
Maximum (10mm)	2801	2440	1732	1536	727	661	328	1098	1240	1560	2045	3190
Skewness	1.041	0.981	0.179	0.4425	1.00036	2.5	2.01	2.27	1.53	0.3464	-0.6581	0.814
Coefficient of Variation	0.535	0.576	0.62	0.7226	0.91452	1.75	1.62	1.87	1.11	0.5094	0.3635	0.473

0518859W												
	Jan	Feb	Mar	Apr	May	Jun	Jul	Aug	Sep	Oct	Nov	Dec
Mean (10mm)	1181	1112.1	806.91	653.91	216	96.2	86.86	153	308	785	1341.2	1299
Standard Deviation (10mm)	821	586.35	443.76	476.6	212	153	117.1	230	364	341.2	622.41	645.12
Minimum (10mm)	285	110	150	0	0	0	0	0	0	325	284	455
Maximum (10mm)	3990	2218	1835	1605	718	601	365	800	1325	1625	2655	2587
Skewness	1.85	0.2538	0.5728	0.5468	1.22	2.43	1.402	1.65	1.6	0.993	0.2009	0.3194
Coefficient of Variation	0.7	0.5272	0.5499	0.7288	0.98	1.59	1.348	1.51	1.18	0.435	0.4641	0.4966

0518886W												
	Jan	Feb	Mar	Apr	May	Jun	Jul	Aug	Sep	Oct	Nov	Dec
Mean (10mm)	1042	1089.2	703.8	617.5	235	91.1	75.7	142	322	757.8	1189.9	1368.2
Standard Deviation (10mm)	568.9	589.76	433.1	431.5	229	144	120	255	342	396.9	444.28	634.08
Minimum (10mm)	280	155	180	15	0	0	0	0	0	200	278	340
Maximum (10mm)	2482	2460	1860	1475	970	565	380	947	1389	1714	1872	2897
Skewness	0.998	0.5752	1.008	0.38	1.7	2.19	1.58	2.23	1.47	1.067	-0.2617	0.2771
Coefficient of Variation	0.546	0.5414	0.615	0.699	0.97	1.58	1.58	1.8	1.06	0.524	0.3734	0.4634

0519134W												
	Jan	Feb	Mar	Apr	May	Jun	Jul	Aug	Sep	Oct	Nov	Dec
Mean (10mm)	932	931.1	692.5	562.8	232	87.8	64.9	121	276	653	1052	1306
Standard Deviation (10mm)	538.2	545.6	492	434.1	239	151	111	254	300	338	448.2	618.15
Minimum (10mm)	250	298	67	0	0	0	0	0	0	233	187	356
Maximum (10mm)	2208	2214	1752	1332	934	575	387	1123	1123	1590	2156	2516
Skewness	1.042	1.17	0.593	0.321	1.43	2.41	2.16	3.07	1.24	1.24	0.354	0.131
Coefficient of Variation	0.577	0.586	0.711	0.771	1.03	1.73	1.71	2.11	1.09	0.52	0.426	0.4733

0519310W												
	Jan	Feb	Mar	Apr	May	Jun	Jul	Aug	Sep	Oct	Nov	Dec
Mean (10mm)	1290.6	1005	692.82	526.9	252	112	85.7	127	292	698	1107	1231.59
Standard Deviation (10mm)	984.82	681.4	411.75	356	234.28	158	141	215	352	460	600	542.272
Minimum (10mm)	105	294	110	39	0	0	0	0	0	120	78	306
Maximum (10mm)	3597	2835	1505	1075	780	630	505	925	1475	2035	2814	2264
Skewness	0.9064	1.233	0.4125	0.197	0.9514	2.1	2.28	2.57	1.79	1.45	0.79	-0.04056
Coefficient of Variation	0.7631	0.678	0.5943	0.676	0.9297	1.41	1.64	1.7	1.21	0.66	0.542	0.4403

GEORGE

0014393W												
	Jan	Feb	Mar	Apr	May	Jun	Jul	Aug	Sep	Oct	Nov	Dec
Mean (10mm)	809	650	842	794	888	742.44	754.528	1071.8	863	872.6	860.92	710
Standard Deviation (10mm)	419	367	506	568	549	451.64	532.105	485.69	496	426.3	510.63	422
Minimum (10mm)	210	72	190	117	132	85	20	317	128	100	124	241
Maximum (10mm)	2350	1675	2479	2875	2545	1840	2118	2250	2518	2036	2260	2155
Skewness	1.59	1.33	1.38	2	1.06	0.4871	0.73891	0.5089	1.56	0.517	0.6915	1.71
Coefficient of Variation	0.52	0.56	0.6	0.72	0.62	0.6083	0.70522	0.4532	0.58	0.489	0.5931	0.6

0014633W												
	Jan	Feb	Mar	Apr	May	Jun	Jul	Aug	Sep	Oct	Nov	Dec
Mean (10mm)	456	478	579	590	654.6	552.2	552.08	828.7	581.3	629	643.64	388
Standard Deviation (10mm)	390	413	426	457	440.7	350.5	396.25	458	362.2	382	460.98	277
Minimum (10mm)	0	110	11	75	80	25	0	162	15	75	38	65
Maximum (10mm)	1715	2128	1805	2145	1825	1455	1410	2055	1640	1715	1715	1295
Skewness	1.61	2.24	1.3	1.65	0.95	0.784	0.6046	0.891	0.959	1.12	0.6982	1.17
Coefficient of Variation	0.86	0.86	0.74	0.77	0.673	0.635	0.7177	0.553	0.623	0.61	0.7162	0.71

0029805W												
	Jan	Feb	Mar	Apr	May	Jun	Jul	Aug	Sep	Oct	Nov	Dec
Mean (10mm)	743	766	811	651	709	531	546.4	849	702	817	827	653
Standard Deviation (10mm)	437	505	446	491	530	389	454.6	608	501	494.69	556	438
Minimum (10mm)	20	215	193	188	127	13	38	127	177	207	115	60
Maximum (10mm)	2066	2563	2605	2452	2645	1653	1810	2943	2880	2075	2876	1996
Skewness	1.3	1.87	1.87	2.09	1.75	1.19	1.192	1.53	2.78	0.8074	1.7	1.35
Coefficient of Variation	0.59	0.66	0.55	0.75	0.75	0.73	0.832	0.72	0.71	0.6055	0.67	0.67

0030088W												
	Jan	Feb	Mar	Apr	May	Jun	Jul	Aug	Sep	Oct	Nov	Dec
Mean (10mm)	844	764	913	764	718.9	547.7	675.1	957	775	919.5	872.5	745
Standard Deviation (10mm)	431	475	499.4	493	477.1	361	538.2	655	416	472.4	476.2	378
Minimum (10mm)	290	255	167	162	0	28	31	205	225	255	132	235
Maximum (10mm)	2030	2555	2260	2545	1955	1484	2155	3352	2402	2009	2300	2185
Skewness	1.11	2.2	0.854	1.97	0.826	0.958	1.01	1.87	1.87	0.648	0.844	1.63
Coefficient of Variation	0.51	0.62	0.547	0.65	0.664	0.659	0.797	0.68	0.54	0.514	0.546	0.51

0030090W												
	Jan	Feb	Mar	Apr	May	Jun	Jul	Aug	Sep	Oct	Nov	Dec
Mean (10mm)	741.5	623	775.4	730	786	638.8	656.58	857	713	793.3	727.56	605
Standard Deviation (10mm)	409.7	389	429.6	509	529	427.7	433.55	506	409	445.7	436.63	327
Minimum (10mm)	118	110	165	185	160	43	0	45	120	100	115	130
Maximum (10mm)	1790	2246	1903	2698	2257	1760	1721	2296	1979	1951	1910	1880
Skewness	0.926	2.33	0.956	2.01	1.09	0.802	0.7014	1.27	1.14	0.898	0.5866	1.64
Coefficient of Variation	0.553	0.62	0.554	0.7	0.67	0.67	0.6603	0.59	0.57	0.562	0.6001	0.54

0030265W												
	Jan	Feb	Mar	Apr	May	Jun	Jul	Aug	Sep	Oct	Nov	Dec
Mean (10mm)	998	932	980.6	896	882	707	799	1227	926.3	1058.9	1033	860
Standard Deviation (10mm)	455	488	467.1	703	561	492	568	780	423.7	528.72	503.8	381
Minimum (10mm)	273	422	212	155	120	19	40	232	277	235	240	270
Maximum (10mm)	2409	2464	2403	3523	3034	2530	2306	4156	2209	2390	2526	2130
Skewness	1.22	1.61	0.828	2.61	1.66	1.69	1.27	1.73	0.856	0.8201	0.939	1.22
Coefficient of Variation	0.46	0.52	0.476	0.78	0.64	0.7	0.71	0.64	0.457	0.4993	0.488	0.44

0030446W												
	Jan	Feb	Mar	Apr	May	Jun	Jul	Aug	Sep	Oct	Nov	Dec
Mean (10mm)	811.92	693	821.9	697	673	520.4	587.1	892	737	842.1	793.1	668
Standard Deviation (10mm)	441	373	465.9	516	505	349.7	441.2	574	417	454.1	435.8	325
Minimum (10mm)	185	225	215	105	135	3	30	180	215	155	180	167
Maximum (10mm)	1851	1999	2150	2550	2610	1525	1733	2650	2095	2073	1827	1870
Skewness	0.4796	1.74	0.858	2.05	1.93	1.109	1.102	1.43	1.22	0.889	0.817	1.45
Coefficient of Variation	0.5432	0.54	0.567	0.74	0.75	0.672	0.751	0.64	0.57	0.539	0.55	0.49

0030775W												
	Jan	Feb	Mar	Apr	May	Jun	Jul	Aug	Sep	Oct	Nov	Dec
Mean (10mm)	829	816	868	659	639	460	565	875	679	818	790.4	629.11
Standard Deviation (10mm)	445.23	515	504.5	486	528	330.3	512	659	456	562.9	520.2	302.43
Minimum (10mm)	106	115	99	64	35	8	0	106	92	170	30	170
Maximum (10mm)	1873	2705	2424	2425	2674	1435	2008	2835	1925	2347	2259	1360
Skewness	0.4048	1.78	0.76	2.15	1.88	1.052	1.38	1.08	1.11	1.291	0.995	0.7117
Coefficient of Variation	0.5371	0.63	0.581	0.74	0.83	0.718	0.91	0.75	0.67	0.688	0.658	0.4807

LIEBENBERGSVLEI

0297721W												
	Jan	Feb	Mar	Apr	May	Jun	Jul	Aug	Sep	Oct	Nov	Dec
Mean (10mm)	1138.5	808.4	901.8	605.73	326.23	116	137	128.85	293	940	935.077	917.7
Standard Deviation (10mm)	613.54	370.3	542.2	348.72	300.03	191	202	162.32	453	729.04	411.681	509.4
Minimum (10mm)	290	280	110	0	0	0	0	0	0	100	0	170
Maximum (10mm)	2710	1729	2300	1270	1020	660	820	520	2390	2640	1728	2260
Skewness	0.5684	0.825	0.617	0.0711	0.8882	1.88	1.83	1.1266	4	0.72	-0.14843	0.697
Coefficient of Variation	0.5389	0.458	0.601	0.5757	0.9197	1.64	1.48	1.2598	1.55	0.7756	0.44026	0.555

0298512W												
	Jan	Feb	Mar	Apr	May	Jun	Jul	Aug	Sep	Oct	Nov	Dec
Mean (10mm)	1379	1015.3	964	549.9	259	130	129	140.8	364	880	969.54	1123
Standard Deviation (10mm)	647	512.71	609	304.9	314	232	216	203	540	579	598.04	595.9
Minimum (10mm)	509	260	43	26	0	0	0	0	0	90	58	300
Maximum (10mm)	3126	2165	2761	1362	1475	1016	915	605	2810	2838	2148	2940
Skewness	1.037	0.7474	1.01	0.652	2.4	2.49	2.31	1.287	3.74	1.61	0.3712	0.812
Coefficient of Variation	0.469	0.505	0.63	0.554	1.22	1.78	1.68	1.441	1.48	0.66	0.6168	0.531

0331474W												
	Jan	Feb	Mar	Apr	May	Jun	Jul	Aug	Sep	Oct	Nov	Dec
Mean (10mm)	1058.3	865.5	782	583.96	311	110	159	84	290	800.08	794.3	1030.7
Standard Deviation (10mm)	498.53	555.6	535	390.08	393	244	284	166	556	562.43	453.4	555.54
Minimum (10mm)	305	0	157	0	0	0	0	0	0	0	25	89
Maximum (10mm)	2024	1879	2455	1389	1653	1021	1107	638	2916	2055	2062	2323
Skewness	0.3276	0.245	1.22	0.3368	1.82	2.61	2.06	2.28	4.27	0.5649	0.646	0.2676
Coefficient of Variation	0.4711	0.642	0.68	0.668	1.27	2.21	1.79	1.98	1.92	0.703	0.571	0.539

0331554W												
	Jan	Feb	Mar	Apr	May	Jun	Jul	Aug	Sep	Oct	Nov	Dec
Mean (10mm)	1105.08	791.6	874.7	487.92	286	105	137	89	296	764.4	767.231	966.85
Standard Deviation (10mm)	639.11	378.5	374.5	296.21	350	171	231	118.6	519	545.6	308.134	469.64
Minimum (10mm)	259	166	61	0	0	0	0	0	0	35	125	157
Maximum (10mm)	2593	1509	1820	1021	1287	648	951	367	2716	2208	1466	1684
Skewness	0.80112	0.175	0.607	0.174	1.54	2.14	2.44	1.231	4.1	0.878	-0.08613	-0.1827
Coefficient of Variation	0.57834	0.478	0.428	0.6071	1.22	1.63	1.69	1.333	1.75	0.714	0.40162	0.4857

0331740W												
	Jan	Feb	Mar	Apr	May	Jun	Jul	Aug	Sep	Oct	Nov	Dec
Mean (10mm)	1244.3	789.19	870.69	597.04	311	125	129	119.08	299	814.3	851.62	1111.62
Standard Deviation (10mm)	599.26	373.05	554.66	339.56	336	200	229	145.78	477	530.8	344.94	575.579
Minimum (10mm)	460	198	104	0	0	0	0	0	0	76	74	140
Maximum (10mm)	2569	1577	1974	1189	1270	761	1006	445	2520	2004	1640	2122
Skewness	0.5946	0.483	0.6111	0.1598	1.51	2.15	2.61	1.0177	4.08	0.659	-0.2352	-0.01037
Coefficient of Variation	0.4816	0.4727	0.637	0.5687	1.08	1.6	1.78	1.2243	1.6	0.652	0.405	0.51779

0331828W												
	Jan	Feb	Mar	Apr	May	Jun	Jul	Aug	Sep	Oct	Nov	Dec
Mean (10mm)	1219.5	752.88	860	582	287.9	100	124	107.9	277	779.7	852.1	1058.4
Standard Deviation (10mm)	700.75	354.31	516.8	323.91	303.4	175	208	148.1	442	546	386.7	536.09
Minimum (10mm)	271	246	135	0	0	0	0	0	0	99	20	133
Maximum (10mm)	2823	1579	1937	1174	1125	678	854	425	2324	2072	1723	2154
Skewness	0.695	0.7183	0.723	0.0612	1.224	2.46	2.43	1.135	4.03	0.796	-0.185	0.1365
Coefficient of Variation	0.5746	0.4706	0.601	0.5565	1.054	1.75	1.68	1.373	1.59	0.7	0.454	0.5065

0332206W												
	Jan	Feb	Mar	Apr	May	Jun	Jul	Aug	Sep	Oct	Nov	Dec
Mean (10mm)	1239	986.8	823	704.12	369.77	141	114	115	377	936.73	945.5	951.5
Standard Deviation (10mm)	464.6	586.1	525	377.55	377.19	238	189	159	529	575.43	546.7	471.88
Minimum (10mm)	739	124	6	55	0	0	0	0	0	71	0	132
Maximum (10mm)	2480	2531	2228	1387	1325	920	836	514	2722	2087	2306	2005
Skewness	1.017	0.884	1.09	0.0477	0.9535	2.26	2.53	1.23	3.53	0.5268	0.723	0.0993
Coefficient of Variation	0.375	0.594	0.64	0.5362	1.0201	1.69	1.65	1.38	1.4	0.6143	0.578	0.4959

0332349W												
	Jan	Feb	Mar	Apr	May	Jun	Jul	Aug	Sep	Oct	Nov	Dec
Mean (10mm)	1118	912	789.8	542.31	240	119	123	116.38	306	873	958	962
Standard Deviation (10mm)	639.8	406.4	433.3	390.91	263	214	223	151.31	471	501.4	437.8	571
Minimum (10mm)	38	303	160	0	0	0	0	0	0	84	127	158
Maximum (10mm)	3095	1935	1882	1445	1182	793	874	423	2483	1782	2305	2724
Skewness	0.959	0.7546	0.869	0.4202	1.99	2.09	2.13	1.0303	3.99	0.349	0.708	1.09
Coefficient of Variation	0.572	0.4456	0.549	0.7208	1.1	1.79	1.82	1.3001	1.54	0.574	0.457	0.59

LOUIS TRICHARDT

0722529W												
	Jan	Feb	Mar	Apr	May	Jun	Jul	Aug	Sep	Oct	Nov	Dec
Mean (10mm)	991	728.9	492.8	219.9	146.57	44.4	26.9	27.9	135	371.43	617.7	604.29
Standard Deviation (10mm)	788	554.67	379.5	216.76	194.38	73.9	65.5	81.7	204.6	329.05	322.1	385.05
Minimum (10mm)	65	0	0	0	0	0	0	0	0	0	150	0
Maximum (10mm)	3175	2044	1450	675	640	251	250	325	645	1127	1120	1520
Skewness	1.34	0.7011	0.79	0.7062	1.1032	1.72	2.51	3.04	1.399	0.9356	0.203	0.3945
Coefficient of Variation	0.8	0.761	0.77	0.9857	1.3262	1.66	2.44	2.93	1.516	0.8859	0.521	0.6372

00722571W												
	Jan	Feb	Mar	Apr	May	Jun	Jul	Aug	Sep	Oct	Nov	Dec
Mean (10mm)	1416	1213	676.5	324	210	93.5	38.8	119	193	451	877.3	890.4
Standard Deviation (10mm)	989	755.2	568.7	282	185.9	114	54.7	250	236	402	515.2	452.1
Minimum (10mm)	153	238	30	11	10	0	0	0	0	45	145	315
Maximum (10mm)	4368	2550	2258	1129	515	474	227	974	840	1749	1999	2110
Skewness	1.22	0.564	1.137	1.16	0.478	1.83	2.12	2.54	1.47	1.83	0.498	1.039
Coefficient of Variation	0.7	0.623	0.841	0.87	0.885	1.22	1.41	2.1	1.22	0.89	0.587	0.508

0722614W												
	Jan	Feb	Mar	Apr	May	Jun	Jul	Aug	Sep	Oct	Nov	Dec
Mean (10mm)	973.3	897.2	520	283	176.4762	62.3	22.7	66.4	140.952	403.6	694.5	711.81
Standard Deviation (10mm)	718.8	642.6	443	252.6	209.7566	139	43.9	149	197.639	273.8	394.8	294.97
Minimum (10mm)	70	160	0	0	0	0	0	0	0	0	221	260
Maximum (10mm)	2945	2560	1815	880	695	579	160	650	550	1070	1599	1320
Skewness	0.907	0.993	1.37	0.877	1.048212	2.89	2.03	3.15	1.26088	0.824	1.07	0.5631
Coefficient of Variation	0.739	0.716	0.85	0.893	1.188583	2.23	1.94	2.24	1.40217	0.678	0.568	0.4144

0722700W												
	Jan	Feb	Mar	Apr	May	Jun	Jul	Aug	Sep	Oct	Nov	Dec
Mean (10mm)	1026.4	855.5	560.7	207.14	148.1	48.4	22.9	55.6	122	354	644.4	716.29
Standard Deviation (10mm)	731.25	597.8	471	214.17	175.83	95.7	43.4	128	188	271	435.8	360.03
Minimum (10mm)	0	240	0	0	0	0	0	0	0	0	80	190
Maximum (10mm)	2535	2475	1745	630	515	360	130	535	620	1180	1500	1485
Skewness	0.6598	1.215	0.939	0.6814	0.9843	2.25	1.75	2.9	1.64	1.52	0.434	0.5972
Coefficient of Variation	0.7124	0.699	0.84	1.0339	1.1873	1.98	1.9	2.3	1.55	0.77	0.676	0.5026

0722721W												
	Jan	Feb	Mar	Apr	May	Jun	Jul	Aug	Sep	Oct	Nov	Dec
Mean (10mm)	1448.5	1356.2	797	343.71	224.5	98.286	59.6	97.2	246	420	904.48	899.1
Standard Deviation (10mm)	1064.3	932.25	662	306.44	219.9	110.09	85.3	201	452	386	611.47	461.3
Minimum (10mm)	150	233	0	0	0	0	0	0	0	30	85	285
Maximum (10mm)	4102	3565	2589	1020	635	355	280	762	1975	1640	2175	2055
Skewness	0.8623	0.8506	1.2	0.6965	0.628	0.9759	1.58	2.63	2.97	1.88	0.4801	0.627
Coefficient of Variation	0.7347	0.6874	0.83	0.8916	0.979	1.1201	1.43	2.07	1.84	0.92	0.676	0.513

0723070W												
	Jan	Feb	Mar	Apr	May	Jun	Jul	Aug	Sep	Oct	Nov	Dec
Mean (10mm)	1519.7	1382	878.9	384	200	91.3	51.3	86	217	500.1	833.2	959
Standard Deviation (10mm)	1159.3	909.2	652	346	207	140	63.9	127	311	302.7	504.9	509
Minimum (10mm)	20	63	53	0	0	0	0	0	0	50	86	429
Maximum (10mm)	4147	2924	2600	1490	694	525	232	404	1231	1200	1871	2508
Skewness	0.9077	0.425	1.031	1.62	1.17	2.26	1.61	1.57	2.04	0.581	0.43	1.76
Coefficient of Variation	0.7629	0.658	0.742	0.9	1.03	1.54	1.24	1.47	1.43	0.605	0.606	0.53

0723155W												
	Jan	Feb	Mar	Apr	May	Jun	Jul	Aug	Sep	Oct	Nov	Dec
Mean (10mm)	1463.4	1367	938.1	386.57	246	122.7	53.8	109.29	235	467	857.3	880.86
Standard Deviation (10mm)	993.45	1107	771.1	330.88	325	122.6	75	103.3	267	371	519.5	510.98
Minimum (10mm)	90	0	2	0	0	0	0	0	0	27	25	120
Maximum (10mm)	3925	4047	2935	1206	1245	440	300	370	1125	1655	1795	1855
Skewness	0.6438	1.053	1.11	0.8796	1.83	0.839	1.84	0.9236	1.88	1.64	0.338	0.3674
Coefficient of Variation	0.6789	0.81	0.822	0.8559	1.32	0.999	1.39	0.9453	1.13	0.79	0.606	0.5801

0723334W												
	Jan	Feb	Mar	Apr	May	Jun	Jul	Aug	Sep	Oct	Nov	Dec
Mean (10mm)	2054	1853	1173.3	483.81	311	116	47.6	107.7	347	669	1182.6	1221
Standard Deviation (10mm)	1457	1449	933.15	392.994	343	144	74	125.1	389	484	657.51	743
Minimum (10mm)	135	80	50	0	0	0	0	0	0	0	8	405
Maximum (10mm)	4920	4366	3163	1468	1285	635	265	415	1550	1897	2285	3735
Skewness	0.452	0.597	0.9671	0.71773	1.36	2.31	1.61	1.336	1.69	1	0.0873	1.99
Coefficient of Variation	0.709	0.782	0.7953	0.81229	1.1	1.24	1.56	1.161	1.12	0.72	0.556	0.61

MURRAYSBURG

0094513W												
	Jan	Feb	Mar	Apr	May	Jun	Jul	Aug	Sep	Oct	Nov	Dec
Mean (10mm)	318	383.8	660	287.17	285	127.21	151.1	131	78.5	212	287.96	255.5
Standard Deviation (10mm)	376	360.6	513.9	214.39	260.52	111.94	189.1	136	94	238	225.56	265.5
Minimum (10mm)	0	0	0	0	0	0	0	0	0	0	0	0
Maximum (10mm)	1590	1341	1920	715	880	370	645	485	335	975	760	870
Skewness	2	1.053	1.217	0.5169	0.7228	0.7051	1.227	1.4	1.45	1.53	0.6079	0.7367
Coefficient of Variation	1.18	0.94	0.779	0.7466	0.9141	0.88	1.251	1.04	1.2	1.12	0.7833	1.0391

0094578W												
	Jan	Feb	Mar	Apr	May	Jun	Jul	Aug	Sep	Oct	Nov	Dec
Mean (10mm)	306	351	663	308.88	297.71	170.21	174.96	268	79.96	265	293.38	239.5
Standard Deviation (10mm)	415	318.56	551.4	222.9	276.6	150.42	203.9	319	88.78	274	224.59	250.8
Minimum (10mm)	0	0	0	25	0	0	0	0	0	0	0	0
Maximum (10mm)	1429	1142	2028	758	979	497	618	1159	305	1215	762	951
Skewness	1.75	0.8074	1.063	0.7396	0.9008	0.8232	1.0552	1.93	1.019	1.93	0.5277	1.007
Coefficient of Variation	1.36	0.9076	0.832	0.7217	0.9291	0.8837	1.1654	1.19	1.11	1.03	0.7655	1.047

0094730W												
	Jan	Feb	Mar	Apr	May	Jun	Jul	Aug	Sep	Oct	Nov	Dec
Mean (10mm)	390	413	703.3	392.5	361.9	224	180.3	325	163	365	388	317.67
Standard Deviation (10mm)	476	405	529.8	270.1	293.7	199	213.7	433	170	334	349	318.34
Minimum (10mm)	0	0	0	0	0	0	0	11	0	0	13	0
Maximum (10mm)	1746	1613	1917	1126	1064	803	785	1932	640	1477	1467	1052
Skewness	1.85	1.44	0.912	0.639	0.911	1.38	1.304	2.67	1.46	1.7	1.53	0.899
Coefficient of Variation	1.22	0.98	0.753	0.688	0.811	0.89	1.185	1.33	1.05	0.92	0.9	1.0021

0095006W												
	Jan	Feb	Mar	Apr	May	Jun	Jul	Aug	Sep	Oct	Nov	Dec
Mean (10mm)	490.25	448	694.21	424	314	201.2	166	296	129	305	298.21	288
Standard Deviation (10mm)	477.38	416	489.57	328	273	163.5	204	372	153	249	243.48	283
Minimum (10mm)	0	0	0	0	0	0	0	10	0	0	30	0
Maximum (10mm)	1505	1560	1745	1300	1075	605	750	1401	630	1000	825	1110
Skewness	0.8268	1.25	0.7715	1.23	1.24	1.133	1.52	1.96	1.76	1.12	0.7472	1.3
Coefficient of Variation	0.9737	0.93	0.7052	0.77	0.87	0.813	1.23	1.26	1.19	0.81	0.8165	0.98

0095123W												
	Jan	Feb	Mar	Apr	May	Jun	Jul	Aug	Sep	Oct	Nov	Dec
Mean (10mm)	477	405	784.88	417.5	359	219.5	183	328	148.6	338.58	361.13	383
Standard Deviation (10mm)	496	299	553.22	265.883	314	186.8	228	450	141.4	262.02	277.78	327
Minimum (10mm)	0	0	0	0	0	13	0	0	0	0	45	0
Maximum (10mm)	1908	1465	1981	1041	1365	700	875	1935	520	950	945	1270
Skewness	1.48	1.71	0.6661	0.50321	1.46	1.081	1.65	2.57	1.16	0.9286	0.7986	1.25
Coefficient of Variation	1.04	0.74	0.7048	0.63685	0.87	0.851	1.24	1.37	0.952	0.7739	0.7692	0.85

0117447W												
	Jan	Feb	Mar	Apr	May	Jun	Jul	Aug	Sep	Oct	Nov	Dec
Mean (10mm)	317	385	572.88	304.75	204.63	103	121	115	54.25	158	274.33	227
Standard Deviation (10mm)	408	404	453.75	273.42	194.5	103	172	141	65.85	151.3	235.8	241.11
Minimum (10mm)	0	0	0	2	0	0	0	0	0	0	0	0
Maximum (10mm)	1458	1830	1501	989	653	415	630	505	243	585	783	810
Skewness	1.76	2.09	0.6985	0.8105	0.8564	1.48	1.7	1.49	1.202	1.024	0.7866	1.0271
Coefficient of Variation	1.29	1.05	0.7921	0.8972	0.9505	1.01	1.42	1.23	1.214	0.957	0.8595	1.0621

0117749W												
	Jan	Feb	Mar	Apr	May	Jun	Jul	Aug	Sep	Oct	Nov	Dec
Mean (10mm)	329	375.4	609	317.46	209.9	111	111	98.13	67.5	175.08	293	233.83
Standard Deviation (10mm)	380	339.9	484.16	243.05	233.2	105.8	167	127.8	76.074	183.09	276.42	232.78
Minimum (10mm)	0	0	0	0	0	0	0	0	0	0	0	0
Maximum (10mm)	1441	1280	1665	695	808	383	604	448	249	587	895	749
Skewness	1.67	1.01	0.6947	0.0613	1.07	1.218	1.76	1.371	0.7084	0.9359	0.9814	0.8719
Coefficient of Variation	1.15	0.905	0.795	0.7656	1.111	0.954	1.5	1.302	1.127	1.0457	0.9434	0.9955

0118029W												
	Jan	Feb	Mar	Apr	May	Jun	Jul	Aug	Sep	Oct	Nov	Dec
Mean (10mm)	466.3	384.25	709.792	382.7	266.75	195.9	131.7	271.9	75.29	272	329.75	310.75
Standard Deviation (10mm)	496.7	315.78	517.891	332.3	274.92	207.9	214.4	530.8	107	317.6	284.6	281.09
Minimum (10mm)	0	0	0	0	0	0	0	0	0	0	0	0
Maximum (10mm)	1790	1020	1964	1194	924	744	1040	2650	351	1210	1050	893
Skewness	1.188	0.6929	0.95486	1.353	1.2841	1.316	3.386	3.963	1.598	1.661	0.9274	0.7578
Coefficient of Variation	1.065	0.8218	0.72964	0.868	1.0306	1.062	1.629	1.952	1.421	1.168	0.8631	0.9045

PRIESKA

0224734W												
	Jan	Feb	Mar	Apr	May	Jun	Jul	Aug	Sep	Oct	Nov	Dec
Mean (10mm)	210	323.7	487.7	309.1	114	58	57.09	29.7	35.9	166.97	154	205
Standard Deviation (10mm)	283	274.6	432.9	344.3	185	120	90.55	95.1	73.6	180.93	197	384
Minimum (10mm)	0	0	0	0	0	0	0	0	0	0	0	0
Maximum (10mm)	1364	1123	1661	1217	909	554	290	480	345	562	735	2126
Skewness	2.41	1.084	0.979	1.258	2.73	2.8	1.338	3.96	2.72	0.9874	1.51	3.87
Coefficient of Variation	1.35	0.848	0.888	1.114	1.63	2.07	1.586	3.2	2.05	1.0836	1.28	1.87

0225065W												
	Jan	Feb	Mar	Apr	May	Jun	Jul	Aug	Sep	Oct	Nov	Dec
Mean (10mm)	240	362	436	360.5	131	50.9	53.3	38.8	50.4	173	193.7	151
Standard Deviation (10mm)	280	327	409	354.56	204	93.4	89.2	96.6	90.6	184	217	183
Minimum (10mm)	0	0	0	0	0	0	0	0	0	0	0	0
Maximum (10mm)	1320	1336	1604	1215	942	405	375	507	432	769	802	730
Skewness	2.05	1.36	1.47	1.1017	2.55	2.59	2.13	3.78	2.68	1.6	1.329	1.51
Coefficient of Variation	1.17	0.9	0.94	0.9835	1.55	1.84	1.67	2.49	1.8	1.06	1.12	1.21

0225118W												
	Jan	Feb	Mar	Apr	May	Jun	Jul	Aug	Sep	Oct	Nov	Dec
Mean (10mm)	249.1	335.3	432	300.26	106	72.4	67.3	45.9	50.3	145.265	182	130
Standard Deviation (10mm)	299.2	272.7	390	320.16	160	122	115	107	121	172.698	228	166
Minimum (10mm)	0	0	0	0	0	0	0	0	0	0	0	0
Maximum (10mm)	1143	1110	1625	1017	581	420	405	536	475	550	920	711
Skewness	1.12	0.864	1.37	1.0115	1.59	1.67	1.79	3.31	2.58	1.07446	1.86	1.83
Coefficient of Variation	1.201	0.813	0.9	1.0663	1.51	1.69	1.71	2.34	2.41	1.18885	1.25	1.28

0225311W												
	Jan	Feb	Mar	Apr	May	Jun	Jul	Aug	Sep	Oct	Nov	Dec
Mean (10mm)	207	323	409	311.8	148	53.5	54	37.9	44.3	161	207.1	192
Standard Deviation (10mm)	250	253	374	309.3	207	94.3	101	97.9	87	149	219.2	220.3
Minimum (10mm)	0	0	0	0	0	0	0	0	0	0	0	0
Maximum (10mm)	1047	1074	1511	1095	863	375	500	564	381	671	745	862
Skewness	1.96	1.05	1.46	1.041	2.25	2.12	2.93	4.77	2.45	1.18	1.239	1.199
Coefficient of Variation	1.21	0.78	0.92	0.992	1.4	1.76	1.88	2.58	1.97	0.93	1.059	1.147

0225395W												
	Jan	Feb	Mar	Apr	May	Jun	Jul	Aug	Sep	Oct	Nov	Dec
Mean (10mm)	254	378.06	485.471	384	136	57.4	50.6	46.3	54.5	174.6	215	237
Standard Deviation (10mm)	287	323.33	418.714	394	202	96.7	88.9	112	90.1	167.5	260	261
Minimum (10mm)	0	0	0	0	0	0	0	0	0	0	0	0
Maximum (10mm)	1325	1156	1509	1757	882	400	400	603	310	584	1165	1115
Skewness	2.39	0.8231	0.87693	1.57	2.54	2.08	2.4	4.02	1.6	0.867	1.88	1.59
Coefficient of Variation	1.13	0.8552	0.86249	1.03	1.48	1.69	1.76	2.42	1.65	0.959	1.21	1.1

0225413W												
	Jan	Feb	Mar	Apr	May	Jun	Jul	Aug	Sep	Oct	Nov	Dec
Mean (10mm)	228.18	266.3	413.06	293.5	119	54.9	53.2	37.3	43.5	140	180	163.3
Standard Deviation (10mm)	239.5	237.5	375.96	349.6	166	111	85.7	99.4	84.3	182	205	185.1
Minimum (10mm)	0	0	0	0	0	0	0	0	0	0	0	0
Maximum (10mm)	770	893	1202	1201	678	475	325	510	368	721	851	713
Skewness	0.9871	1.095	0.8166	1.331	1.77	2.56	1.79	3.61	2.37	1.87	1.36	1.275
Coefficient of Variation	1.0496	0.892	0.9102	1.191	1.39	2.02	1.61	2.67	1.94	1.3	1.14	1.134

0225540W												
	Jan	Feb	Mar	Apr	May	Jun	Jul	Aug	Sep	Oct	Nov	Dec
Mean (10mm)	219	346	383.26	292	120	65.9	61.7	57.3	50	144.4	202	160
Standard Deviation (10mm)	291	325	340.22	340	163	108	99.3	112	88.7	137.9	222	184
Minimum (10mm)	0	0	0	0	0	0	0	0	0	0	0	0
Maximum (10mm)	1430	1343	1150	1275	713	355	360	569	414	500	928	791
Skewness	2.45	1.6	0.716	1.44	2.14	1.8	1.69	3.15	2.57	1.029	1.42	1.5
Kurtosis	7.33	2.28	-0.5551	1.11	4.57	2.02	1.89	11.7	7.31	0.133	1.8	2.47
Coefficient of Variation	1.33	0.94	0.8877	1.17	1.35	1.64	1.61	1.95	1.78	0.955	1.1	1.15

0225679W												
	Jan	Feb	Mar	Apr	May	Jun	Jul	Aug	Sep	Oct	Nov	Dec
Mean (10mm)	248	337	446	348.5	157	58.2	62.9	53.8	58.3	199	227	188
Standard Deviation (10mm)	309	367	459	379.2	268	98.8	121	127	98.7	217	301	246
Minimum (10mm)	0	0	0	0	0	0	0	0	0	0	0	0
Maximum (10mm)	1247	1559	1816	1328	1144	417	470	683	349	1083	1363	970
Skewness	1.51	1.41	1.45	1.186	2.85	2.21	2.35	3.88	1.85	2.15	2.13	1.72
Coefficient of Variation	1.25	1.09	1.03	1.088	1.71	1.7	1.92	2.36	1.69	1.09	1.33	1.31

TZANEEN

0678776W												
	Jan	Feb	Mar	Apr	May	Jun	Jul	Aug	Sep	Oct	Nov	Dec
Mean (10mm)	1650	1530	907.8	486	176.889	126	127	110	207	630.18	1165	1286
Standard Deviation (10mm)	1129	1366	702.24	449	212.358	213	299	167	221	341.95	575.1	728.5
Minimum (10mm)	73	150	45	0	0	0	0	0	0	170	60	233
Maximum (10mm)	4988	7280	2713	2451	696	838	1875	850	1011	1475	3009	3329
Skewness	1.23	2.10	0.98	2.15	1.07	2.19	4.73	2.66	1.77	0.65	0.57	1.11
Coefficient of Variation	0.68	0.89	0.77	0.92	1.20	1.69	2.36	1.52	1.07	0.54	0.49	0.57

0678836W												
	Jan	Feb	Mar	Apr	May	Jun	Jul	Aug	Sep	Oct	Nov	Dec
Mean (10mm)	2033	2015	1164	593	229.6	181	152	176	360	797.3	1446	1590
Standard Deviation (10mm)	1395	1741	753.14	473	229	223	241	188	314	427.8	602.7	710
Minimum (10mm)	155	260	0	30	0	0	0	0	0	260	205	470
Maximum (10mm)	5785	9477	3110	2670	835	980	1340	840	1245	1980	2940	3550
Skewness	1.14	2.21	0.83	2.24	1.17	2.02	3.13	1.73	1.39	0.95	0.47	1.02
Coefficient of Variation	0.69	0.86	0.65	0.80	1.00	1.23	1.59	1.07	0.87	0.54	0.42	0.45

0678 858W												
	Jan	Feb	Mar	Apr	May	Jun	Jul	Aug	Sep	Oct	Nov	Dec
Mean (10mm)	6011.5	3482	2361.7	1071	396.4	356.8	313	287.1	522.33	1112.9	1891.5	2703.6
Standard Deviation (10mm)	12800	2253	1643	816.8	456.3	438.4	474	303.1	467.44	606.53	882.91	1400.2
Minimum (10mm)	927	40	317	27	0	0	0	0	15	105	447	545
Maximum (10mm)	66361	9500	7451	4485	2316	2110	2492	1327	1922	2758	4772	6864
Skewness	4.3324	0.628	1.1565	1.92	2.21	1.93	2.824	1.666	1.2546	0.5473	0.9492	1.0431
Coefficient of Variation	2.1292	0.647	0.6957	0.763	1.151	1.229	1.514	1.056	0.8949	0.545	0.4668	0.5179

0679086W												
	Jan	Feb	Mar	Apr	May	Jun	Jul	Aug	Sep	Oct	Nov	Dec
Mean (10mm)	2678.4	1729	1266	598.9	206.3	159.3	122.4	110.4	263.7	620.11	1295.6	1688
Standard Deviation (10mm)	4167.3	1367	926	508.4	211.1	261.4	198	144.8	335.5	353.02	676.36	919.48
Minimum (10mm)	311	149	130	0	0	0	0	0	0	80	210	409
Maximum (10mm)	28381	6636	3968	2240	862	1042	1068	750	1630	1445	3216	4781
Skewness	5.3873	1.507	1.059	1.671	1.453	2.34	3.013	2.298	2.138	0.5243	0.8725	0.9633
Coefficient of Variation	1.5559	0.791	0.731	0.849	1.023	1.641	1.618	1.312	1.272	0.5693	0.5221	0.5447

0679141W												
	Jan	Feb	Mar	Apr	May	Jun	Jul	Aug	Sep	Oct	Nov	Dec
Mean (10mm)	3454.7	2205	1741	841.6	316.4	187.7	148.6	182.1	391.1	979.9	1675.1	2216.04
Standard Deviation (10mm)	7040.1	1406	1275.8	782.1	350.9	243	241.5	198.1	403.2	605.8	838.23	1185.01
Minimum (10mm)	455	0	260	32	0	0	0	0	0	50	394	330
Maximum (10mm)	48171	7434	5818	4481	1540	1246	1350	895	1780	3265	4053	5303
Skewness	5.888	1.177	1	2.679	1.607	2.199	3.258	1.532	1.709	1.255	0.747	0.70177
Coefficient of Variation	2.0378	0.638	0.7328	0.929	1.109	1.295	1.626	1.088	1.031	0.618	0.5004	0.53474

0679164W												
	Jan	Feb	Mar	Apr	May	Jun	Jul	Aug	Sep	Oct	Nov	Dec
Mean (10mm)	2944.6	2139	1445	661.8	267	162.5	157.2	130.4	307.2	721.2	1321.9	1703.47
Standard Deviation (10mm)	4901.5	1346.7	1065	558.7	331.4	200.9	264.7	160	362.6	472.1	688.1	865.864
Minimum (10mm)	303	186	134	0	0	0	0	0	0	116	225	469
Maximum (10mm)	33681	6481	5192	2632	1793	817	1368	754	1605	2250	2796	3914
Skewness	5.6611	0.9672	1.471	1.614	2.565	1.325	3.071	1.787	1.95	1.366	0.4086	0.66022
Coefficient of Variation	1.6646	0.6296	0.737	0.844	1.241	1.236	1.684	1.227	1.18	0.655	0.5205	0.50829

0679197W												
	Jan	Feb	Mar	Apr	May	Jun	Jul	Aug	Sep	Oct	Nov	Dec
Mean (10mm)	2706.1	1905	1309	622.7	237	172	128.2	142.7	265	683.02	1333.4	1727
Standard Deviation (10mm)	4569.6	1293	1146	582.3	253.7	240.7	206.3	149.9	355.1	443.5	712.36	1065
Minimum (10mm)	306	230	45	35	0	0	0	0	0	50	95	0
Maximum (10mm)	31251	6533	6405	3325	1085	1275	1165	665	1655	1910	3060	5140
Skewness	5.593	1.241	2.252	2.55	1.814	2.482	3.25	1.596	2.25	1.009	0.4438	1.022
Coefficient of Variation	1.6886	0.679	0.875	0.935	1.071	1.399	1.61	1.051	1.34	0.6493	0.5342	0.617

0679267W												
	Jan	Feb	Mar	Apr	May	Jun	Jul	Aug	Sep	Oct	Nov	Dec
Mean (10mm)	3394.2	2168	1747.4	726.2	291.3	231.111	180.2	165.5	436.5	933.33	1851	2289.8
Standard Deviation (10mm)	6177.4	1437	1231	593.6	311.3	284.822	283.7	191.7	444.6	525.77	1098	1073.2
Minimum (10mm)	490	173	185	63	0	0	0	0	0	142	341	407
Maximum (10mm)	42701	6994	4829	2677	1391	965	1492	908	1828	2418	6198	4715
Skewness	5.9048	1.058	1.0417	1.573	1.7	1.15532	2.692	2.122	1.966	0.9634	1.997	0.3275
Coefficient of Variation	1.82	0.663	0.7044	0.817	1.069	1.2324	1.574	1.158	1.019	0.5633	0.593	0.4687

APPENDIX B

FIGURE B1

Balfour Catchment_Combination 1_Rain gauge groupings

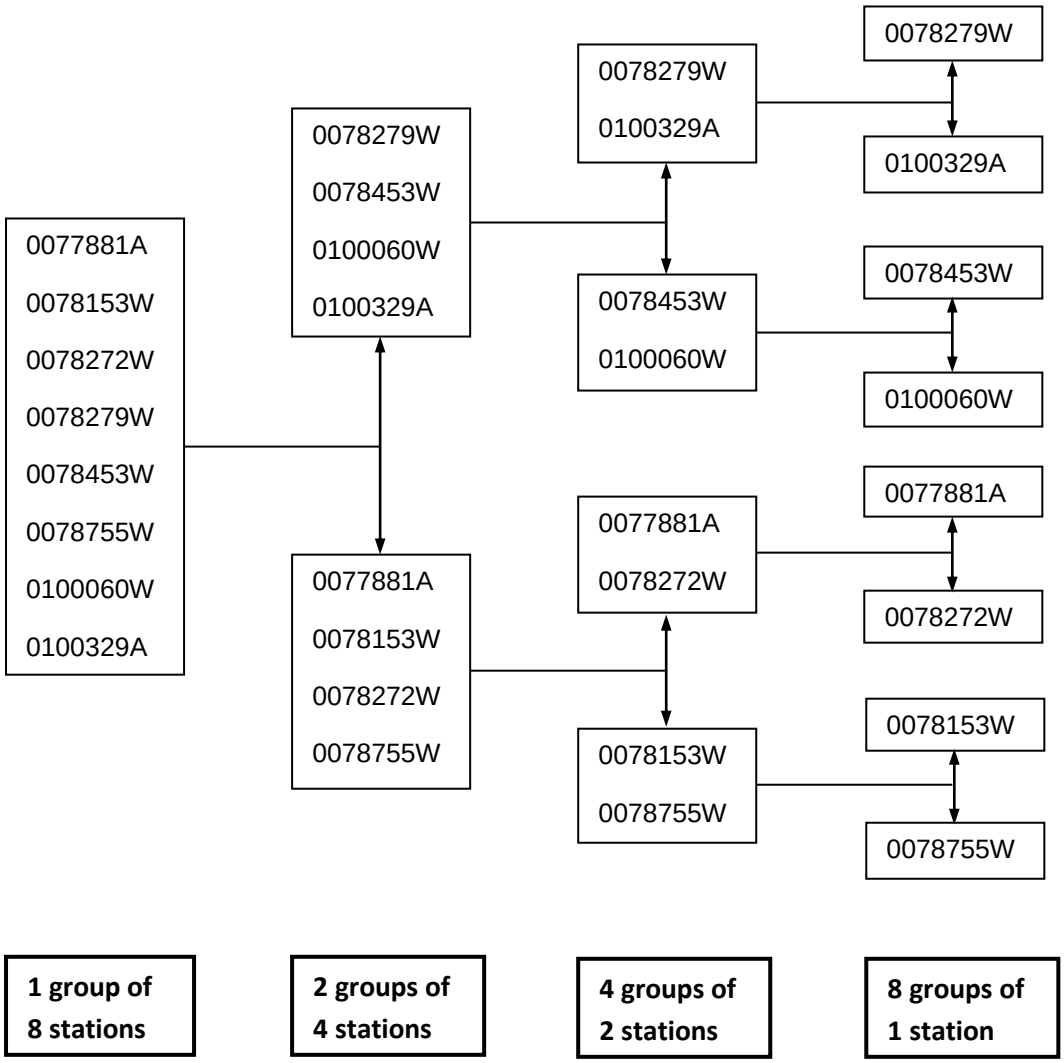

FIGURE B2

Balfour Catchment_Combination 2_Rain gauge groupings

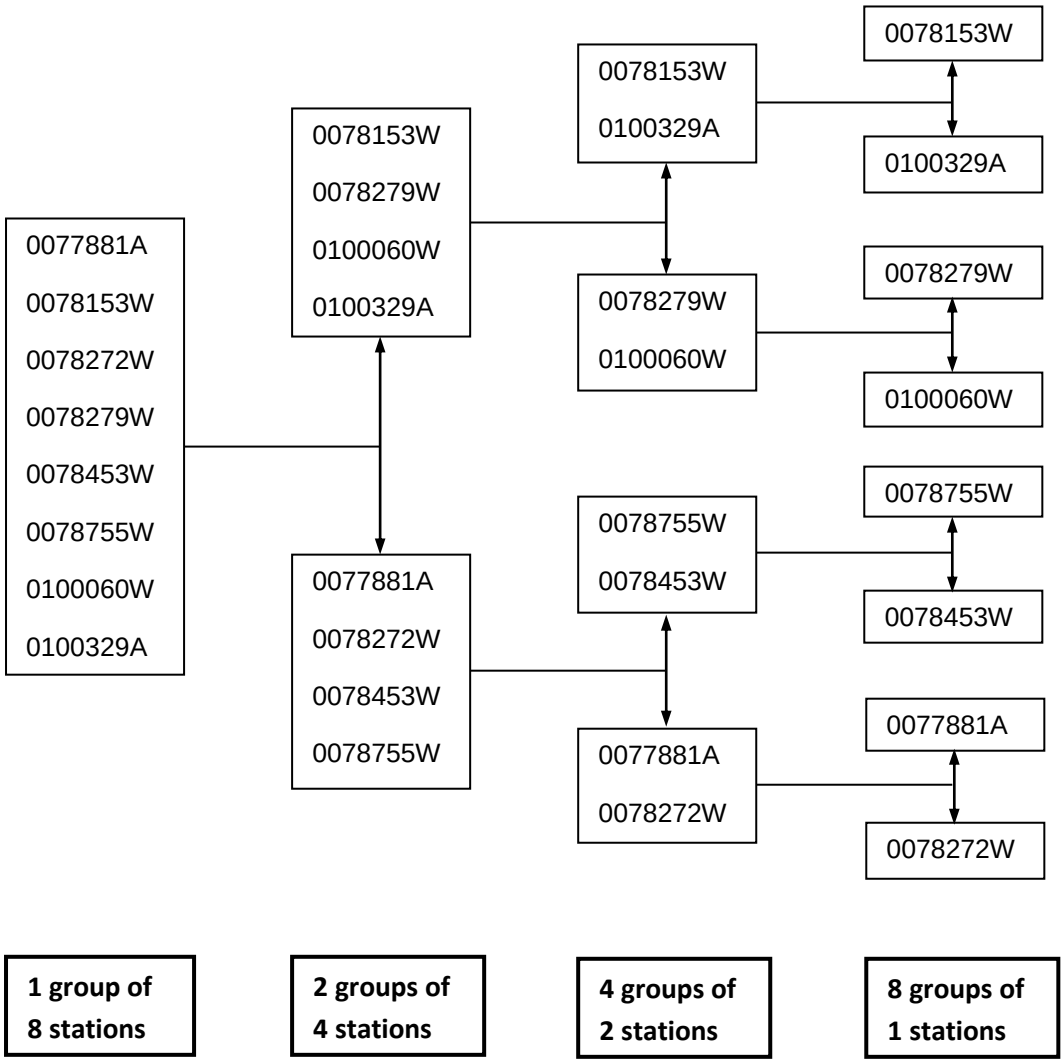

FIGURE B3

Balfour Catchment_Combination 3_Rain gauge groupings

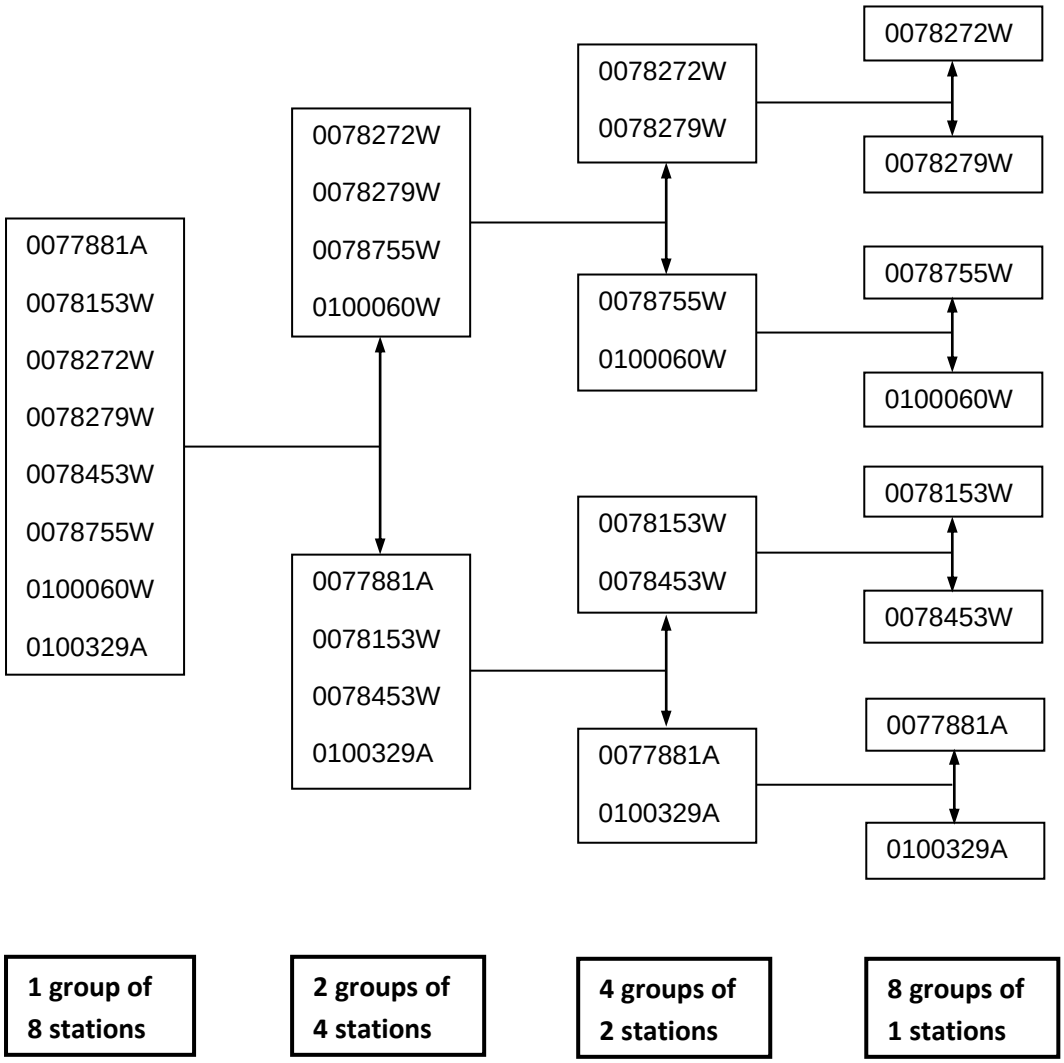

FIGURE B4

Balfour Catchment_Combination 4_Rain gauge groupings

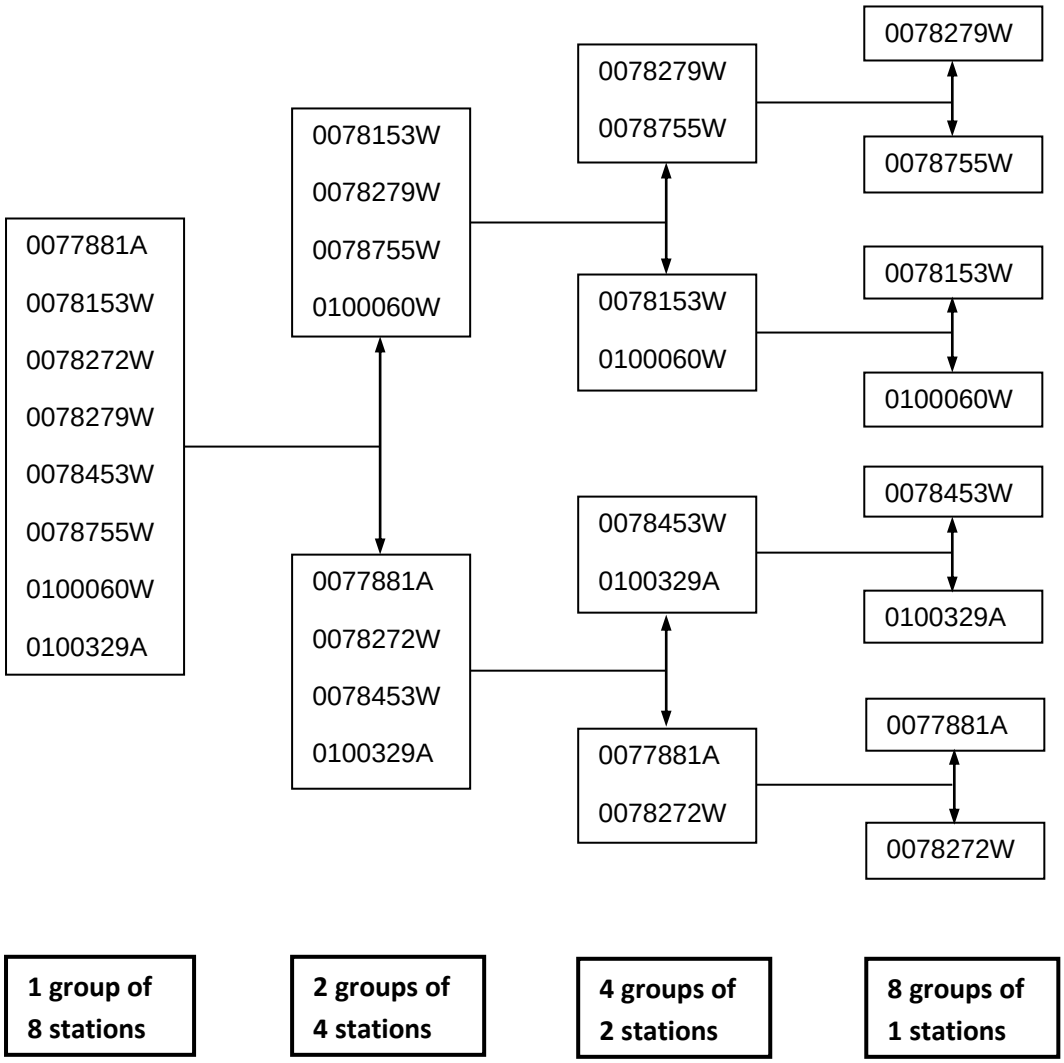

FIGURE B5

Barberton Catchment_Combination 1_Rain gauge groupings

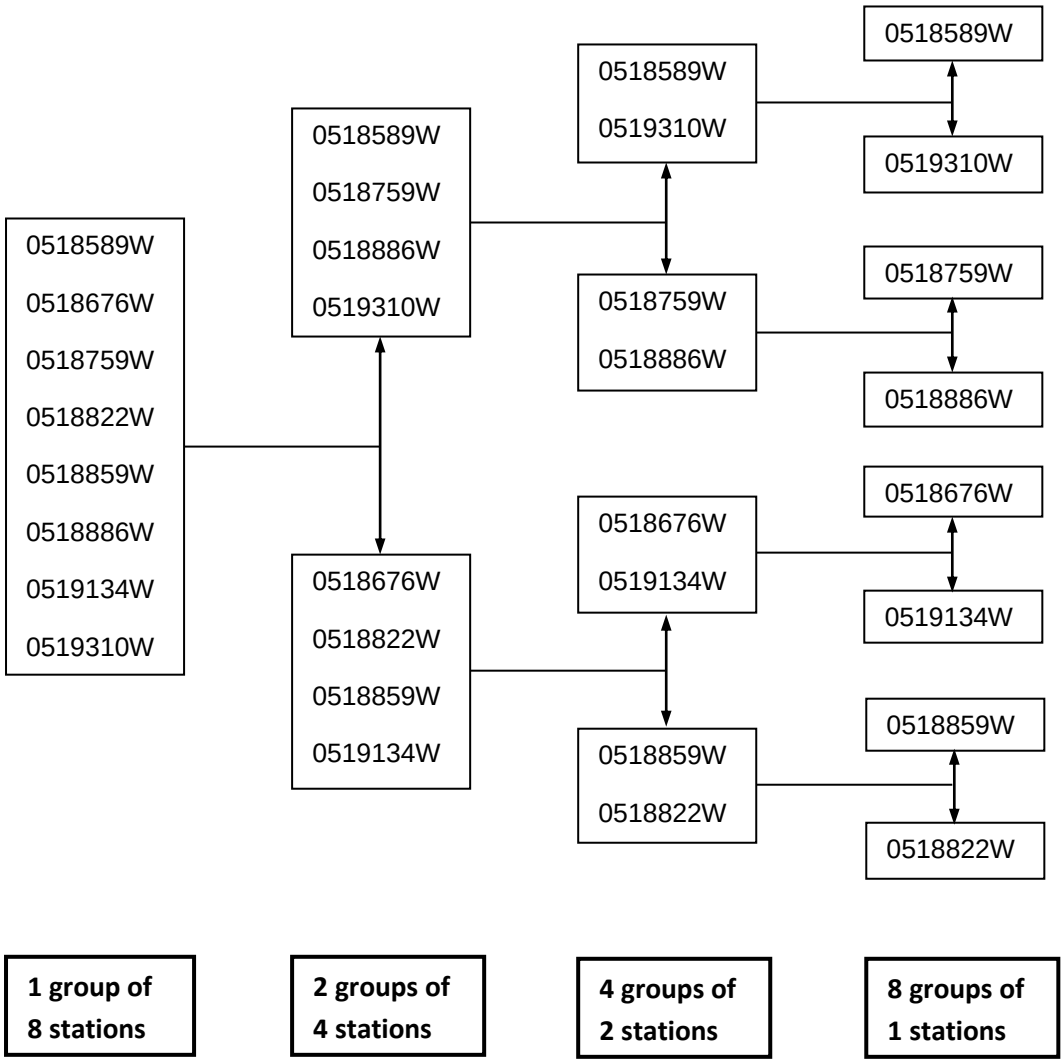

FIGURE B6

Barberton Catchment_Combination 2_Rain gauge groupings

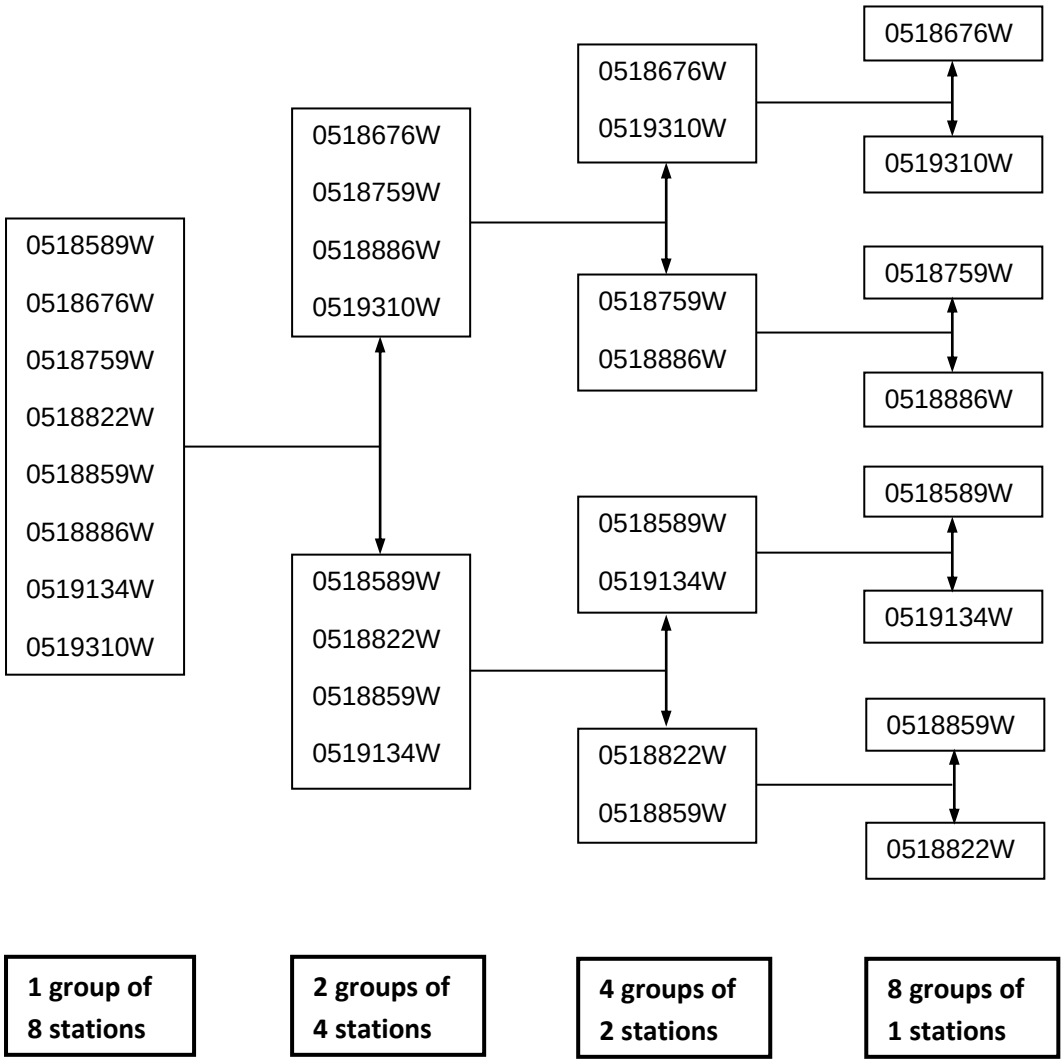

FIGURE B7

Barberton Catchment_Combination 3_Rain gauge groupings

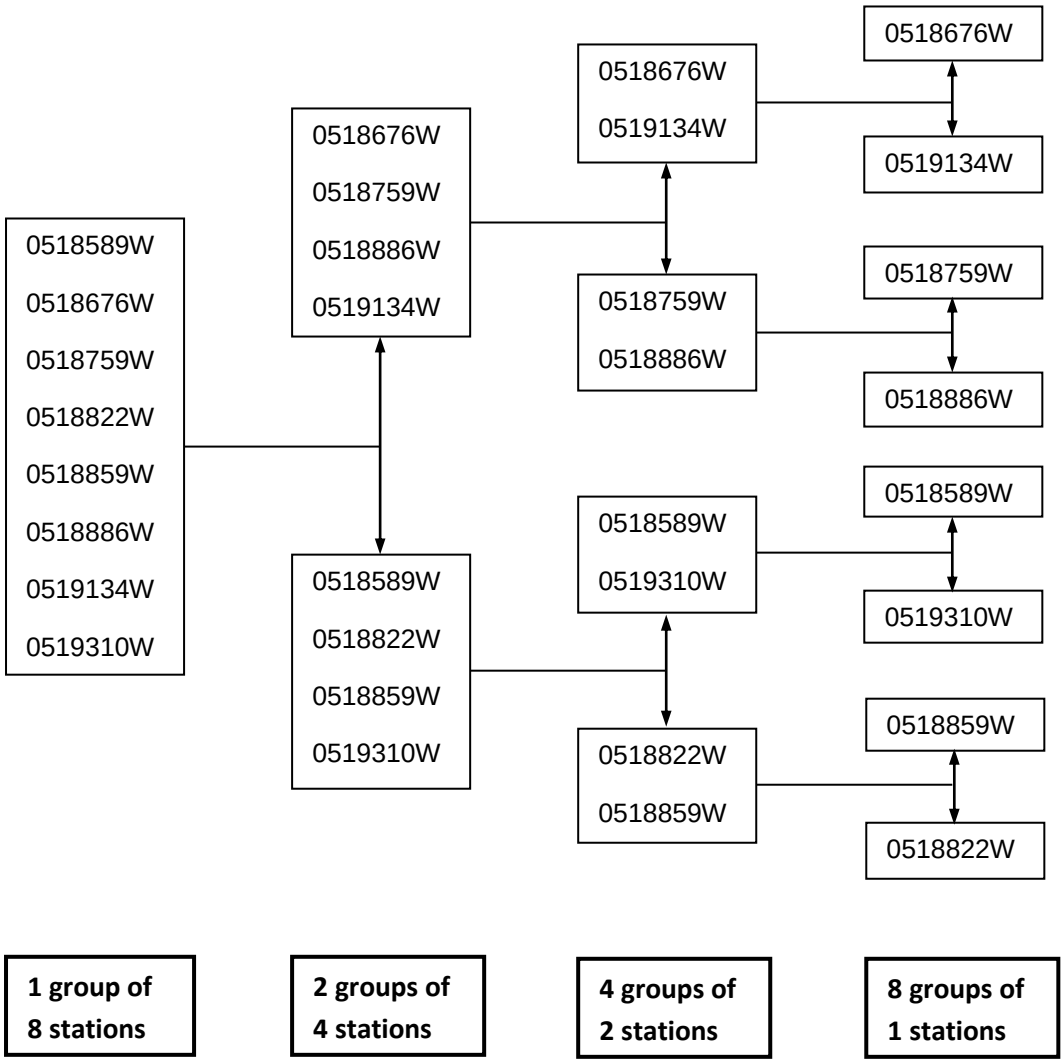

FIGURE B8

Barberton Catchment_Combination 4_Rain gauge groupings

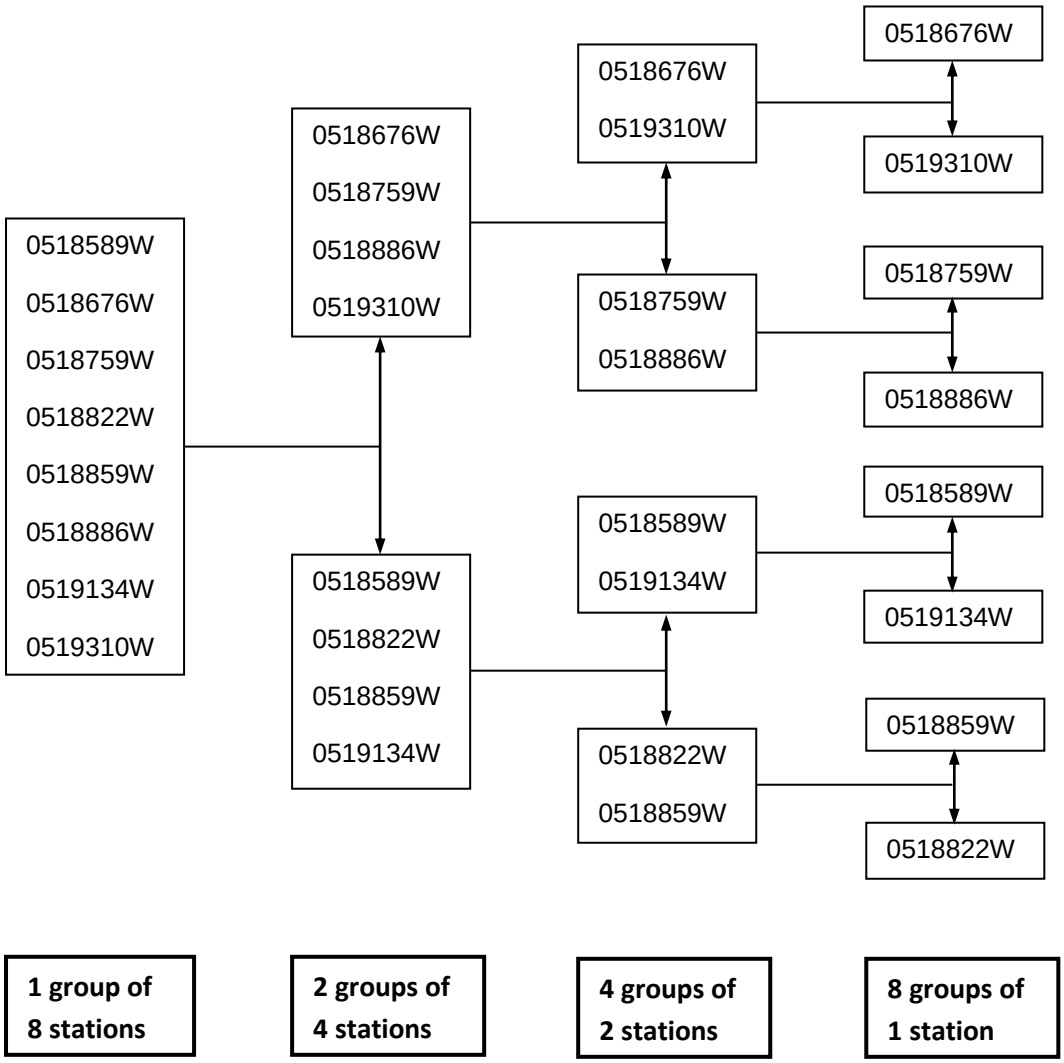

FIGURE B9

George Catchment_Combination 1_Rain gauge groupings

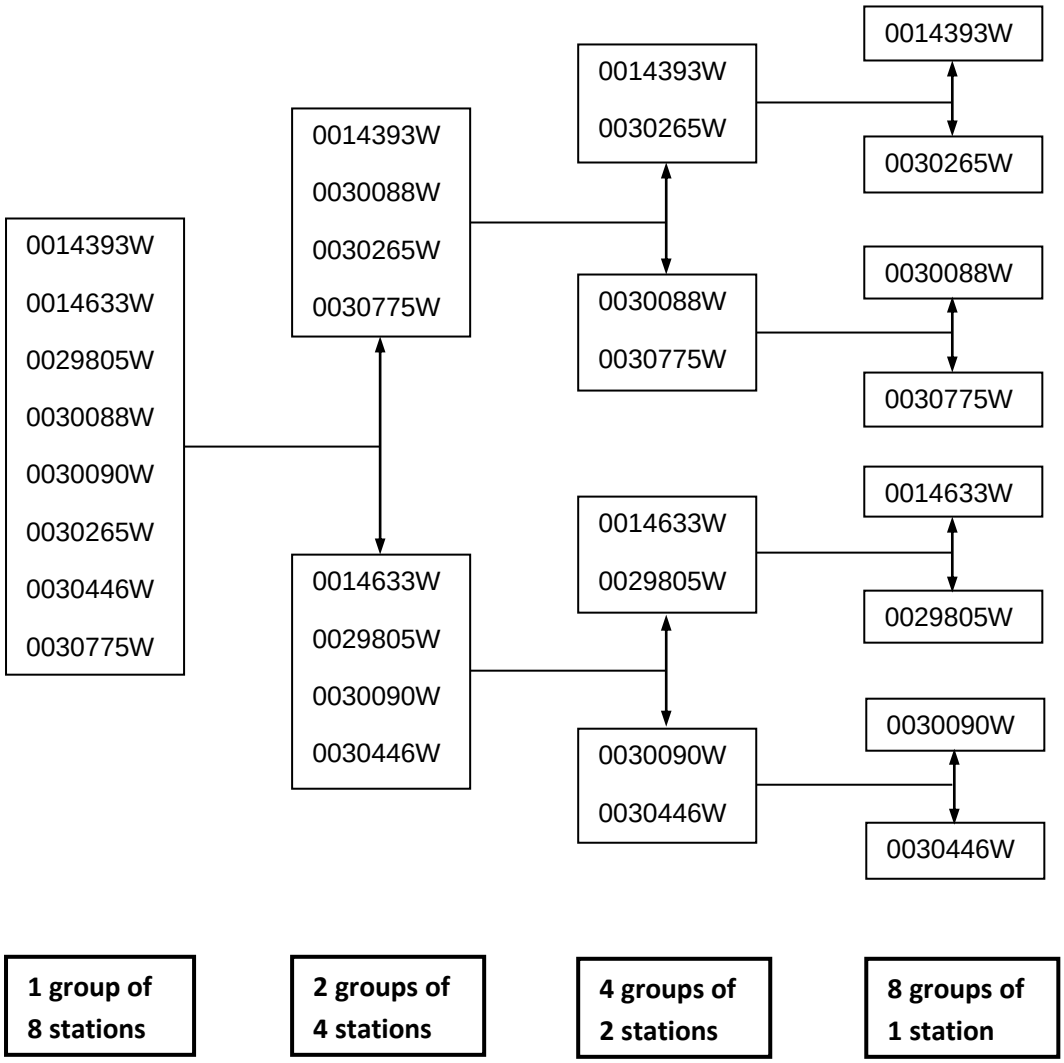

FIGURE B10

George Catchment_Combination 2_Rain gauge groupings

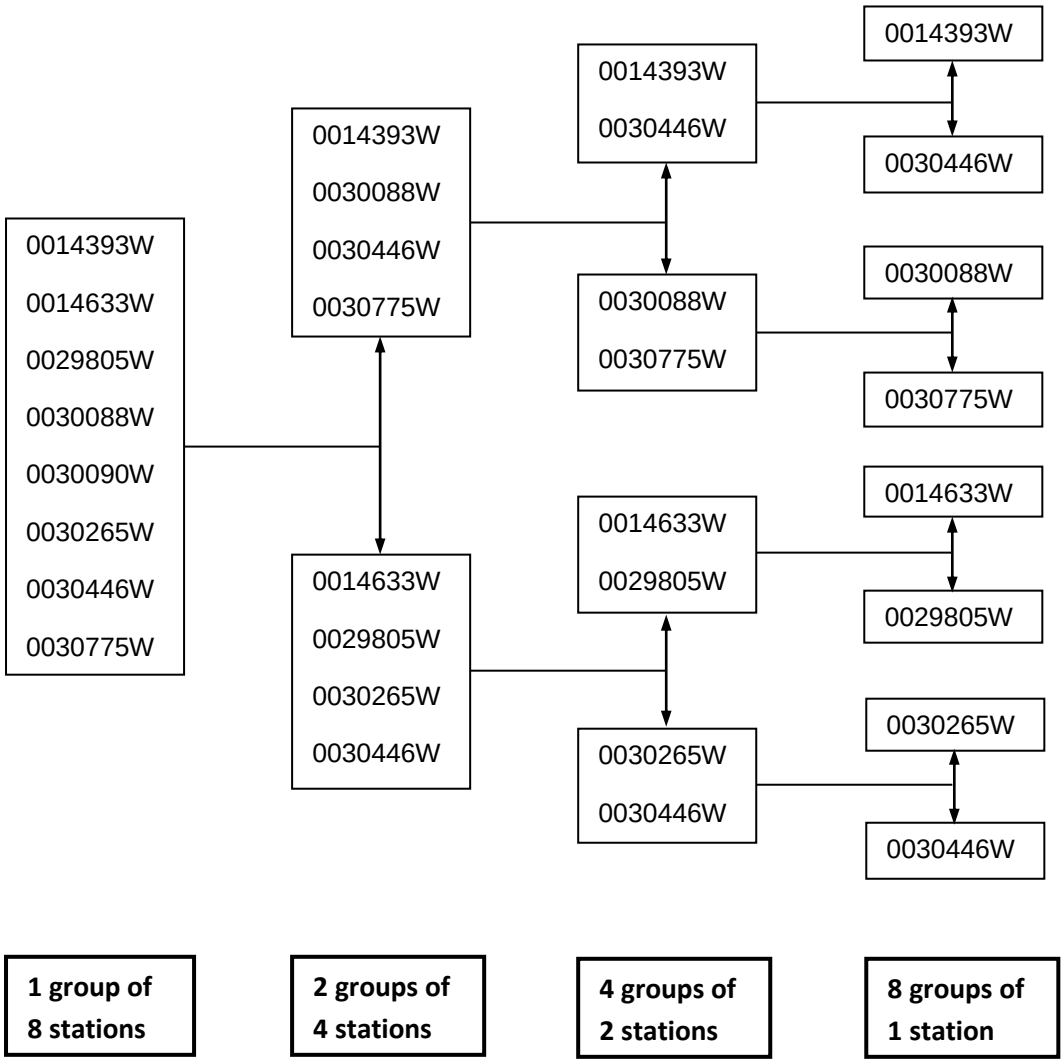

FIGURE B11

George Catchment_Combination 3_Rain gauge groupings

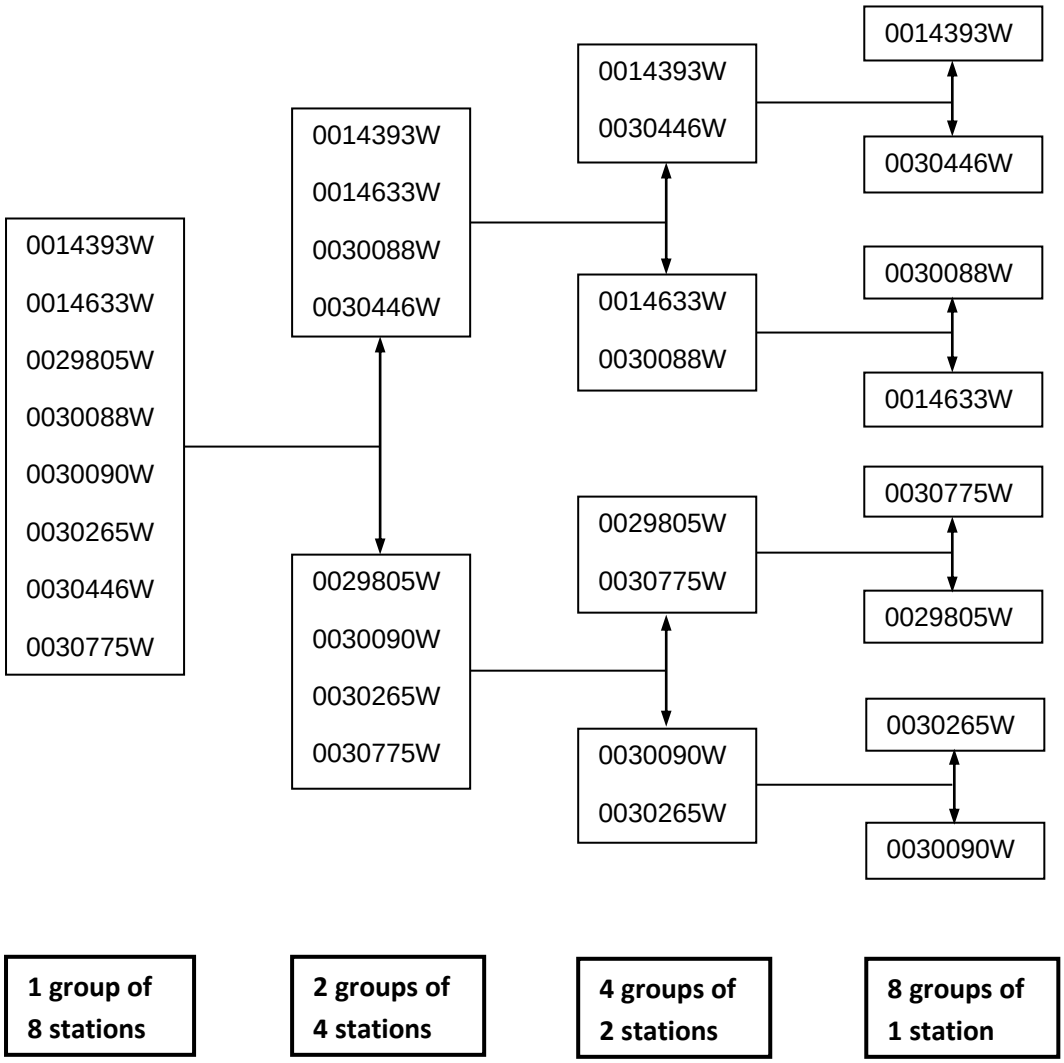

FIGURE B12

George Catchment_Combination 4_Rain gauge groupings

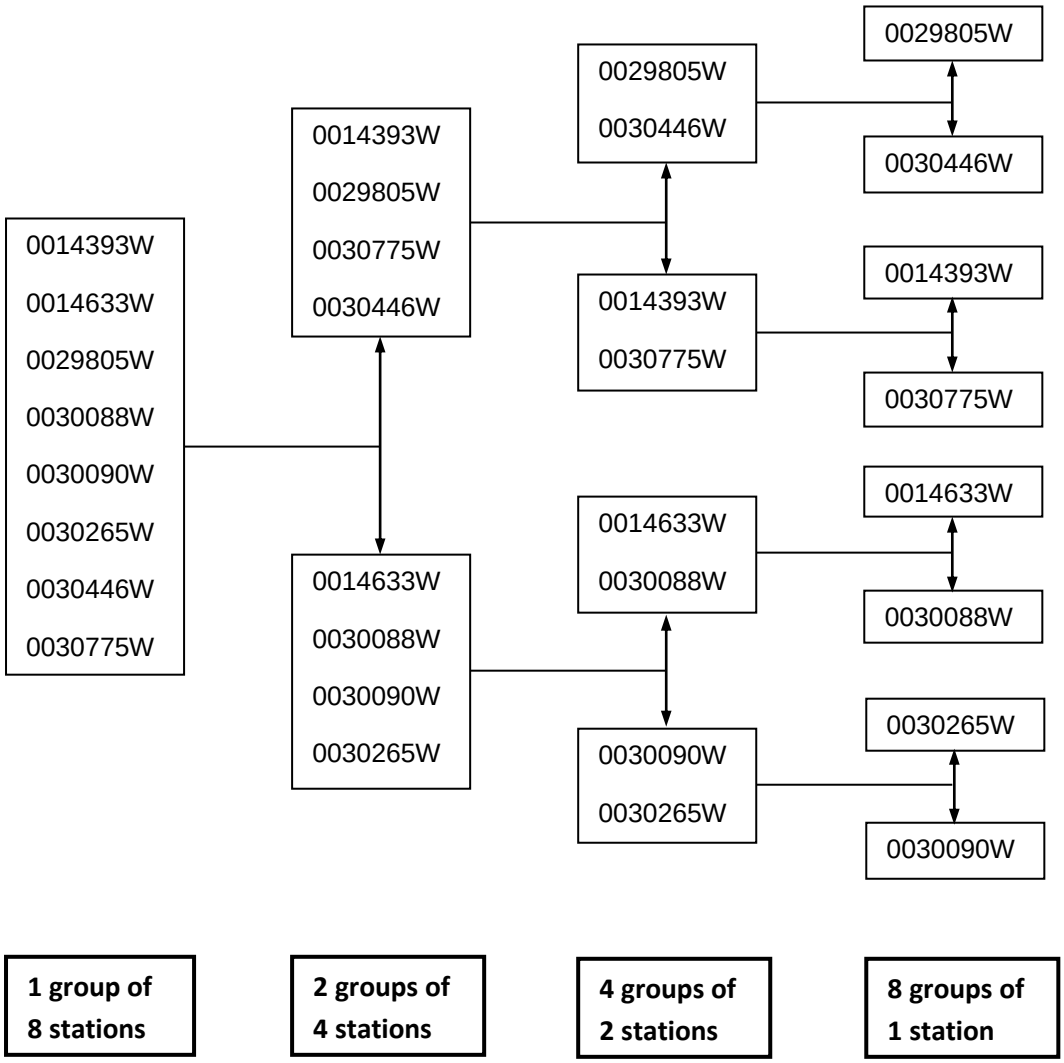

FIGURE B13

Liebenbergsvlei Catchment_Combination 1_Rain gauge groupings

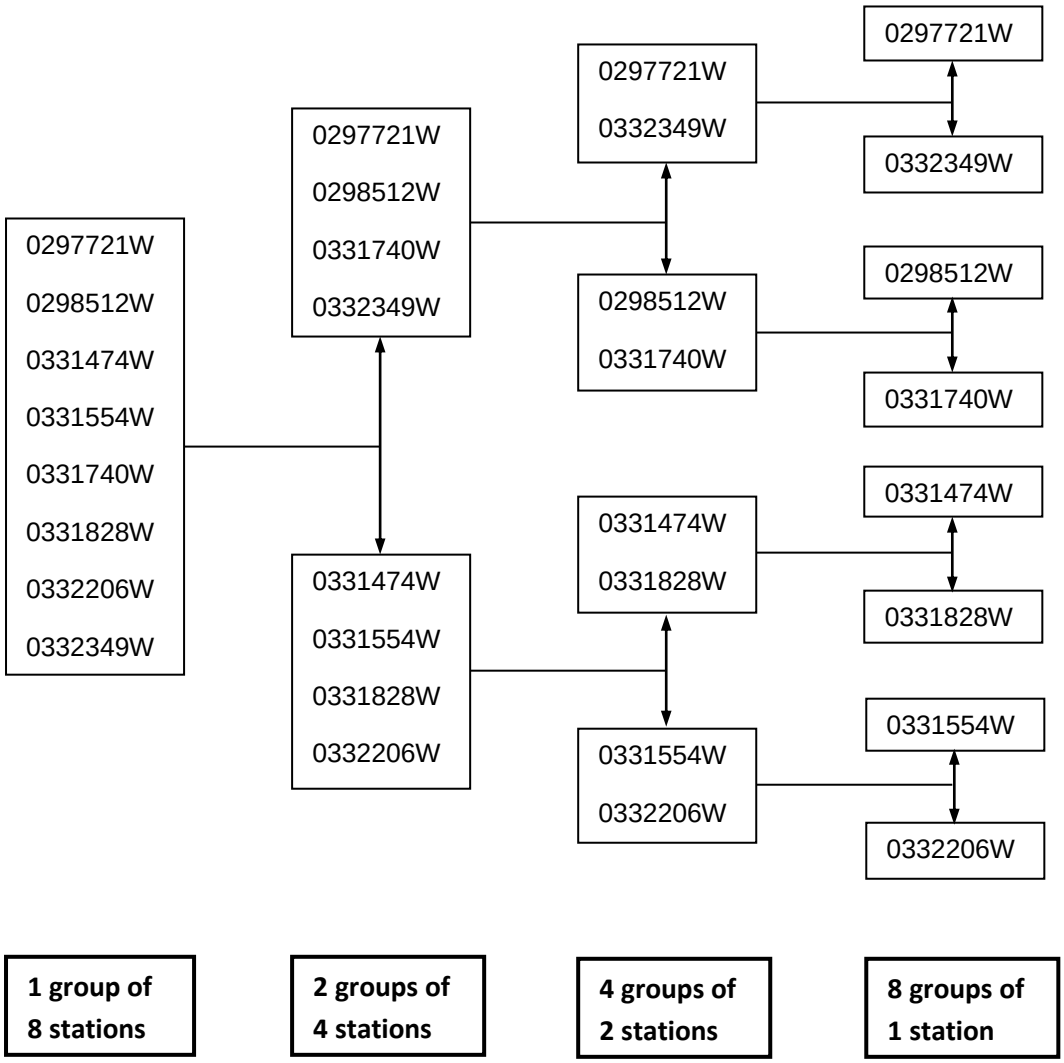

FIGURE B14

Liebenbergsvlei Catchment_Combination 2_Rain gauge groupings

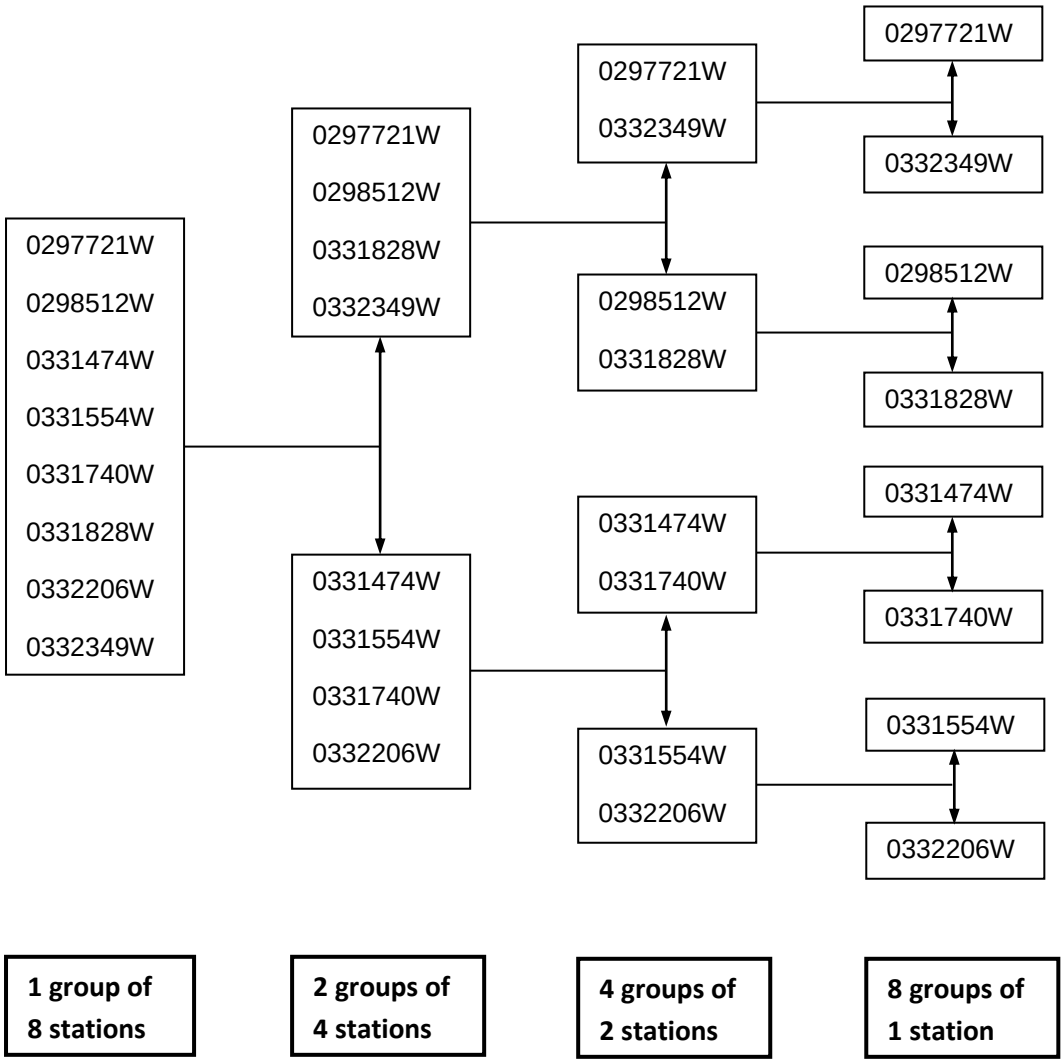

FIGURE B15

Liebenbergsvlei Catchment_Combination 3_Rain gauge groupings

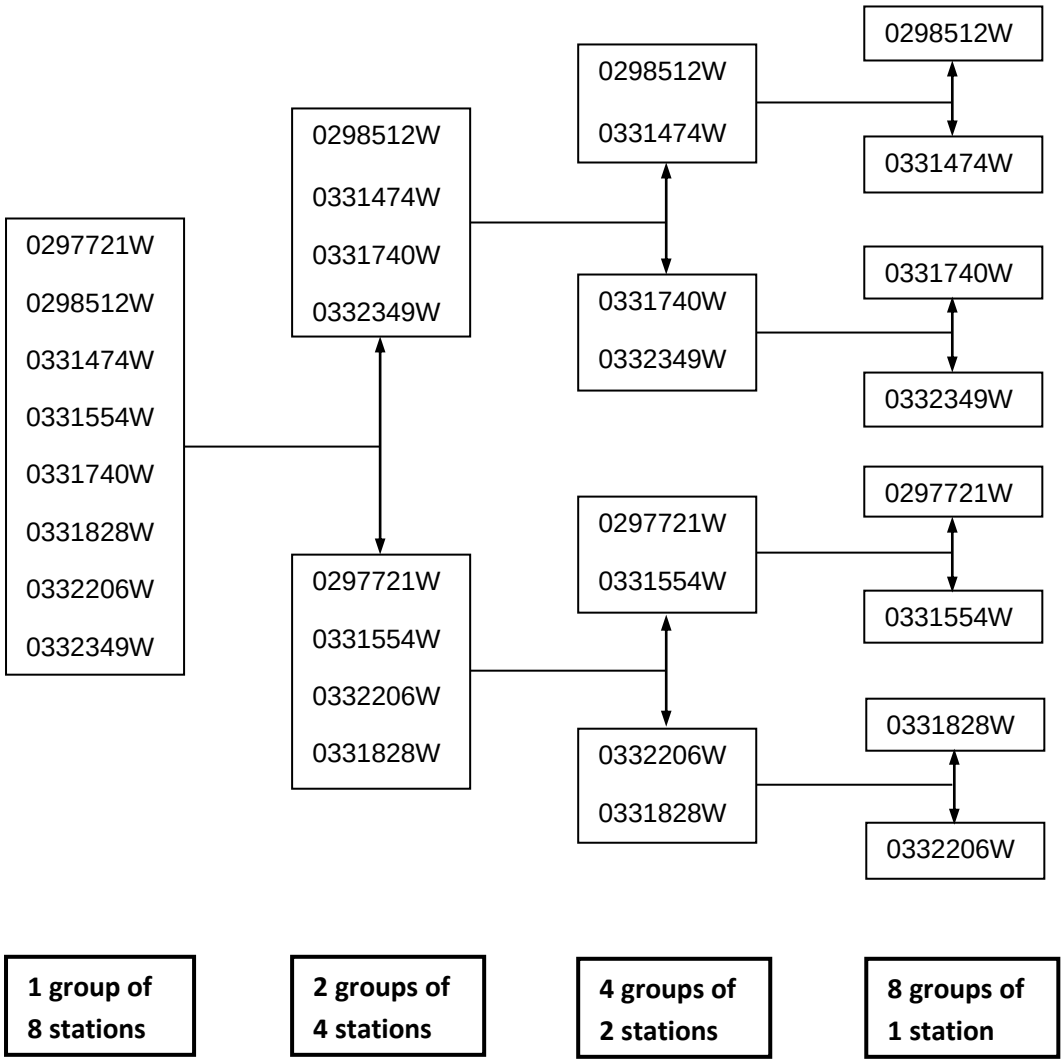

FIGURE B16

Liebenbergsvlei Catchment_Combination 4_Rain gauge groupings

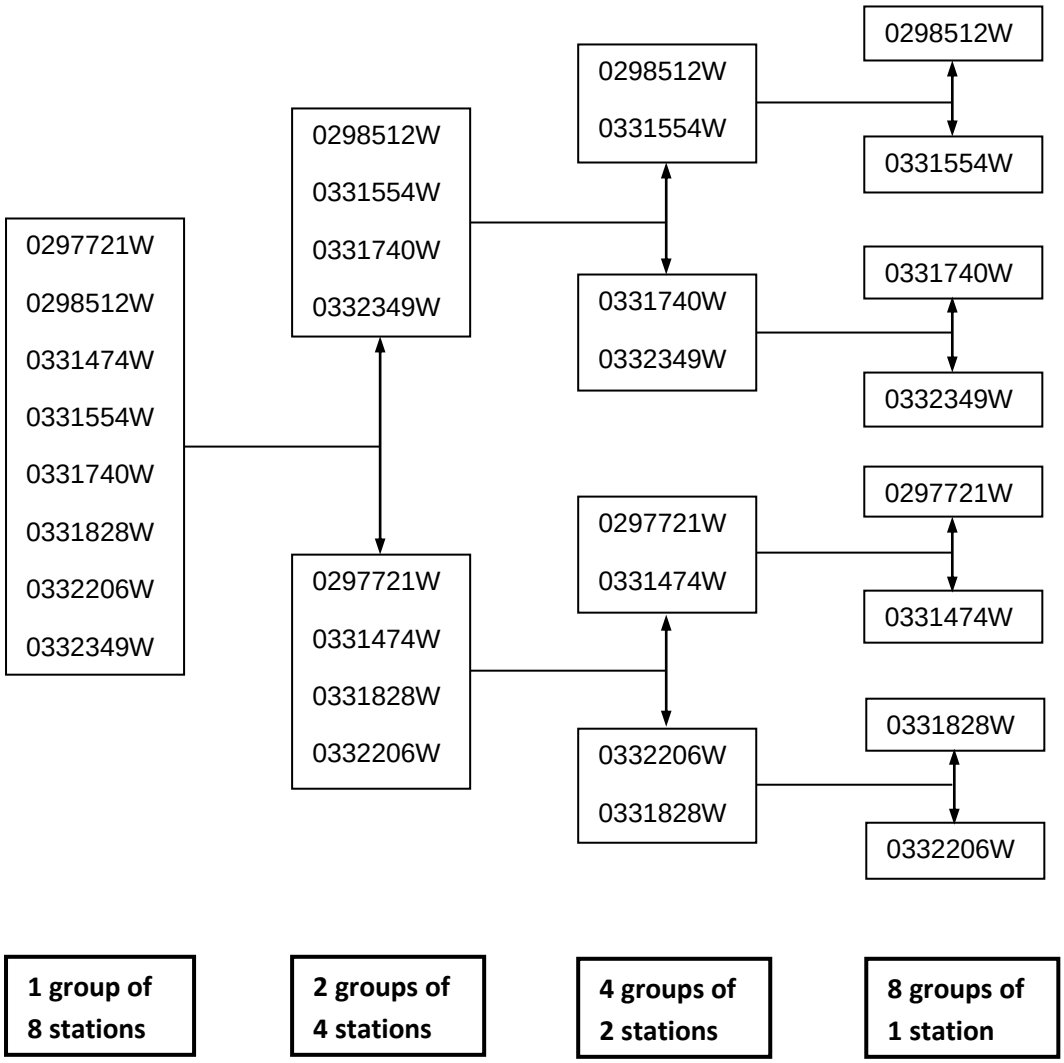

FIGURE B17

Louis Trichardt Catchment_Combination 1_Rain gauge groupings

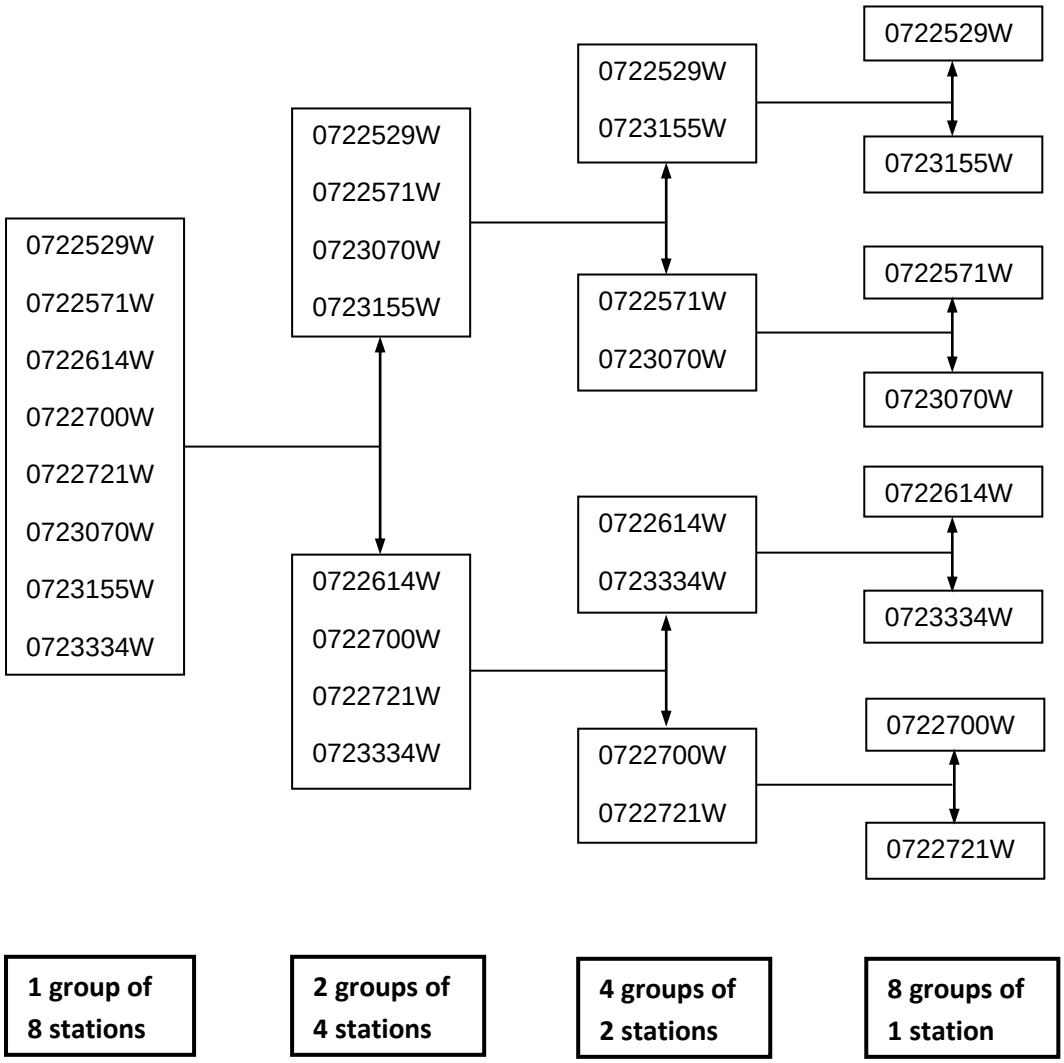

FIGURE B18

Louis Trichardt Catchment_Combination 2_Rain gauge groupings

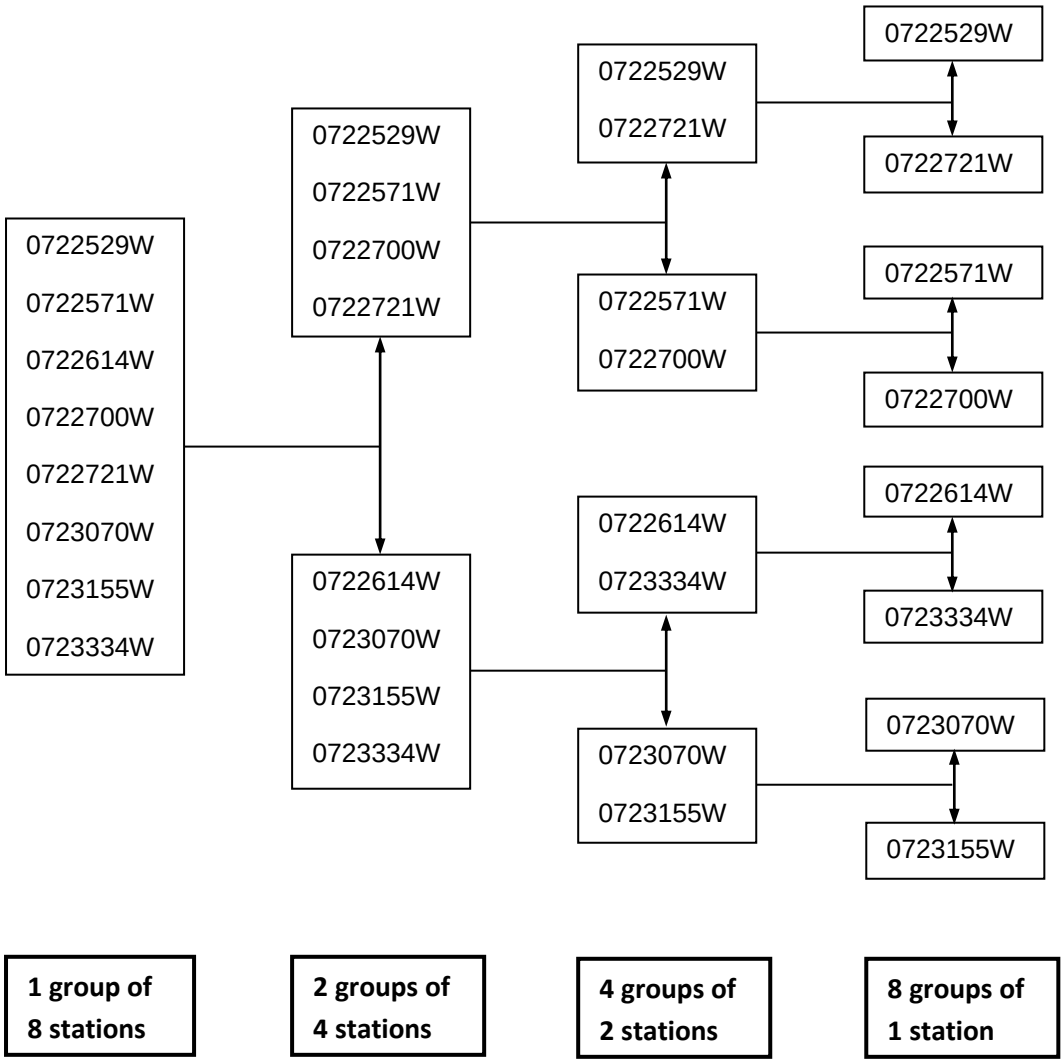

FIGURE B19

Louis Trichardt Catchment_Combination 3_Rain gauge groupings

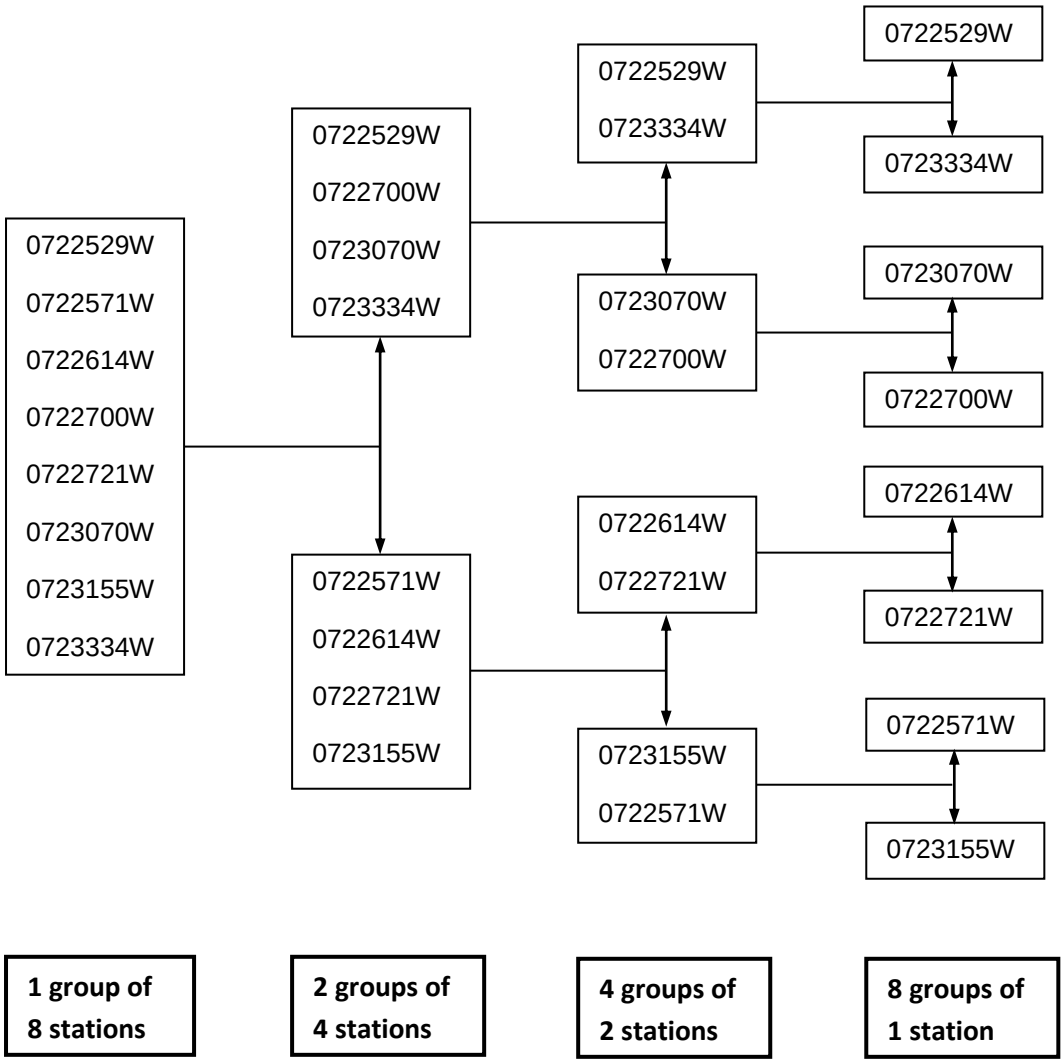

FIGURE B20

Louis Trichardt Catchment_Combination 4_Rain gauge groupings

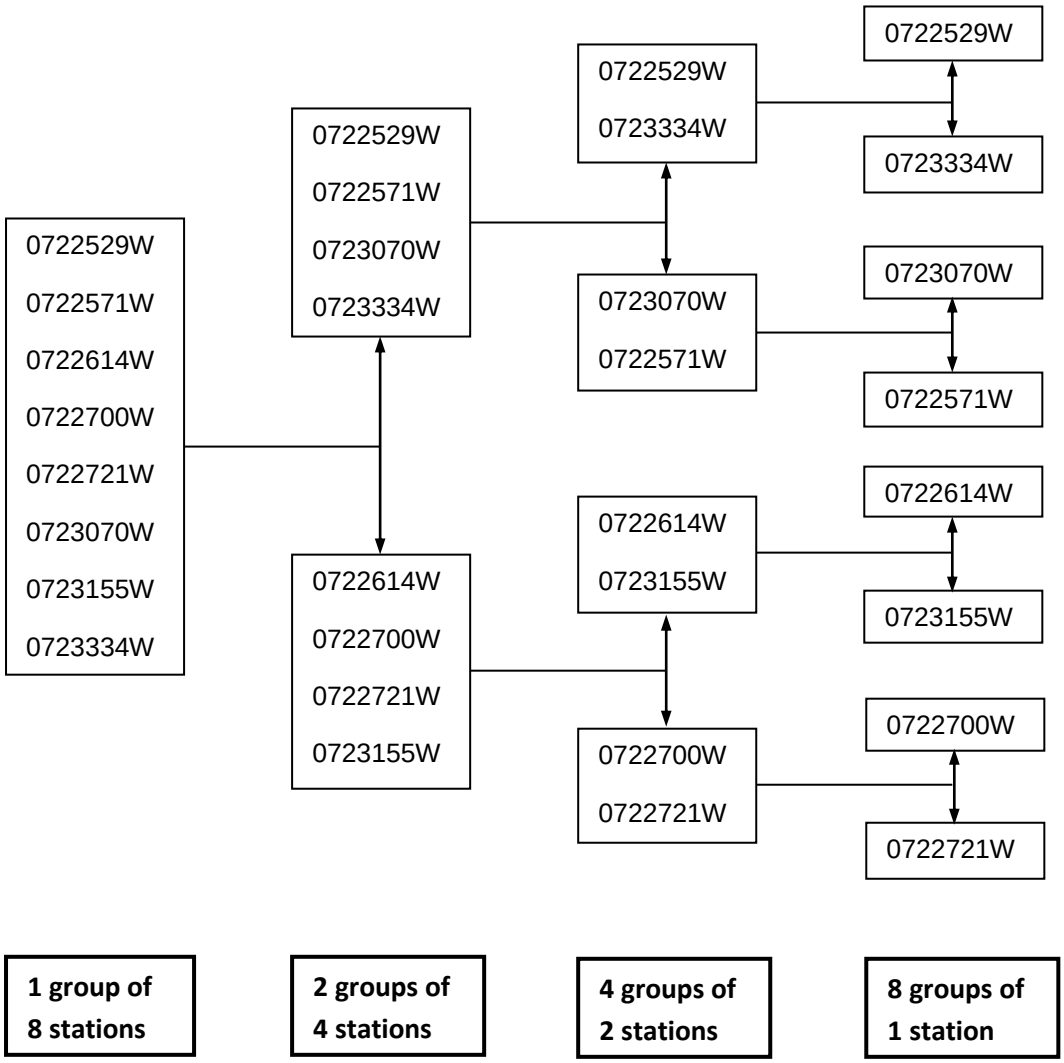

FIGURE B21

Murraysburg Catchment_Combination 1_Rain gauge groupings

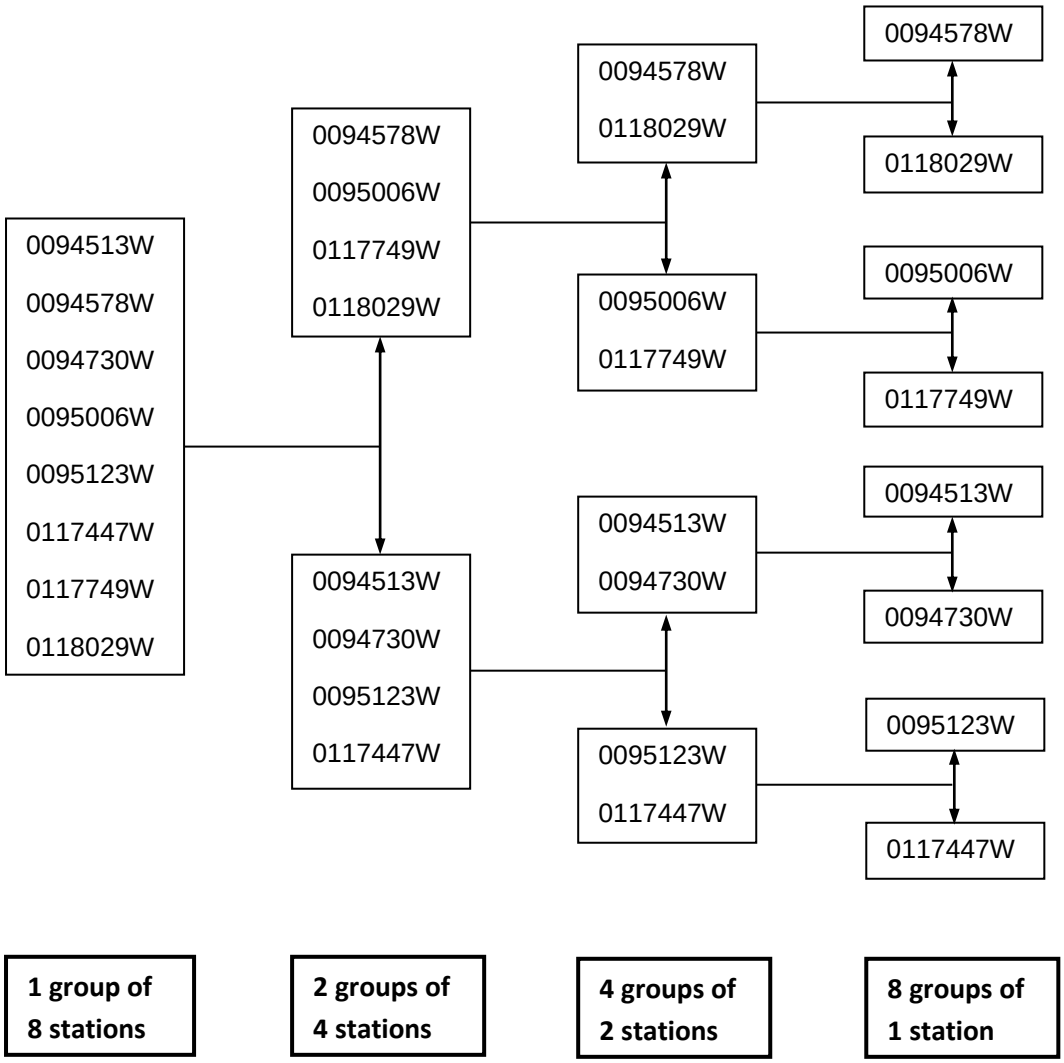

FIGURE B22

Murraysburg Catchment_Combination 2_Rain gauge groupings

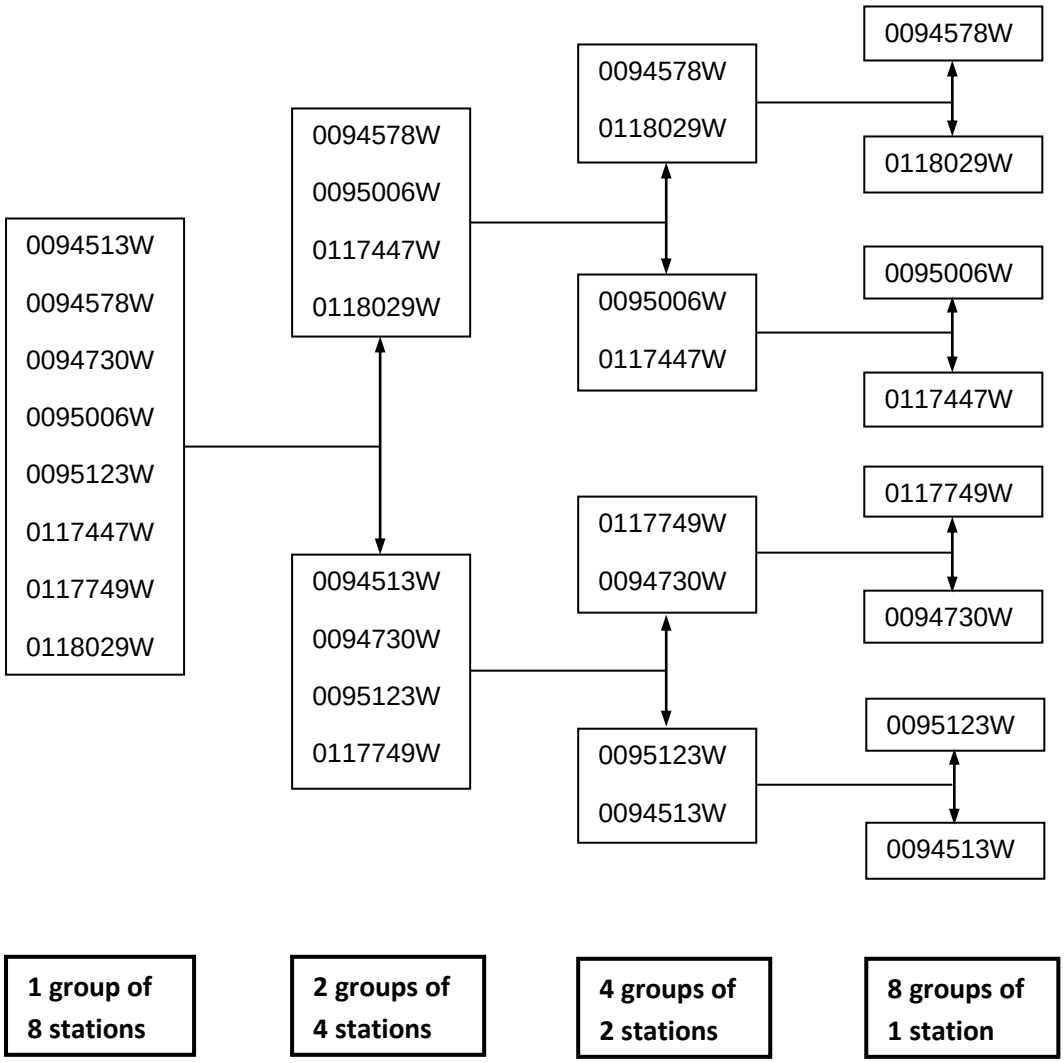

FIGURE B23

Murraysburg Catchment_Combination 3_Rain gauge groupings

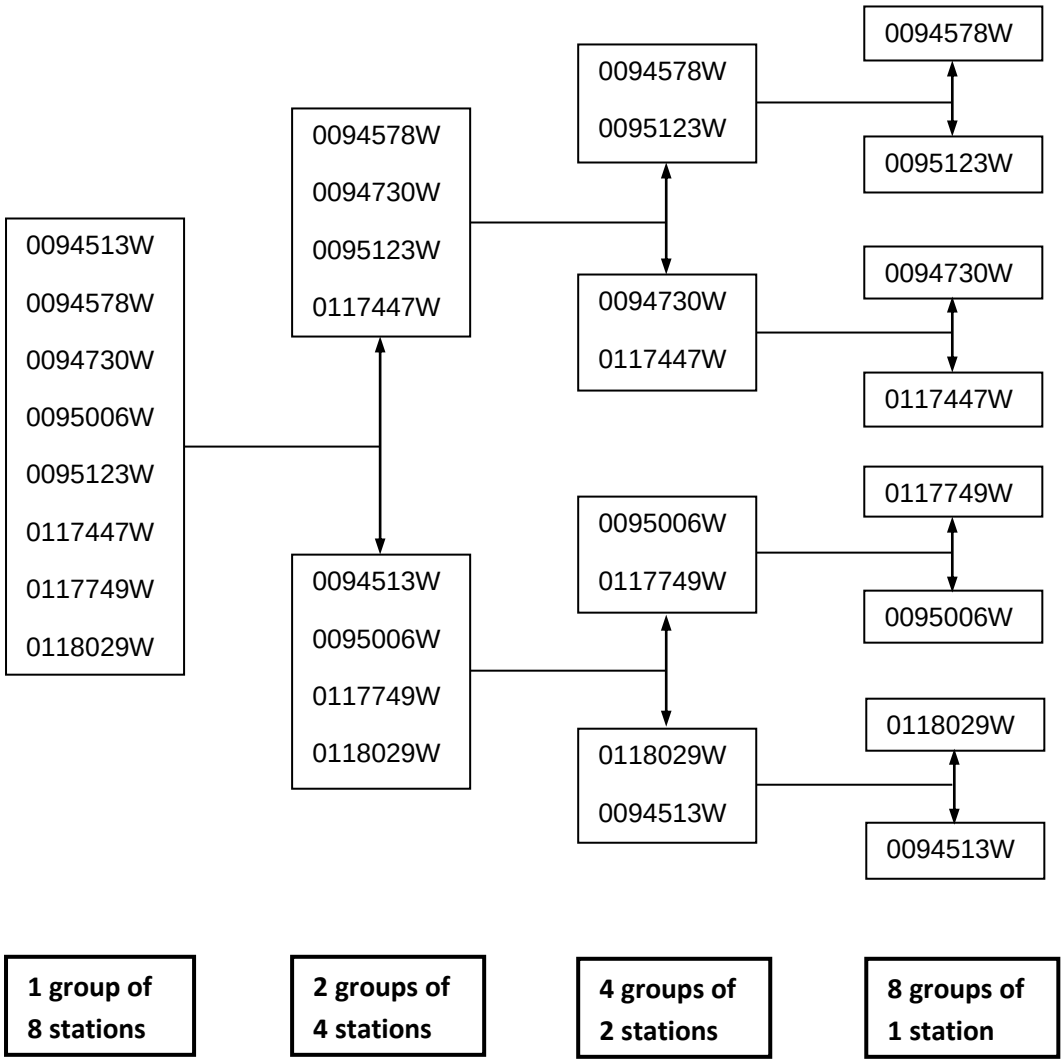

FIGURE B24

Murraysburg Catchment_Combination 4_Rain gauge groupings

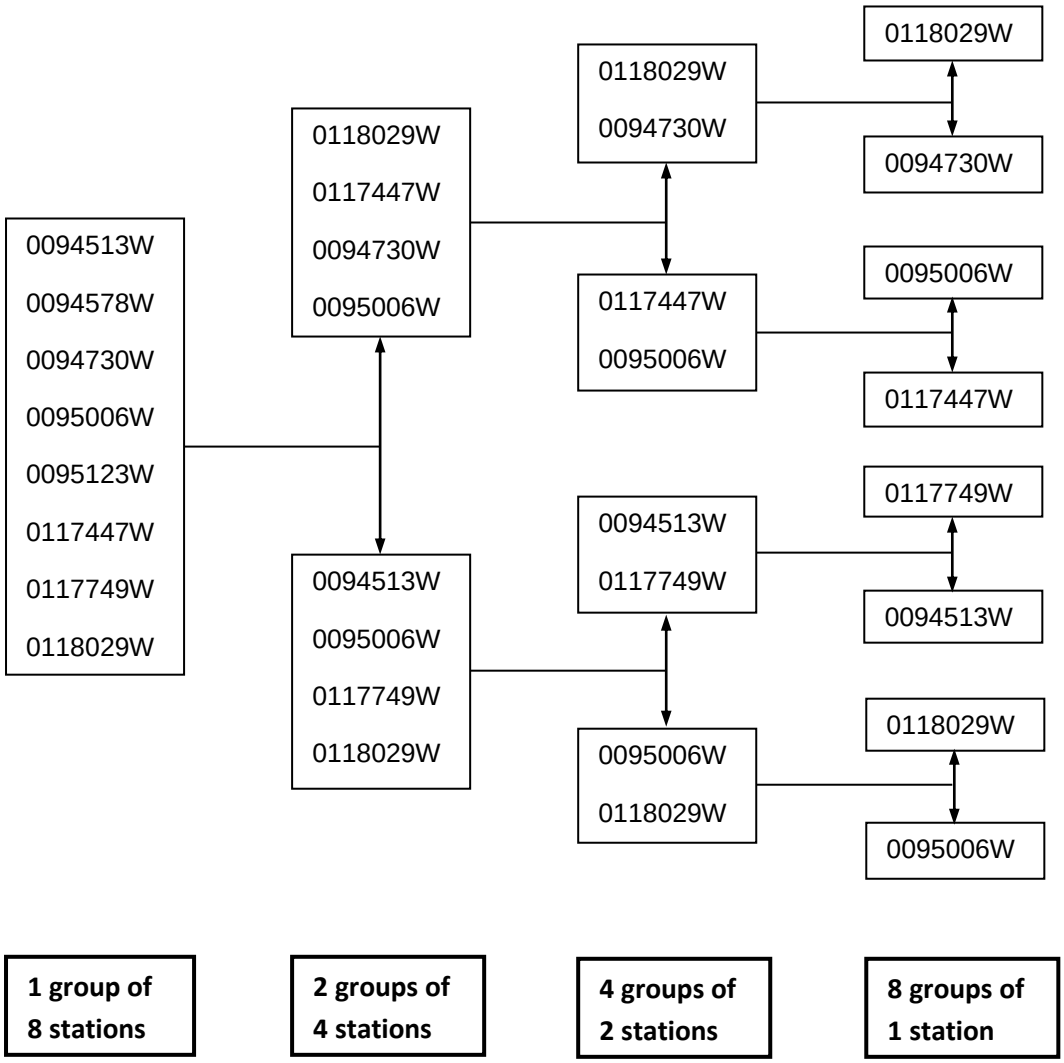

FIGURE B25

Prieska Catchment_Combination 1_Rain gauge groupings

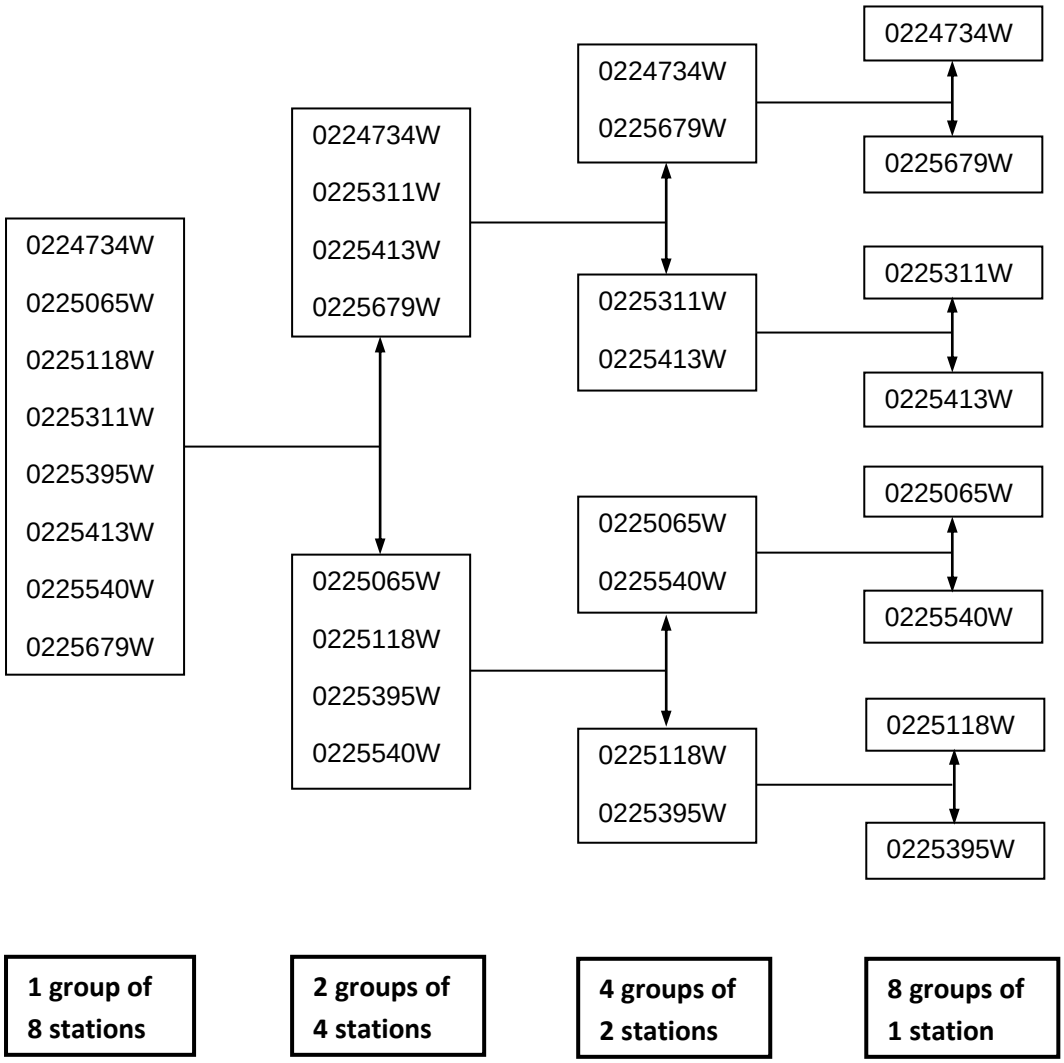

FIGURE B26

Prieska Catchment_Combination 2_Rain gauge groupings

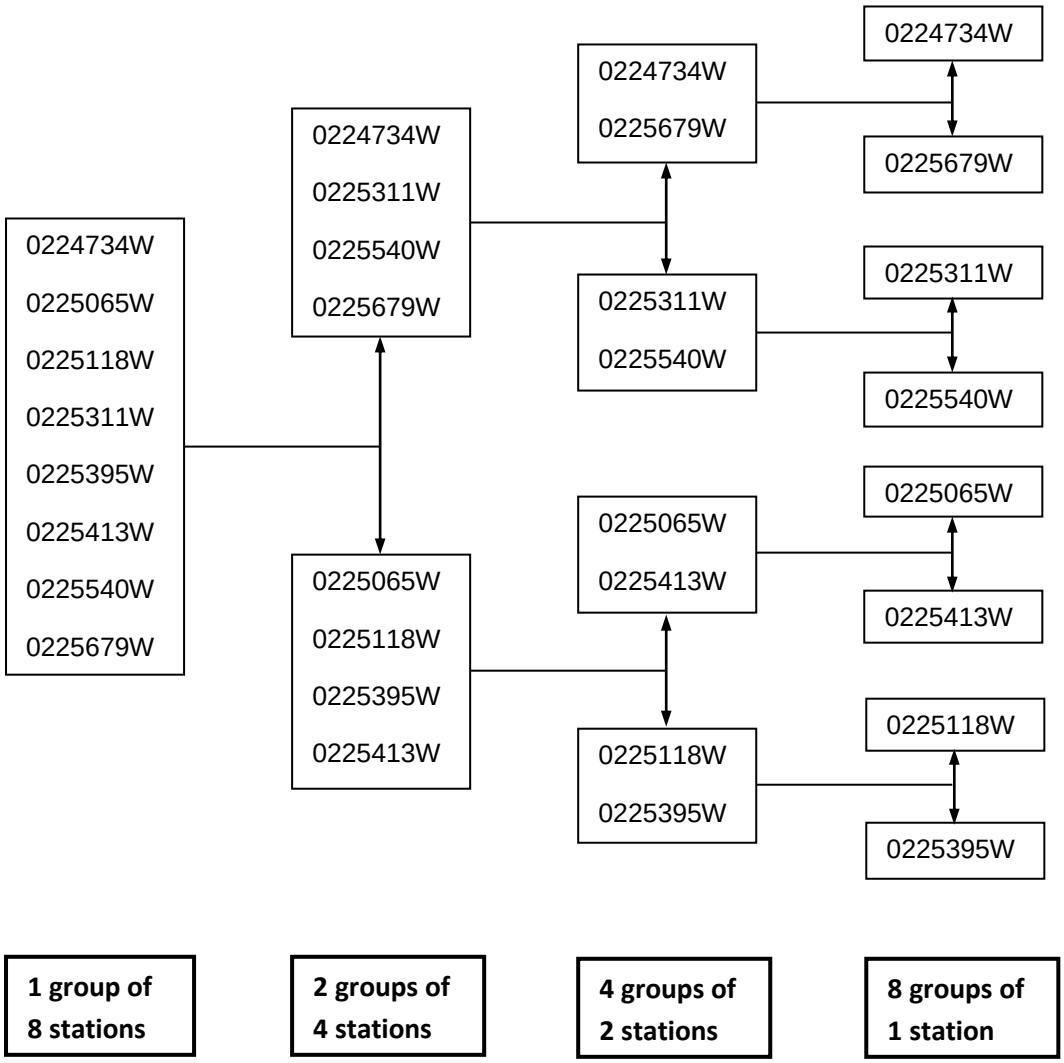

FIGURE B27

Prieska Catchment_Combination 3_Rain gauge groupings

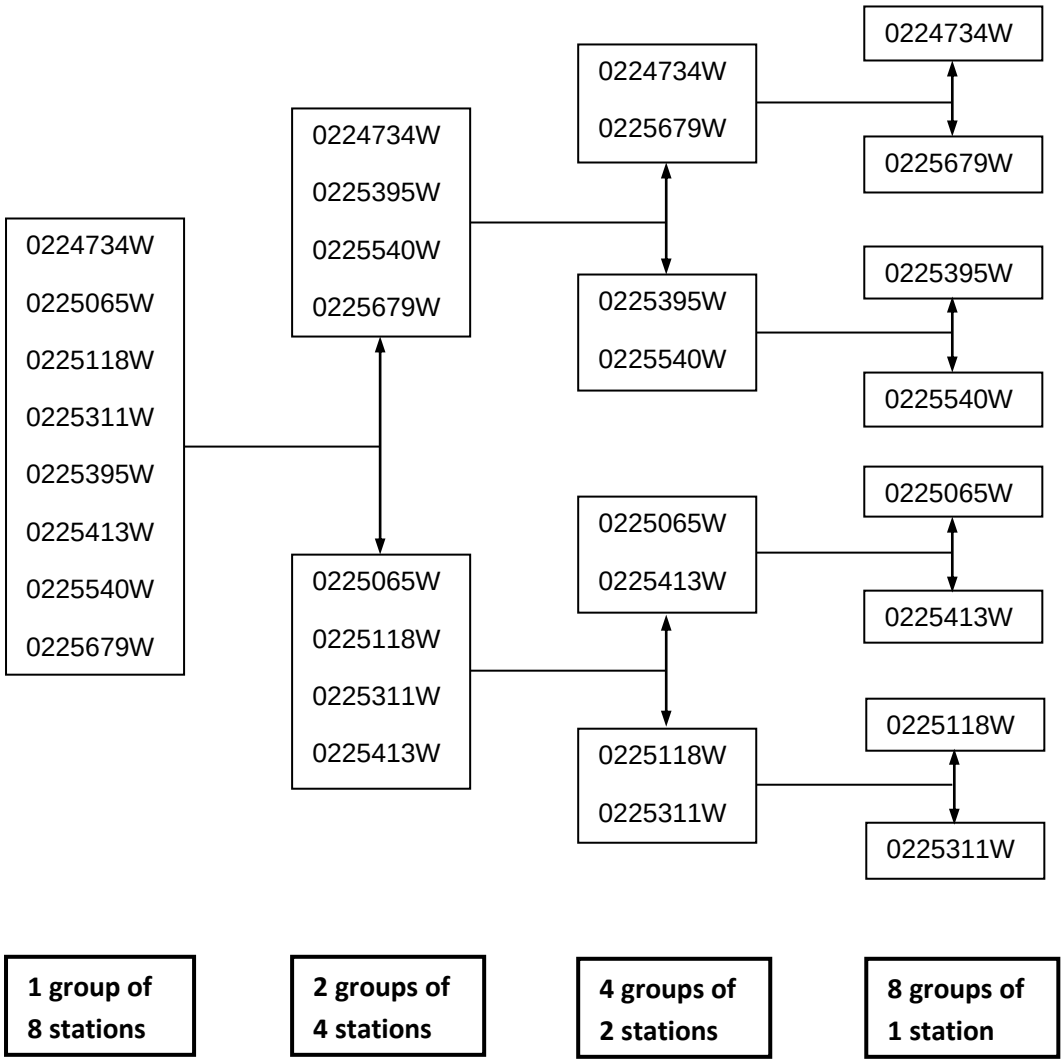

FIGURE B28

Prieska Catchment_Combination 4_Rain gauge groupings

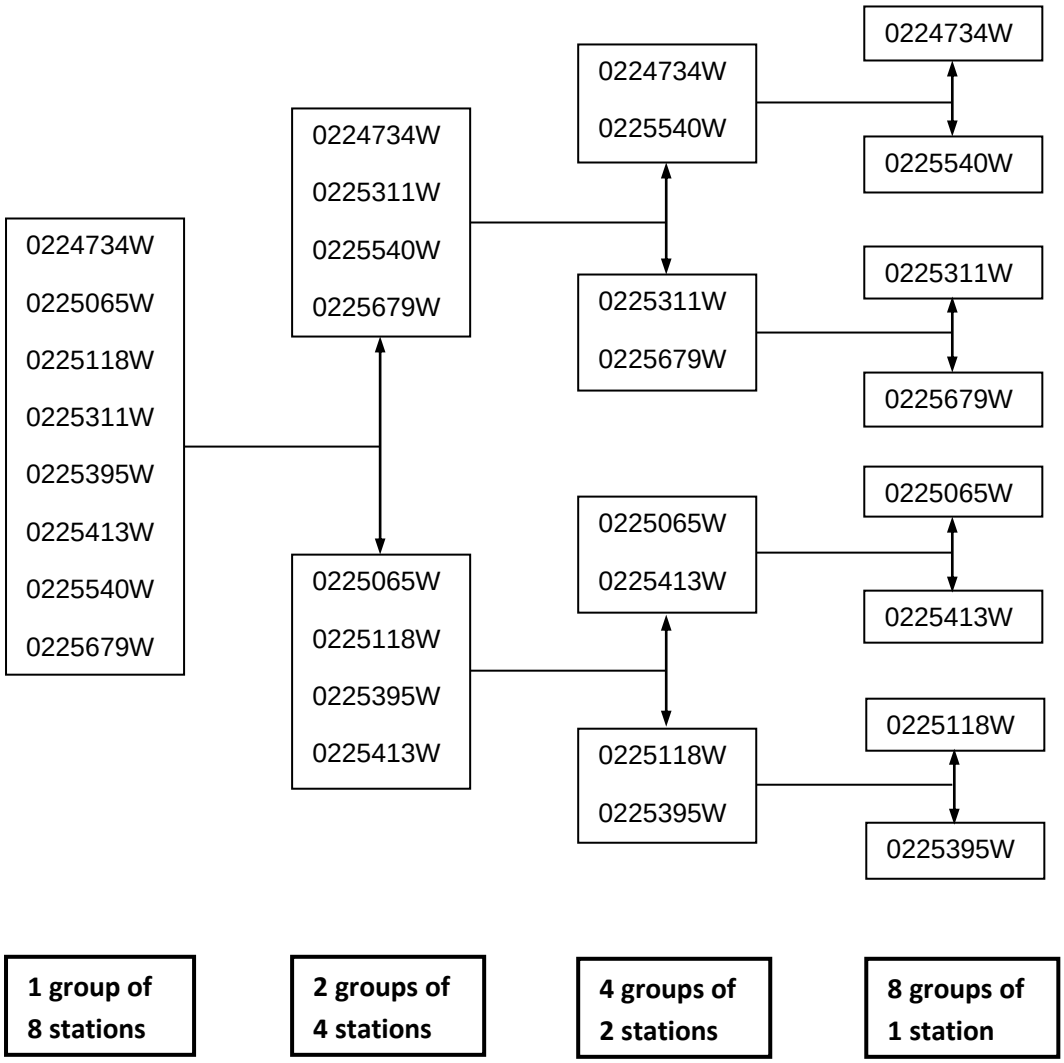

FIGURE B29

Tzaneen Catchment_Combination 1_Rain gauge groupings

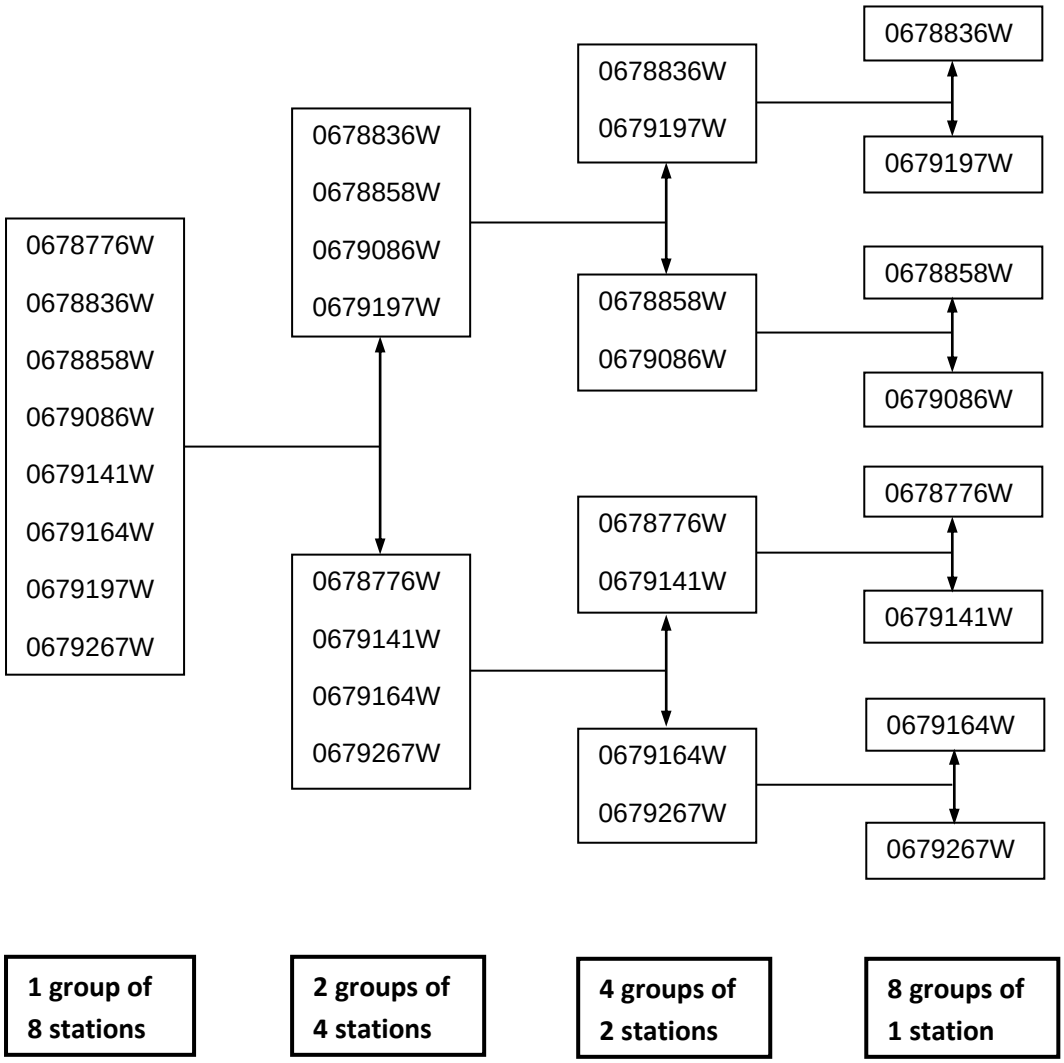

FIGURE B30

Tzaneen Catchment_Combination 2_Rain gauge groupings

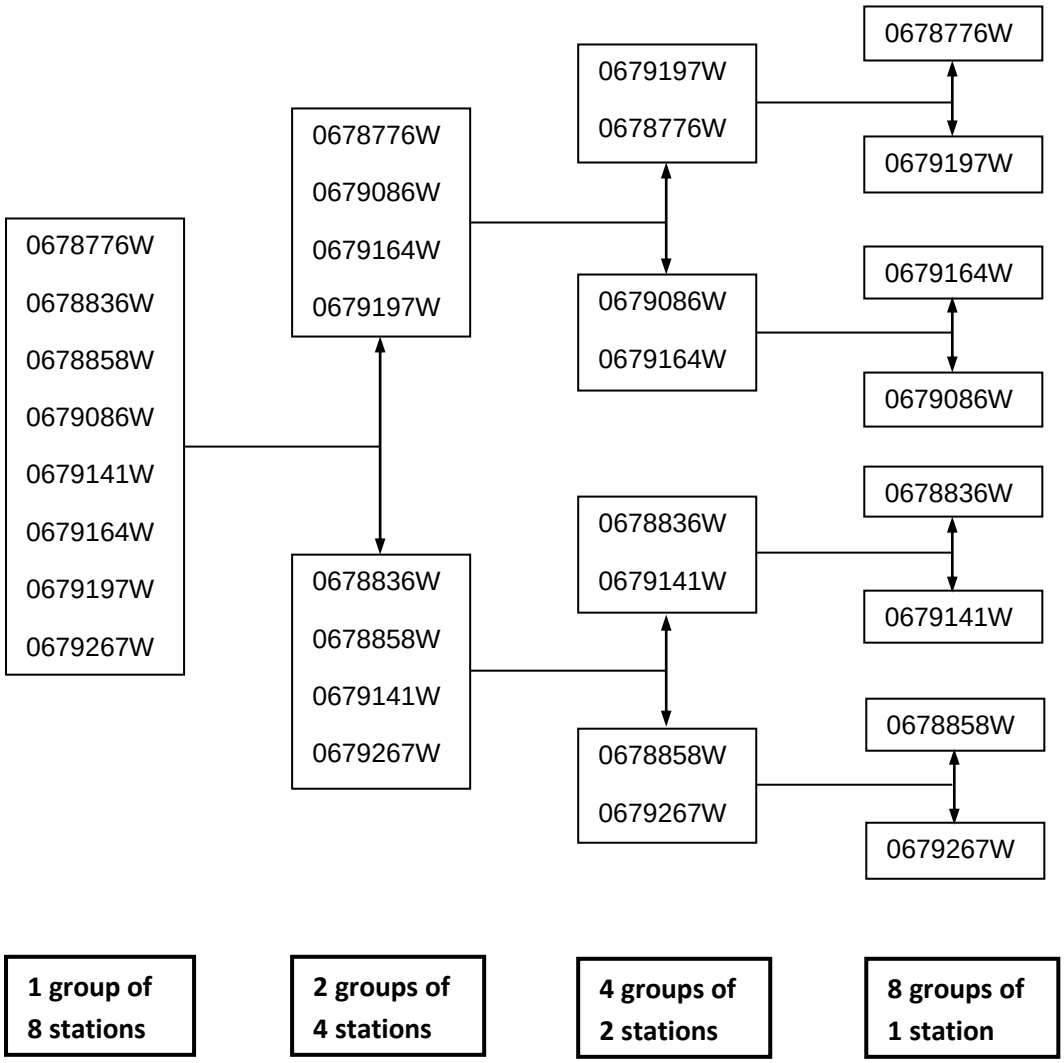

FIGURE B31

Tzaneen Catchment_Combination 3_Rain gauge groupings

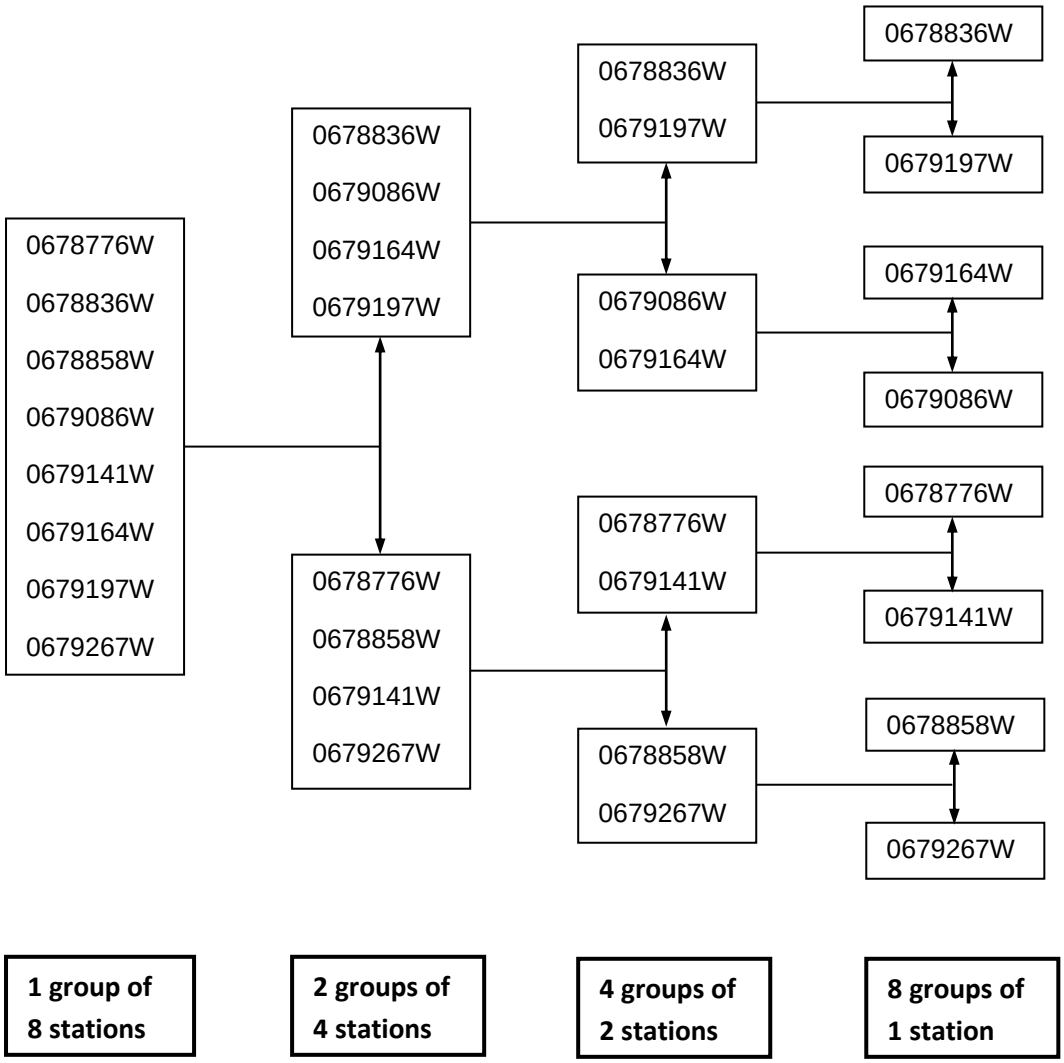

FIGURE B32

Tzaneen Catchment_Combination 4_Rain gauge groupings

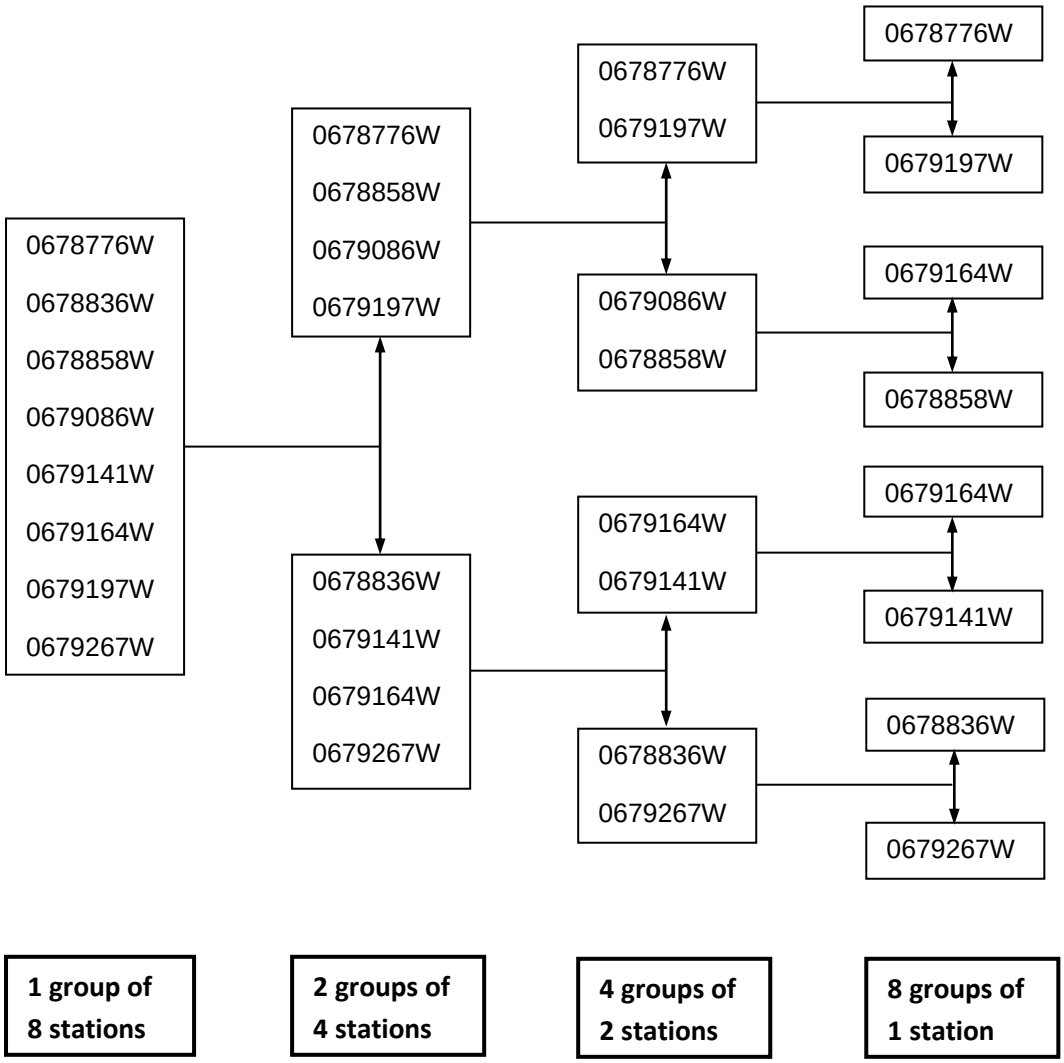

APPENDIX C

Balfour average catchment rainfall

Year	Jan	Feb	Mar	Apr	May	Jun	Jul	Aug	Sep	Oct	Nov	Dec
1920	731	791	1297	1680	315	165	144	120	317	521	673	1650
1921	1097	709	498	685	611	586	181	482	827	468	1251	1351
1922	1537	955	1365	276	357	247	537	89	227	828	2490	606
1923	716	1027	603	331	174	103	43	454	347	423	641	835
1924	628	615	2184	1253	350	263	255	128	1002	130	486	1297
1925	610	798	1504	225	298	478	92	187	821	375	1001	949
1926	470	541	1256	146	266	14	133	170	86	421	1320	881
1927	806	623	1637	360	218	182	151	410	550	454	347	386
1928	609	716	943	61	237	642	389	332	1401	794	677	1310
1929	765	789	1671	318	229	465	189	919	546	1129	457	1159
1930	1476	573	721	958	54	126	1397	208	104	997	340	955
1931	892	402	716	20	538	218	561	81	1589	856	836	1513
1932	240	888	1376	785	233	133	39	349	274	1027	1269	578
1933	1266	1657	1617	368	231	240	652	30	319	298	2016	986
1934	849	521	944	973	1494	310	21	302	295	791	647	725
1935	402	873	1209	237	717	146	560	48	542	584	814	846
1936	650	906	1538	124	182	46	262	22	529	1141	1433	416
1937	969	874	569	836	234	412	132	405	414	417	1113	1848
1938	928	2165	979	200	204	32	333	419	920	782	1364	1211
1939	652	1793	1841	342	607	11	256	25	1082	992	566	675
1940	1253	1418	368	705	123	208	78	115	221	419	1192	508
1941	1350	1020	981	656	488	150	129	279	496	1125	514	756
1942	950	517	606	1028	425	647	44	612	553	999	1065	1041
1943	673	1313	1639	230	1189	459	275	43	726	244	2700	1133
1944	886	513	929	368	327	236	166	73	90	753	191	261
1945	853	1108	1253	281	335	205	231	212	209	853	231	437
1946	1012	567	1088	396	239	383	428	56	985	988	979	541
1947	977	887	1047	1937	63	110	307	49	300	571	856	1278
1948	498	655	462	598	205	2	63	219	329	682	701	571
1949	498	1333	1297	514	1451	4	253	575	314	362	804	581
1950	1148	625	515	149	183	222	413	435	916	1581	1003	1938

APPENDIX D

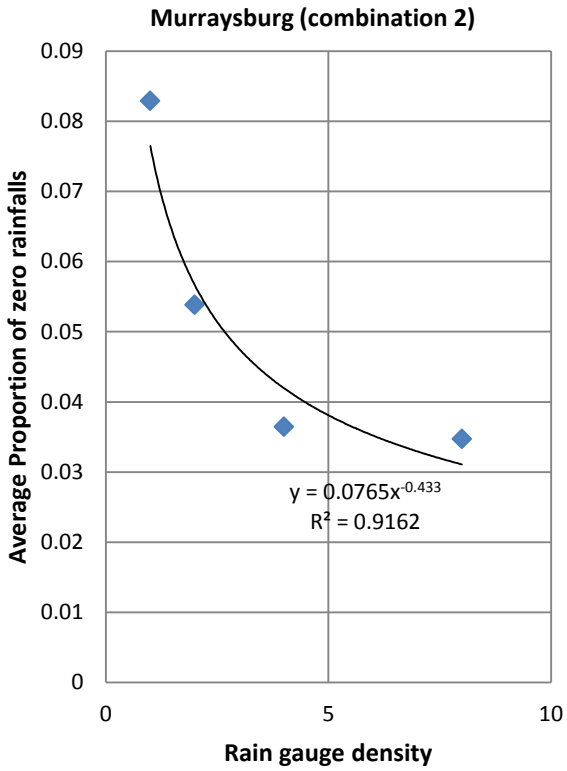
Murraysburg (combination 2)
Average Proportion of zero rainfalls
Rain gauge density
y = 0.0765x-0.433
R² = 0.9162
0.09
0.08
0.07
0.06
0.05
0.04
0.03
0.02
0.01
0
0
5
10

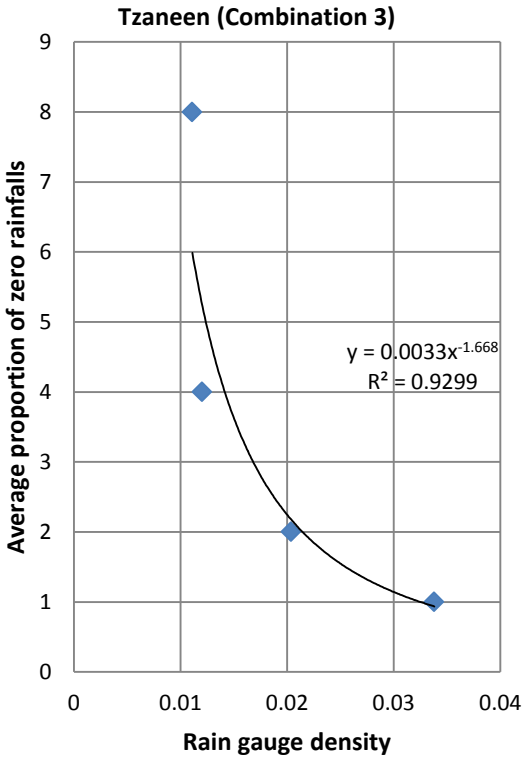
Tzaneen (Combination 3)
Average proportion of zero rainfalls
Rain gauge density
y = 0.0033x-1.668
R² = 0.9299
9
8
7
6
5
4
3
2
1
0
0
0.01
0.02
0.03
0.04

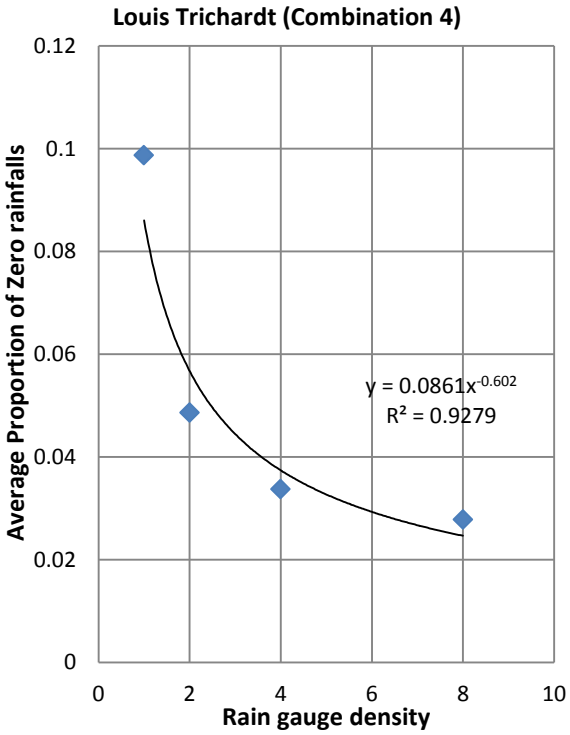
Louis Trichardt (Combination 4)
Average Proportion of Zero rainfalls
Rain gauge density
y = 0.0861x-0.602
R² = 0.9279
0.12
0.1
0.08
0.06
0.04
0.02
0
0
2
4
6
8
10

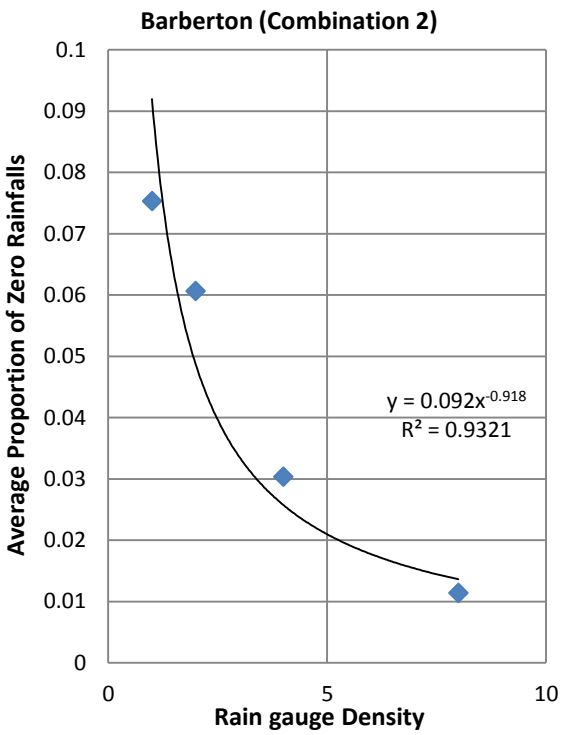
Barberton (Combination 2)
Average Proportion of Zero Rainfalls
Rain gauge Density
y = 0.092x-0.918
R² = 0.9321
0.1
0.09
0.08
0.07
0.06
0.05
0.04
0.03
0.02
0.01
0
0
5
10